‘A Twisted Backbone’ – The Synthesis of Interesting Metallosupramolecular Assemblies Through Steric Control.

A Thesis Submitted in Partial Fulfilment of the Requirements for the Degree of Masters of Science in Chemistry

---

Shane Sandeep Verma

University of Canterbury

2013

Acknowledgements

First and foremost, I would like to thank my supervisor, Professor Paul Kruger, for his continued encouragement, guidance and enthusiasm for research. I would like to extend my gratitude to my co-supervisor Dr Alan Ferguson, for all his help with X-ray crystallography, assistance in the laboratory, insight into the project and many more things that helped my project run smoothly.

To the past and present members of "the office", who created a friendly work environment throughout the past two years. I have been privileged to work alongside some amazing people within the Kruger group; I would like extend my thank you to Dr Chris Hawes and Miss Rosanna Archer for all their help and knowledge in the lab and introducing me to life as a postgraduate student. I would like to thank Samantha Bodman, for all her encouragement, pep-talks and extended coffee breaks during the past year that helped me stay in touch with reality. To Anthony O'Connor and Tamara Muirson for all their encouragement, friendly banter and antics that helped keep me motivated during the past few months.

I am grateful to all the academic staff in the Department of Chemistry who have passed on their knowledge of chemistry throughout my study at the University of Canterbury. To the technical staff, for helping maintain chemical stocks and a well-run department, especially Wayne Mackay and Rob McGregor for fixing anything broken. In particular I would like to thank Dr Meike Holzenkaempfer, Dr Matt Polson and Dr Marie Squire for their assistance, knowledge and help with NMR and Mass Spec. analysis. To the University of Canterbury for kindly providing me with a Masters Scholarship and to the Marsden Fund for additional funding.

Last but not least, the two people who I'll never be able to thank enough, my parents, whose love, belief, encouragement and support have made me the person I am today.

Abstract

This study investigates the self-assembly of ligands consisting of sterically hindered backbones. Ligands synthesised in this study took advantage of the twisted nature of benzil-2,3-dihydrazone brought about by the steric repulsion between two neighbouring phenyl groups. Synthesis of all ligands used a simple imine condensation reaction, where benzil-2,3-dihydrazone was combined with a chosen aromatic aldehyde. Coordination studies were conducted using first row transition metals and described in text are the solid state structures of twelve new discrete supramolecular complexes, characterised by single crystal X-ray crystallography.

Chapter 1 outlines an introduction to the topics discussed in this text, while providing examples drawn from literature and nature. Chapter 2 details the modified synthesis of bis-2-pyridyliminohydrazono-1,2-diphenylethane, **L1**, and the in-depth background of previous studies with the ligand. The complexes of **L1** with Mn(II), Fe(II), Co(II), Cu(I) and Zn(II) determined by single X-ray crystallography are presented, noting the structural effects different metal ion sources have upon **L1**. In chapter 3 the modified synthesis and characterisation of bis-2-imidazolyliminohydrazono-1,2-diphenylethane, **L2**, is presented. Crystallographically characterised complexes from the combination of **L2** with Mn(II), Ni(II), Co(II) and Zn(II) show the formation of interesting topologies which are compared to structures previously determined.

Chapter 4 begins with a brief introduction to clusters, followed by the synthesis and characterisation of a recently synthesised ligand, bis-2-salicyliminohydrazono-1,2-diphenylethane, **L3**,. The formation of a Ni(II) cluster with **L3** is further discussed in detail, and outlines the future scope for the work with these ligands. The synthesis and characterisation of **L4**, and the discussion of mononuclear complex formed between **L4** and Cu(II) is also introduced. The chapter concludes with a discussion with the potential future direction of this work with these ligands and their related compounds. Chapter 5 concludes the results and discussion with a brief summary of these results. Chapter 6 outlines the synthesis and characterisation of all ligands and complexes used in this study as well as potential ligands for future studies.

Table of contents

Abbreviations

Å	Angstroms (10^{-10} m)
°	Degrees
°C	Degrees Celsius
δ	Chemical Shift
1D	One Dimensional
2D	Two Dimensional
^{1}H NMR	Proton Nuclear Magnetic Resonance
^{13}C NMR	Carbon Nuclear Magnetic Resonance
s	Singlet (^{1}H NMR)
d	Doublet (^{1}H NMR)
t	Triplet (^{1}H NMR)
m	Multiplet (^{1}H NMR)
Acac	Acetylacetone
$[BF_4]^{-1}$	Tetrafluoroborate
$CDCl_3$	Deuterated Chloroform
Cl^{-1}	Chloride
$[ClO_4]^{-1}$	Perchlorate
cm^{-1}	Wavenumbers
COSY	Correlation Spectroscopy
DMSO	Deuterated Dimethyl Sulfoxide
kJ/mol	Kilo joules per mole
DNA	Deoxyribonucleic Acid
ES-MS	Electrospray Mass Spectrometry
g	Grams
H_2O	Water
HOMO	High Occupied Molecular Orbital
HPLC	High Performance Liquid Chromatography
HSQC	Heteronuclear Single Quantum Coherence Spectroscopy
Hz	Hertz
IR	Infrared
s	Strong (IR)
m	Medium (IR)
w	Weak (IR)
br	Broad (IR)
KBr	Potassium Bromide

kJ/mol	Kilo joules per mole
LUMO	Lowest Occupied Molecular Ortial
m/z	Mass-to-Charge Ratio
MeCN	Acetonitrile
MeOH	Methanol
MHz	Megahertz
mL	Millilitres
MP	Melting Point
$[NO_3]^{-1}$	Nitrate
NOESY	Nuclear Overhauser Effect Spectroscopy
$[OAc]^{-1}$	Acetate
SMM	Single Molecule Magnets
TOCSY	Total Correlation Spectroscopy

Atomic Colour Scheme

Black	Carbon
Dark Blue	Cobalt
Gold	Iron, Copper
Green	Chloride
Light Blue	Nitrogen
Pink	Manganese
Red	Oxygen
Silver	Zinc
Teal	Nickel
White	Hydrogen

Chapter 1

Introduction

1.1 Supramolecular chemistry

For the past few decades Supramolecular Chemistry has emerged as an important field in the realm of chemistry. Molecular associations have been studied for a long time, and the term "Ubermoleküle" was introduced already in the 1930's to describe the entities of higher molecular organizations.[1] Progress in the field of supramolecular chemistry is attributed to Cram,[2] Lehn[1] and Pederson[3] whose work on crown ethers and cryptates in the area of host-guest chemistry resulted in the honour of them receiving the Nobel Prize for Chemistry in 1987. Supramolecular chemistry as it is known today was famously introduced and described by Lehn in 1988 as "chemistry beyond the molecule".[1] Other classical explanations have been "the chemistry of the non-covalent bond", "non-molecular chemistry" and even "Lego chemistry".[4] However, a more suitable definition may be: "*Supramolecular Chemistry is the chemistry of the intermolecular, non-covalent bond covering the structures and functions of entities formed by the association of two or more chemical species held together by intermolecular force*."[1,5-7] This implies that not only is a single molecule studied, but the assembly of at least two molecules is examined.[8]

Traditional chemistry tends to focus on the study of atoms held together by strong covalent bonds,[9] which together constitute a molecule, whereas the supramolecular chemist uses the molecules themselves as the most basic building block, to construct a much larger aggregate.[10]

1.2 Non-covalent interactions in supramolecular chemistry

A thorough understanding of non-covalent interactions is fundamental in interpreting and predicting the relationships and functions between these architectures in supramolecular chemistry.[11,12] The term non-covalent interaction is not well defined in the above definition of supramolecular chemistry, but is generally accepted as a bonding interaction that cannot be described by the traditional electron sharing between two atomic orbitals to constitute a covalent bond.[8]

Although a single non-covalent interaction is weaker than a covalent bond, by employing a large array of non-covalent interactions a very durable assembly of molecules may be obtained.[8,10,13-16] Non-covalent interactions commonly found in supramolecular chemistry are; van der Waals interactions, π-π interactions, electrostatic interactions, hydrogen bonding interactions and metal coordination bonding interactions.[1,8,10,17] Discussed below in further detail are the interactions relevant to this study.

1.2.1 Hydrogen bonding

A hydrogen bond is a special type of bonding interaction that is ubiquitously found in nature and is responsible for maintaining the double-helical nature of DNA by employing multiple hydrogen bonding interactions between DNA base pairs.[1,8,18-21]

There are many acceptable definitions for hydrogen bonding interactions, the definition used to describe the hydrogen bonding interactions in this study is adopted from the review by Steiner: "*An X-H···A interaction is called a "Hydrogen bond" if 1). It constitutes a local bond and 2). X-H acts as a proton donor to A*".[22] There are four types of accepted hydrogen bonds:[23] 1). X-H···X bond, where X is an electronegative atom such as oxygen, fluorine or nitrogen, this bond arises due to the polarity of the X-H bond, resulting in a partially positive charge on the hydrogen, which interacts with a lone pair of electrons on X from an adjacent molecule;[9,13-15,23-25] 2). X-H···π, where X is an electronegative atom and the π-system of a second molecule acts as the proton acceptor; 3). C-H···n, where carbon is the proton donor and n is a lone pair of electrons; 4). C-H···π, where carbon is the proton donor and a π-system acts as the proton acceptor, it is important to note that the C-H···π interaction is often referred to as an edge-to-face π-π interaction[23,26] (and will for the scope of this study be referred as a edge-to-face π-π interaction) (Figure 1.1).

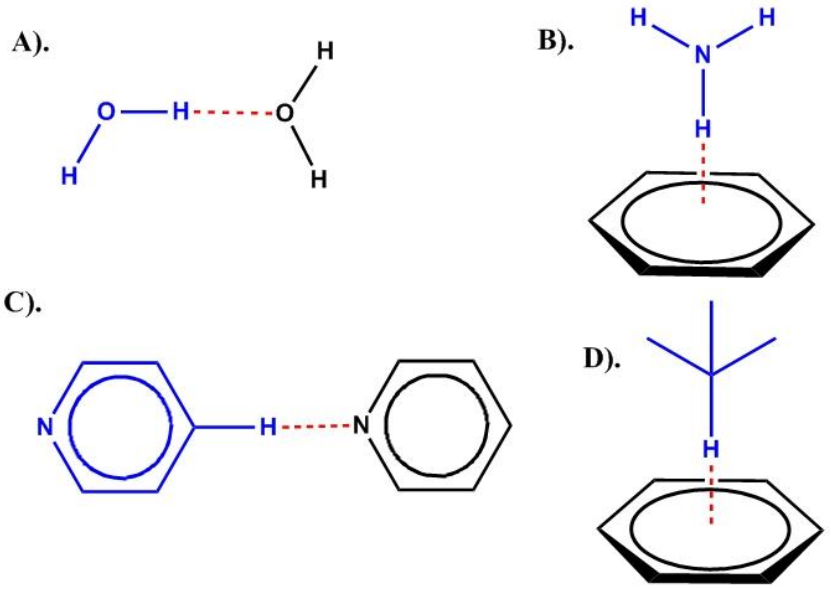

Figure 1.1 – Four types of hydrogen bonding. A). X-H···X bond; B). X-H···π bond; C). C-H···n bond; D). C-H···π bond. Hydrogen donor molecules noted in blue, dashed red bond represents a hydrogen bonding interaction.

1.2.2 π-π interactions

Intermolecular interactions can occur between electron rich and electron deficient π-orbitals of a molecule. Interactions between aromatic groups are widespread in nature and examples are found in the base stacking in DNA, binding in proteins and the intercalation of

certain drugs into DNA.[4,11,12,27,28] π-interactions arise when aromatic systems interact by the way of parallel 'stacking' interactions, in which the π-systems of neighbouring rings overlap[11,28] in a partially off-set arrangement that minimises π-electron repulsion and maximises the interaction between the two stacked rings (π-π interaction)[12]. The terms edge-to-face (see section **1.2.1**), and offset face-to-face interaction[11,12,28] (Figure 1.2) will be used to describe the π interactions in this study.

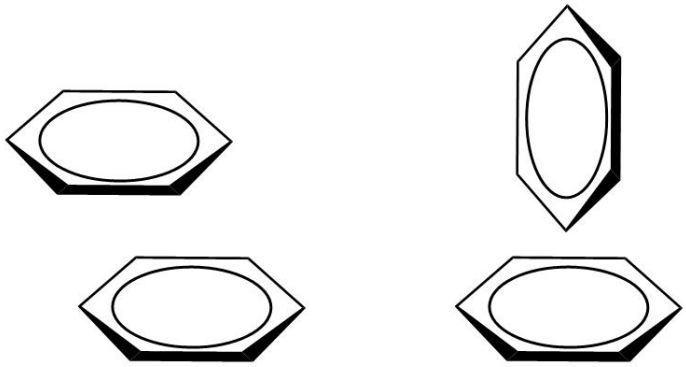

Figure 1.2 – π-interaction displayed between aromatic molecules, with offset face-to-face (left) and edge-to-face (left) interactions shown between benzene molecules.

1.2.3 Metal coordination bonds

It is well established that transition metals form coordination compounds with organic molecules and anions, or better known as *ligands*. The ligand(s) surround the metal ion in a coordination compound and is capable of donating one or more electron pairs to the metal ion (Figure 1.3). The metal ion usually sits between the ligands, acts as an electron acceptor and may be positively charged or uncharged.[9,24,29]

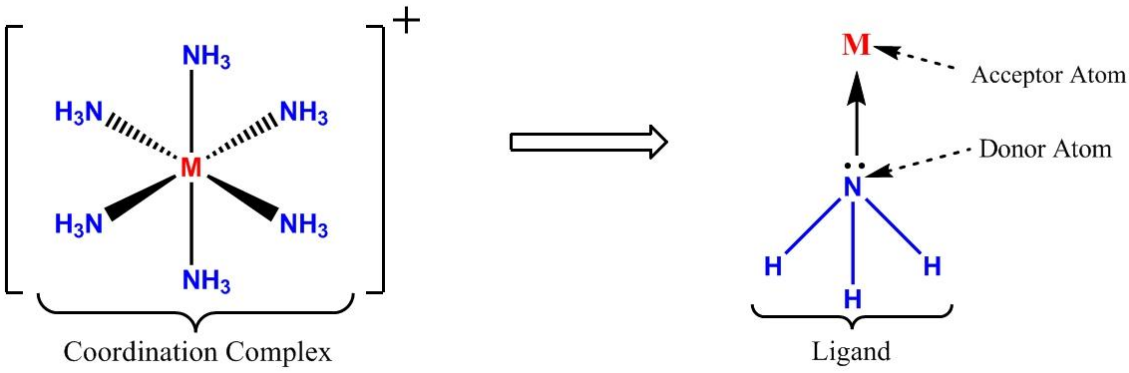

Figure 1.3 – An example of a coordinate bond, where M represents an *octahedral* transition metal and NH_3 the ligand. Note the donation of two electrons to the metal centre.

This electron sharing is generally thought of as a coordinative covalent bond,[9] but in the context of supramolecular chemistry, metal coordination is thought of as a non-covalent

interaction, it is important to note that the metal-ligand interaction is *stable* but *labile* (ligand-metal bond formation is reversible, yet reasonably strong and is dependent upon the metal/ligand used).[8] The atom that is directly bound to the metal atom is known as the donor atom, whereas the metal atom is known as the acceptor atom.[9,24,29]

It is possible to have a ligand with more than one donor atom and these ligands are known as bi-, tri-, or polydentate ligands, and are often referred to as chelating ligands due to their ability to hold onto the metal atom like a claw.[9]

Table 1.1 below summarises the key bonding interactions, bond lengths and energies used in this discussion.

Non-Covalent interaction	Typical bond length (Å)	Typical bond energies (kJ/mol)
offset π-π	3.3-3.8	2-50
edge to face π-π	3.5-3.8	2-8
hydrogen bond N,O donor (donor to acceptor distance)	≤3.2	10-30
hydrogen bond (donor to acceptor distance) C donor	3-3.5	8-15
coordination bond	~1.8-2.5	~50-500

Table 1.1 – Summary of relevant parameters used in this study.[4,11,12,22,23,26-28] Values for typical systems have been chosen. Hydrogen bonding interactions can exhibit bond dissociation enthalpies of over 150 kJ/mol, however the scope of these interactions lies outside this work.[4]

1.3 Metallosupramolecular chemistry

Taking advantage of the coordination bond to control the assembly and properties of supramolecular architectures is highly beneficial[10,17,18,30-32] and is known as '*Metallosupramolecular Chemistry*'- a term coined by Constable in 1994.[33] Traditional organic synthesis usually involves a stepwise synthesis of molecules, requiring the manipulation of various functional groups and usually returns a low yield. However, the metallosupramolecular chemist is able to take advantage of a self-assembly process (see section **1.5.4**) by simply mixing together a pre-chosen metal ion and ligand to obtain a single product in high yield.[17,34]

Metallosupramolecular chemistry involves the use of at least two synthons (building blocks): the metal ion and a predesigned organic molecule, the ligand. The metal ion allows the assembly of diverse and robust structures because the metal-donor bond is highly directional in

nature, is stronger than other non-covalent interactions and in most cases the metal ion displays a preference for a specific geometry[34] which often dictates the structure of the final assembly.[20]

The deliberate design of organic ligands in combination with metal ions has led to the formation of grids, boxes, cylinders, molecular polyhedra, helicates, catenanes, rotaxanes and various other supramolecular structures.[34-37] This can be achieved by fine tuning factors such as the donor atoms, the type of donor atoms, the mode in which the atoms will bind (e.g. bidentate *vs* tridentate) in combination with the variation of spacer groups separating the coordination sites and by employing bridging ligands.

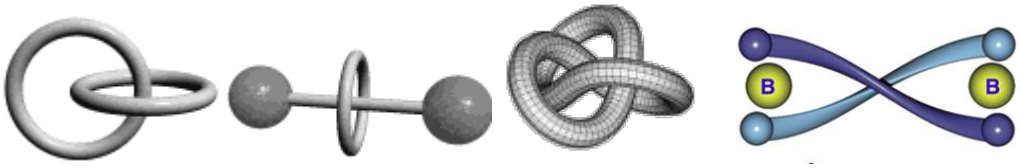

Figure 1.4 – From left to right: structural representations of a catenane, rotaxanes,[38] knot[39] and helicate.[40]

This is metallosupramolecular chemistry, the employment of metal ions in combination with bridging ligands (ligands able to bind to more than one metal) to generate highly interesting architectures, brought on by the spacial and directional information encoded in the building blocks.[10,17,31,41]

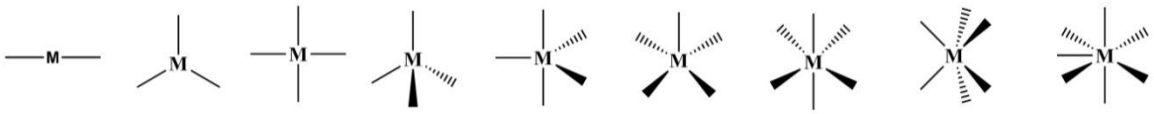

Figure 1.5 – Common metal coordination geometries found in metallosupramolecular chemistry, from left to right: linear, trigonal planar, square planar, tetrahedral, trigonal bipyramidal, square-based pyramidal, octahedral, trigonal prismatic, pentagonal bipyramidal.[24]

1.4 Supramolecular terminology

Supramolecular chemistry contains distinct terminology to describe the theories and processes associated within this field.

1.4.1 Self-organization

Self-organisation refers to systems that are capable of spontaneously forming well defined supramolecular structures from the complementary components (e.g. metal and ligand) under a given set of conditions.[42,43]

1.4.2 Molecular recognition

Molecular recognition is the specific and selective interaction between molecules and/or ions, which are complementary in their geometrical and electronic features. An analogy can be drawn from fitting two pieces of a puzzle together, where two pieces will only fit together if they are complementary in shape.[1,10,17,43] However, binding alone is not recognition; molecular recognition is specifically binding with a purpose. Molecular recognition is a question of the information stored and read out at the supramolecular level, this information may be stored in the structure of the ligand (the nature, number and arrangement of the binding sites offered by the ligand) as well as metal ion (the coordination number, number of donor atoms bound to the metal) and the coordination geometry.[1] This information borne by the ligand and metal is called the *intrinsic information*.[43]

1.4.3 Self-recognition

Defined by Kramer in 1993 as "*the recognition of like from un-like, of self from nonself-embodied in the spontaneous selection and preferential binding of like metal ions by like ligands in a mixture"*.[44]

Self-recognition allows the generation of the desired product from a mixture of different building blocks. This is due to three structural factors:

i. The structural features offered by the ligand (intrinsic information).
ii. The coordination geometry of the metal ions.
iii. The steric and conformational effects between the different possible products which results from the multitude of possible combinations of ligands and metal ions in a given mixture.

As well as due to two thermodynamic factors:

i. "Maximal site occupancy", which means that the final product formed is evolved from the combination of building blocks that occupy the maximum number of binding sites available on both the ligands and the metal ions. This corresponds to the greatest number of coordination bonds and therefore to the most stable product.
ii. The entropic factor, which favours the formation of the largest number of species possible.[42,44]

The spontaneous self-organisation of a number of building blocks into single aggregated structures occurs via molecular recognition in which the intrinsic information of the building blocks leads to the formation of the desired product.[17]

A popular example of the self-recognition process can be taken from Lehn and co-workers where the selective formation of helicates (see section 1.5) was obtained from the mixture of different oligobipyridine strands and suitable metal ions. It was possible that the product generated would contain a mixture of randomly distributed ligand and metal bonded species. However, the species formed showed only the combination of identical ligand strands to central metal ions (Figure 1.6).[44]

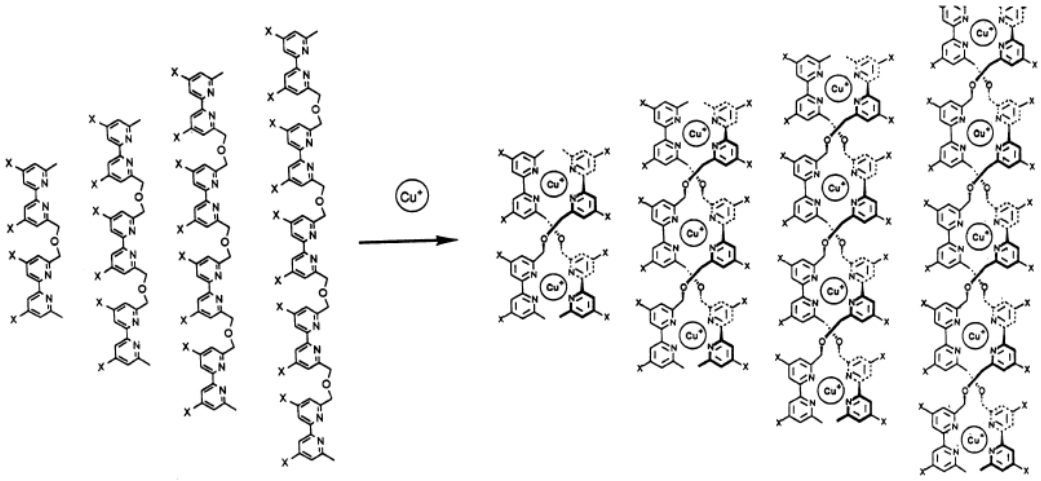

Figure 1.6 – The self-recognition process demonstrated by the mixture of different length oligobipyridine ligands giving a judicious matching of like for like.[44]

1.4.4 Self-assembly

Molecular self-assembly is a process through which complementary molecular building blocks spontaneously assemble into a well-defined product. This is achieved through non-covalent interactions encoded in the building blocks themselves (e.g. hydrogen bond donors, coordination bond donors, groups able to form π-π interactions).[32,43,45-47] The spontaneous and selective formation of supramolecular entities through utilizing the self-assembly process is a subject of great interest in the field of supramolecular chemistry[44,48] due to the unusual structures and special functional properties such as luminescence, redox activity, and magnetism demonstrated by these assemblies.[49]

The non-covalent interactions that drive self-assembly are weak compared to covalent interactions.[45,46] The weak nature of the non-covalent bond allows for their bond formation to be reversible.[8] Since the final product may require the formation of several bonds, the bond formation and dissociation must be rapid. This allows the assembly process to:

i. Explore all potential structures, finally settling on the structure with the lowest energy (thermodynamically most stable structure).[43]

ii. The reversibility of the non-covalent bond allows for any 'errors' to be corrected by the dissociation of the mismatched pair of building blocks.[8,43]

The final product formed by self-assembly corresponds to the thermodynamically most stable complex of all the potential structures that may be formed by the original building blocks.[8,18,37,43,45] Metallosupramolecular chemistry is ideal for the synthesis of structures by self-assembly as the strength of the coordination bond is labile enough to allow the building blocks to continually and reversibly assemble until the most thermodynamically stable structure is finally explored and settled upon, generally in high yield.[17,37,45]

Coordination driven self-assembly relies on the interaction between electron poor transition metals and electron rich organic ligands.[46] Fine tuning of the ligand properties such as the donor, density, types and number of donors as well as the spacer group separating binding domains has led to the assembly of different structural motifs such as grids, boxes, cylinders and helicates.[34,50] In addition to changing the ligand, altering the ratio in which the ligand and metals are mixed together may also affect the final assembly process.[45]

1.5 Helicates

Of the various structures formed in supramolecular chemistry, the helical topology has attracted much interest because of it's prevalence in nature, the information it provide about the self-assembly process and their aesthetic beauty.[35,36] Molecular helicity is a fascinating property displayed by chemical and biological structures, such as the double helix formed by the self-assembly of DNA, where two strands are intertwined and held together through hydrogen bonding interactions between two complementary nucleic bases [19,20,37,43,51,52](Figure 1.7**)**.

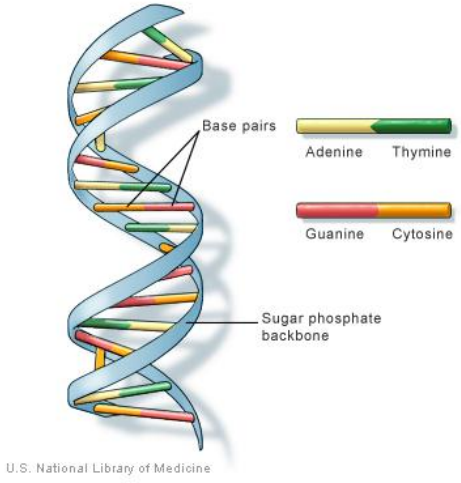

Figure 1.7– Structural representation of DNA.[53]

Nature's most impressive structural architecture, the helix, is now established as a versatile and interesting building block in the field of supramolecular chemistry.[41] A lot of effort has been made in the design and synthesis of artificial helical structures by employing non-covalent interactions such as meal coordination, hydrogen bonding, π-π stacking to mimic the structural and functionality of interesting biomacromolecules.[52]

The term helicate was introduced by Lehn in 1987 for the description of metal complexes whose shape was best described as helical.[51] An acceptable definition of a helicate is "*a discrete supramolecular complex constituted by one or more covalent organic strands wrapped about and coordinated to a series of metal ions defining the helical axis*".[37,42,43,51,52] For a supramolecular entity to be described as a helicate in the scope of this work, it must abide by the following requirements:

i. One or more organic acyclic ligand strands are helically twisted and coordinated to cations or anions by coordinative bonds.
ii. A helicate contains a minimum of two ions and forms a discrete polynuclear structure.[43]

1.5.1 Helicate terminology

A helicate may be right-handed (plus, P; Δ=P) or left-handed (minus, M; Λ=M) according to whether the rotation is clockwise or anticlockwise when the helix is considered to twist from the viewer's eye towards a distant point away from the viewer,[43] as demonstrated below in Figure 1.8.

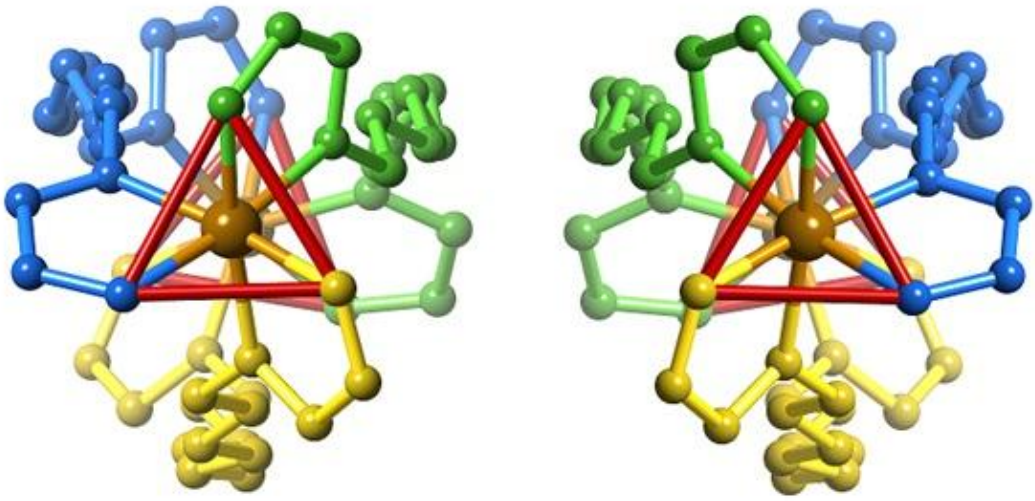

Figure 1.8 – The right-handed (Δ=P) helicate (Figure 1.8 left) and the left-handed (Λ=M) helicate (Figure 1.8 right).[54]

Helicates are generally described by four successive terms, which describes the nature of the helix formed with respect to the ligand (Figure 1.9).

i. The number of strands: single-, double-, triple-, or quadruple-stranded.
ii. The nature of the strands; homotopic (ligand consists of identical binding units) or heterotopic (ligand contains different binding units).
iii. The relative orientation of the strands in the helicate: H= head-to-head (identical binding units bound to the same metal), T= head-to-tail (different binding units bound to the same metal).
iv. Whether the metal ion requires ancillary ligands coordinated to satisfy the coordination sphere; saturated (no extra ligands) or unsaturated (one or more ancillary ligands are coordinated to the metal centre).

As well as describing the helicate by the nature of the ligands and how they are bound, the number of metal ions that constitute the helical axis (the *nuclearity*) are also described.[43]

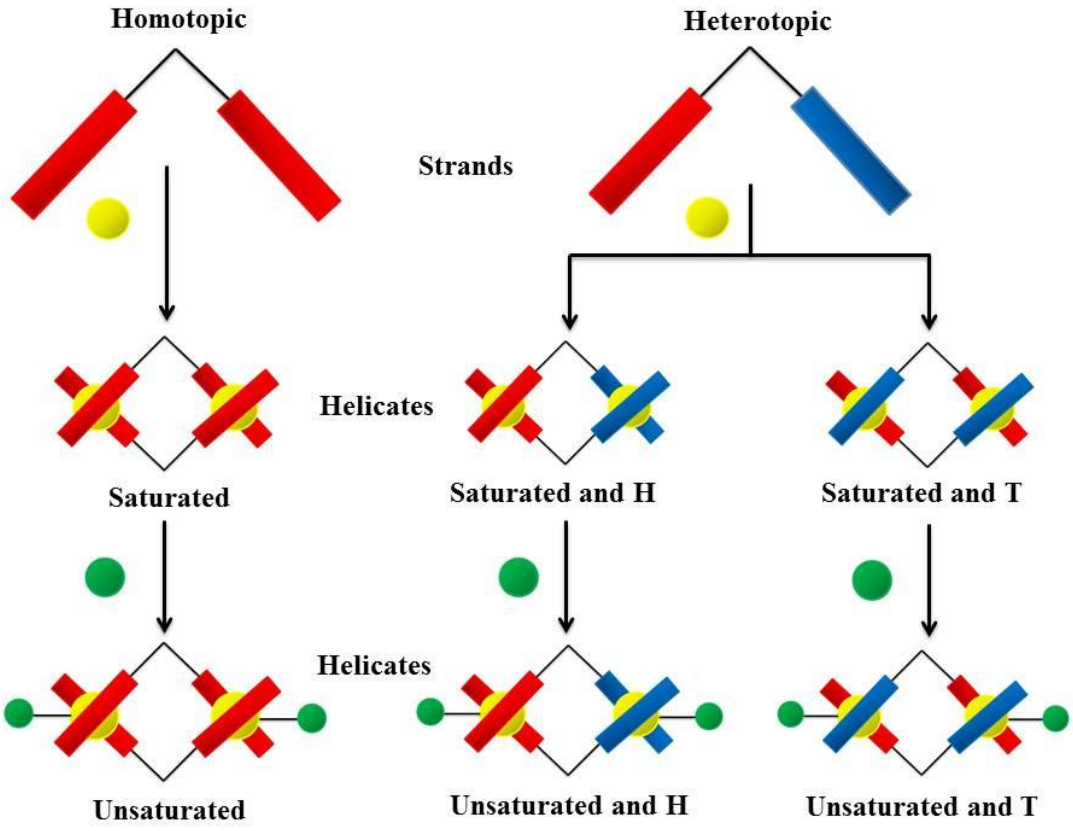

Figure 1.9 – The schematic representation of the different binding modes of a homotopic (all binding modes are identical) and heterotopic (binding modes are different) ligand.[43]

The use of helicates as simple model systems may help answer questions about stereochemistry (study of the spatial arrangement of molecules) and regiochemistry (why one

structural isomer is selectively formed over another) in supramolecular assemblies.[20] This is because the current description and understanding of the thermodynamic self-assembly processes of metallosupramolecular structures is partial and this is shown by the inability to safely predict with 100% certainty that a desired structure will be obtained when a pre-designed ligand and metal are mixed together.[37]

1.5.2 Design principles of a helicate

The generation of a helicate depends on the intrinsic information of the metal ions and the ligands.[20,36,43] Metallic cations are attractive synthons in the synthesis of helicates because they possess useful encoded information that can help direct the assembly of a helicate:

i. A set of coordination numbers and isomeric preferences depending on their size, charge and electronic structure.
ii. A variety in binding strength.
iii. A variation of affinities for different donor groups
iv. They contain specific magnetic, electronic and spectroscopic properties that may be expressed in the final structure.[20]

The use of organic synthesis to prepare organic ligands offers almost an unlimited array of pre-designed receptor sites with suitable encoded information. Ligands suitable for helicate assembly should possess:

i. Several binding units along the organic molecule to allow in the recognition and coordination of various metal ions.
ii. Spacers between the binding units which are rigid enough to prevent the binding of a metal ion to several different binding domains of a single ligand, but at the same time are flexible enough to allow for helix formation and to wrap about the metal ions to produce stable complexes.[37,43]

Changing the intrinsic information of one of the components can lead to the generation of helicates with different topologies. For example the bis-bidentate (two bidentate binding domains) ligand shown in Figure 1.10 possesses binding domains that are compatible with tetrahedral or octahedral metal ions. Reaction of the ligand, **A**, with Cu(I) gives the *dinuclear double helicate*, where the tetrahedral coordination environment of Cu(I) is satisfied by *two* bidentate binding domains. Changing the metal ion to Co(II) resulted in the formation of a *dinuclear triple helicate*, where the octahedral coordination environment of Co(II) is satisfied by *three* bidentate binding domains.[55]

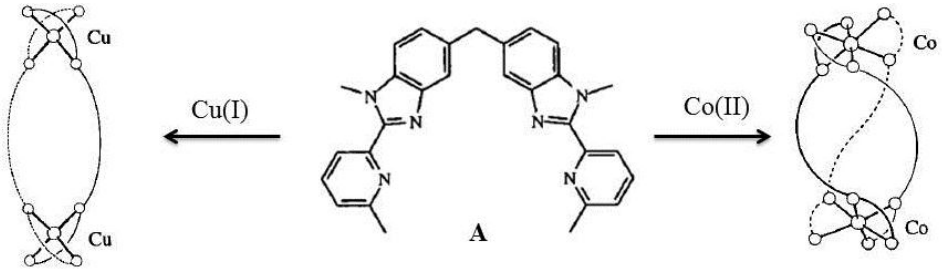

Figure 1.10 – Schematic representation of the double stranded $[Cu_2(\mathbf{A})_2]^{+2}$ and triple stranded $[Co_2(\mathbf{A})_2]^{+4}$ helicates, where the nature of the helicate is dictated by the metal ion.[43]

1.6 Imine-based ligands

Imines, or Schiff base, ligands are straight forward to synthesize,[20,48,56] making them attractive because they are readily available in large amounts to do coordination studies and to probe the properties of different supramolecular architectures.[20,57] Consequently this has greatly increased the knowledge of the self-assembly process.[36] The use of imines in the synthesis of ligands has led to the formation of various supramolecular architectures including helicates,[34-36,48,49,56-66] *meso*-helicates,[41] mononuclear structures,[50] pentafoil knots,[67] tetrahedral cages,[20] clusters[68-70] amongst other structures.

Figure 1.11 below shows the synthetic pathway for the formation of the characteristic C=N bond of an imine functional group. Imines are formed by a reversible nucleophilic substitution reaction, when a primary amine reacts with an aldehyde or ketone. The first step of the reaction involves nucleophilic attack upon the carbonyl group of an aldehyde or ketone giving a dipolar tetrahedral intermediate. Proton migration from the nitrogen to the oxygen leads to a more stable hemiaminal species. Protonation of the hydroxyl group by the aid of an acid catalyst leads to the loss of water by the nitrogen lone pair forming an iminium ion. Subsequent loss of a proton (catalyst regeneration) leads to the imine product.

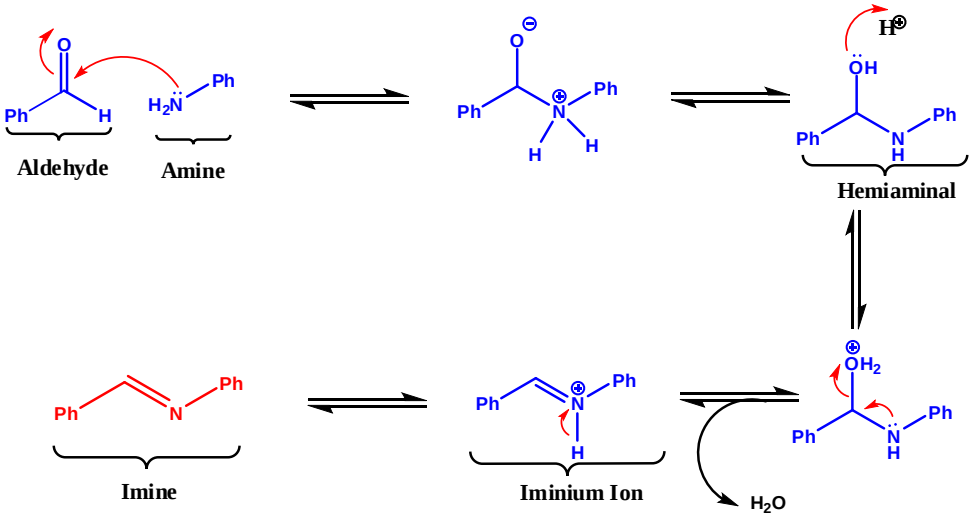

Figure 1.11 - Reaction mechanism for an imine condensation.[71]

Without an acid catalyst the reaction is very slow,[71] though as presented later in this study, is not necessary for the formation of an imine. Imines are generally unstable with respect to their parent carbonyl or amine compounds and are easily hydrolysed by water, so their synthesis usually requires the use of a method which removes water from the reaction mixture e.g. Dean-Stark Trap.[71]

Previous work on helicates within the Kruger group has involved the use of the ligands shown below in Figure 1.12.

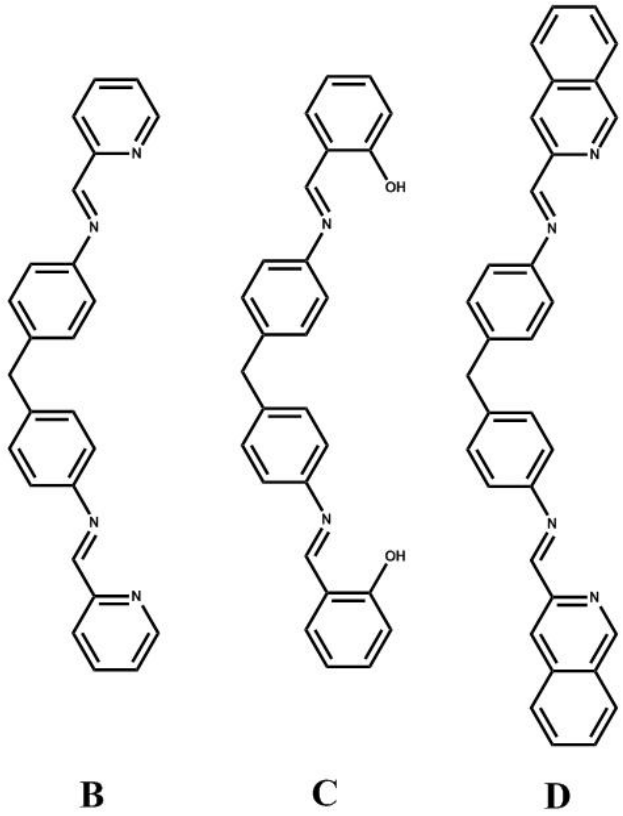

Figure 1.12 – Molecular representations of ligands previously used in the Kruger group to synthesis helicates.[34-36,66]

Ligand **B**, **C** and **D** all consist of a central methylene spacer between two phenyl rings which have an imino functional groups attached. Ligand **B** is known to form a dinuclear triple helicate when reacted with Cu(II) however, it forms a dinuclear molecular square when combined with Cu(I).[66] Once again this represents the influence the nature of the metal ion has upon the final topology of the supramolecular structure.

Functionalization of the ligand, by altering the terminal pyridyl group to a phenolic group allows for the synthesis of a ligand with both nitrogen and oxygen donating groups.[36] Complexation can be achieved by deprotonation of both terminal phenolic groups to form neutral dinuclear double helicates with Co(II) and Cu(II), without the need of anions to balance the charge of the metal centres.[36]

Research within the Kruger group has stemmed from the synthesis of a mononuclear complex where an Fe(II) metal ion is bound to three butane-2,3-dihydrazone ligands in a bidentate fashion (Figure 1.13).[72] This complex exhibits a propeller like twist, which can be taken advantage of to produce a flexible ligand that can display helical behaviour.

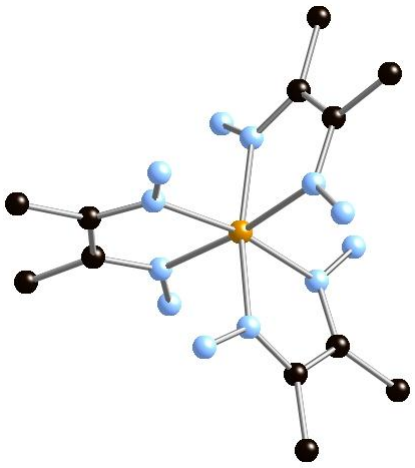

Figure 1.13 – Tris bidentate Fe(II) butane-2,3-dihydrazone complex displaying the propeller like twist. [72]

Polydentate ligands that contain a hydrazone bridge are known to produce a variety of supramolecular architectures such as helices, polygons, polyhedra and oligomers, brought by free rotation of the N-N bond of the hydrazone functional group. Reacting butane-2,3-dihydrazone with 2-imidazolecarbaldehyde capped both sides of butane-2,3-dihyrdrazone and formed two arms of the ligand. Previous research in the Kruger research group has shown formation of a trinuclear triple helicate when this ligand is combined with Fe(II) (Figure 1.14).[73]

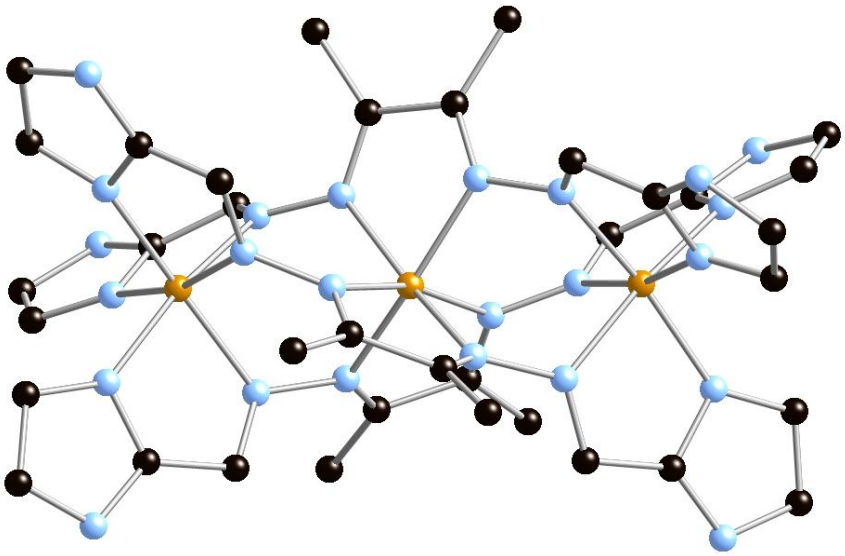

Figure 1.14 – Iron trinuclear triple helicate formed by the extension of the butane-2,3-dihydrazone ligand.[73]

The simple, easily controlled, step-wise construction of ligands, along with the large array of available amines and aldehydes for the formation of imine based ligands, makes this

synthetic strategy an attractive and reasonable way to design interesting supramolecular architectures.

As noted previously the spacer type of the bridging unit of the ligand plays an important role in the outcome of the final structure.[20] Changing the backbone from a small methyl group to a bulky benzil, has an immediate steric effect, resulting in a dihedral angle of 69.5(2)° and 70.7(2)° of benzil dihydrazone (Figure 1.15). Twisting of the backbone of benzil dihydrazone arises from steric repulsion between two large phenyl groups, placing them at angles where the steric interaction is minimised, whereas butane-2,3-dihydrazone is a planar molecule.[74]

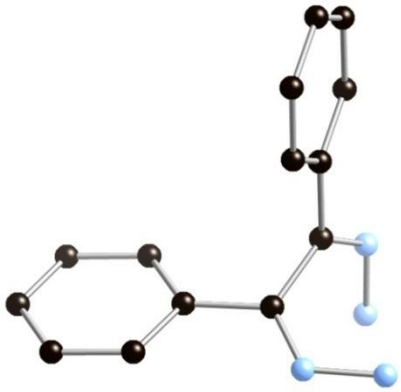

Figure 1.15 - Rotation about the backbone of benzil dihydrazone minimises the steric interaction between two benzil groups.[74]

Exploiting the twist of benzil dihydrazone to design N-helical ligands[67] can be achieved by a simple imine condensation reaction between an appropriate aromatic aldehyde and benzil dihydrazone. This approach has led to the synthesis of three known ligands in the literature (Figure 1.16).

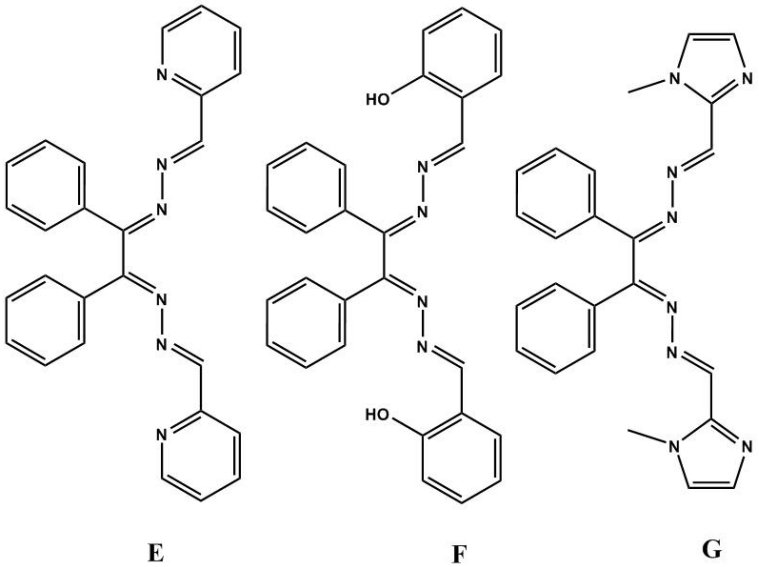

Figure 1.16 – Ligands previously designed, exploiting the dihedral angle of benzil dihydrazone to synthesise interesting supramolecular architectures. [49,56,61-65,67,75-77]

Ligand **E** is the most studied of this family of ligands and is known to form mononuclear structures with Hg(II)[77] and Ru(II),[75,76] as well dinuclear double helicates with Cu(I)[63] and Ag(II).[64,65] Ligand **F** and **G** however, are not as well studied as ligand **E**, but are known to form mononuclear complexes with Cu(II),[56] Co(II)[49] or a Möbius cycle.[67]

1.7 Present Study

As noted previously in the literature[43,55] and within the Kruger research group,[66] changing the transition metal ion from one metal to another or changing the oxidation state of the metal ion can lead to the formation of two unique species. Ligands employed in this study are shown in Figure 1.17**.**

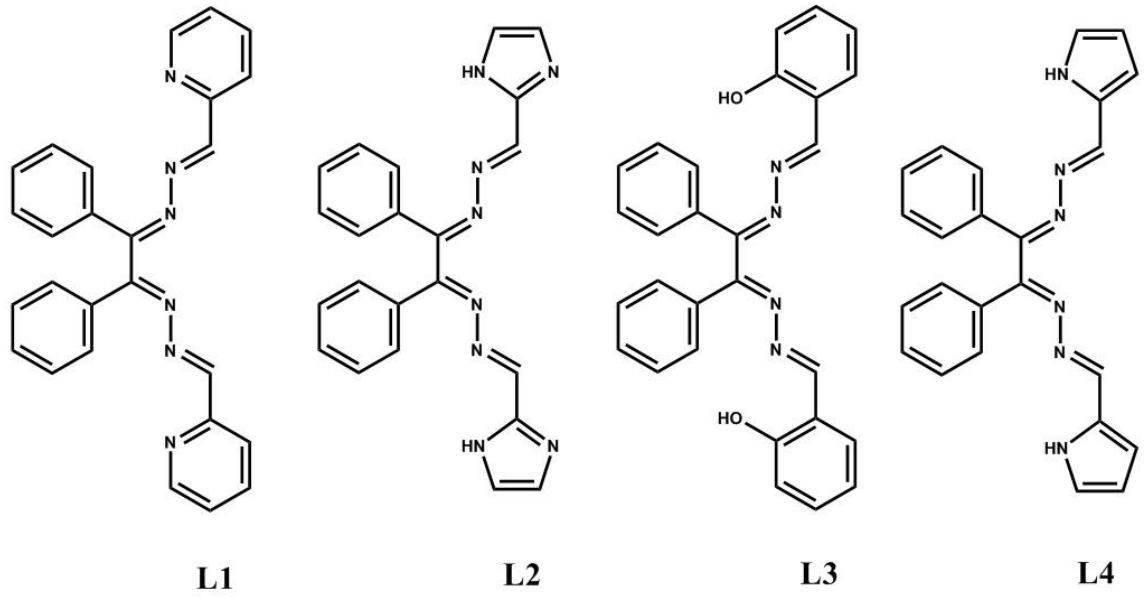

Figure 1.17 – Ligands used in current study.

The main aims of the study were to:

- Exploit the twist of benzil dihydrazone in the synthesis and characterisation of new ligands.
- Investigate the structural difference presented by different head groups bound to benzil dihydrazone.
- Explore the structural effects of complexes formed with first row transition metals formed from different anions and different transition metal ions.
- Add to the library of known structures of **L1** and **L3**.

1.7.1 Methods of synthesis and data collection

The following report details the preparation of ligands based on the twist of benzil dihydrazone and the complexes formed between these ligands and various first row transition metals. The synthetic procedure to synthesise these ligands has been adapted from a simple imine condensation reaction, widely used throughout the Kruger group. All organic precursors and ligand molecules have been fully characterised using nuclear magnetic resonance (NMR), electrospray mass spectrometry (ES-MS), infrared spectroscopy (IR), melting point analysis (MP) as well as single crystal X-ray crystallography where possible.

Single crystal X-ray crystallography was used to determine the structure of metal complexes formed. Slow evaporation and slow diffusion were the chosen methods to grow single crystals, as described by Spingler and co-workers.[78] Diffusions and evaporations were set up so that solutions contained a metal to ligand ratios of 1:1, 1:2, 1:3, 1:4, 2:3, 3:2, 4:1, 3:1, 2:1. Alternative ratios were chosen as it has been noted in literature that changing the ligand and metal ratio can affect the final assembly.[45] Solvents used as in slow evaporations as well as diffusions were; methanol, ethanol, acetonitrile, nitromethane, tetrahydrofuran, chloroform and acetone. The 'anti-solvents' used for slow diffusion studies were diisopropyl ether, diethyl ether, benzene, and toluene. As well as different ratios and solvents, different metal salts were used as the influence of anions can also affect the final architecture formed from the self-assembly process.[66]

The crystallographic refinement details as well as bonding parameters are not fully described within the body of the text. Tables of the crystallographic data (Tables **2.1** – **5**) and bonding parameters (Tables **2.4** – **4.9**) are described in full detail in Appendices 1 and 3, respectively. All crystallographic data is provided in .cif format in the accompanying electronic supplementary information on CD-ROM.

Chapter 2

Bis-2-pyridyliminohydrazono-1,2-diphenylethane, L1

2.1 Synthesis and background of *Bis-2-pyridyliminohydrazono-1,2-diphenylethane,* L1

Previous studies have synthesised **L1** (Figure 2.1) by following the method of Pal and co-workers,[61-65,76,77] maintaining an anhydrous atmosphere, using freshly distilled 2-formyl pyridine and no acid catalyst.[75] In this study, anhydrous conditions were not employed, however the use of an acid catalyst was. This is because it is known that the formation of a stable imine product is achievable if the imine double bond possesses an aromatic substituent or a hydrazone, oximine or semicarbazone functional group.[71] **L1** possesses a hydrazone group, and an aromatic group at each imine functionality, so the formation of a stable imine based ligand was highly likely. Melting point[75] and ^{1}H NMR[64] data was consistent with that reported in literature.

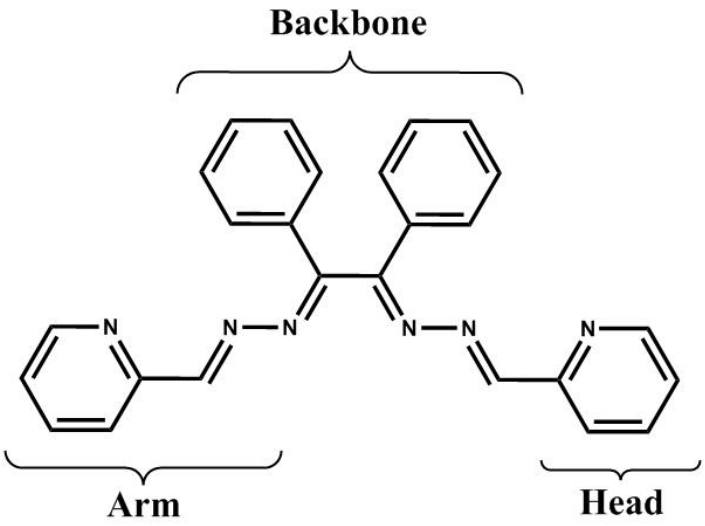

Figure 2.1 – Molecular representation of **L1**, showing the references, arm, head and backbone, used to describe the ligand in text.

Previous research on the crystal structure of this ligand report two different dihedral angles of 85.9°[61] and -99.5(3)°,[63,65] of the backbone between the two benzil groups, which is responsible for the helical nature of the ligand. **L1** is known to form a mononuclear system when reacted with Hg(II) and exhibits a reduction in twisting of the backbone to 83.3°. The crystal packing shows extensive C-H···π and C-H···Cl interactions.[77] A dinuclear helicate is known to form with Cu(I)[61] and Ag(I) showing π-interactions between the aromatic benzil and pyridyl groups.[62,64,65] Interestingly **L1** undergoes a electrocyclic rearrangement when combined with Ru(II).[75,76]

2.2 Synthesis and characterisation of complexes with Bis-2-pyridyliminohydrazono-1,2-diphenylethane, L1

*2.2.1 Crystal structure of {[Mn(L1)Cl_2]·($CH_3CN)_3H_2O$, Complex **1***

Crystals suitable for a single crystal X-ray diffraction study were obtained by vapour diffusion of toluene into an acetonitrile solution consisting of a 1:3, **L1**:$MnCl_2$ molar ratio to obtain a 60% yield of crystals in 4 weeks. The structure for complex **1** was solved and refined in the triclinic *P*-1 space group. The atomic structure and selected atomic numbering scheme is shown in Figure 2.2. The asymmetric unit contains two neutral mononuclear complexes, three acetonitrile solvent molecules and a single water molecule per unit cell.

The geometry of both Mn(II) centres is best described as distorted octahedral. This is indicated by the *trans* bond angles for Mn1 ranging from 146.40(5)° - 175.43(7)° and 146.00(3)° - 176.18(7)° for Mn2, a large variation from the 180° expected for a perfect octahedral structure. The *cis* bonds in both molecules exhibit a large deviation from the expected 90° for a perfect octahedral structure (Mn1, 68.30(7)° - 108.18(3)° and Mn2 68.47(7)° - 113.10(7)°) and the degree of distortion is shown by the large ∑ values of 134.77 (Mn1), 142.11 (Mn2), a large degree of variation of the ideal value of zero for a perfect octahedral structure (for full description on distortion calculations see Appendix **4**).[79] The long Mn-N and Mn-Cl bond lengths (~2.3 Å - ~2.4 Å) exhibited in both molecules suggests that the Mn(II) centre is in a high spin state (bond lengths below 2.15 Å are indicative of a low spin system).[80-82] See Table **2.4** in Appendix **3** for full details on bond lengths and angles.

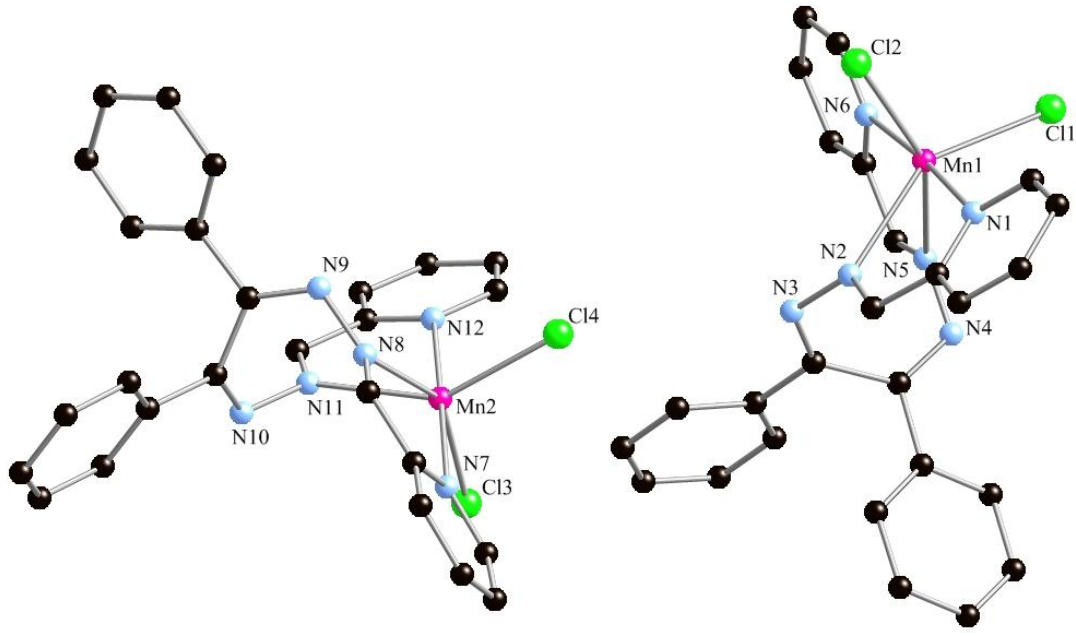

Figure 2.2- Molecular structure and selected atomic numbering scheme for complex **1**. Hydrogen atoms, solvent molecules and carbon numbering omitted for clarity.

Each arm of **L1** binds to the Mn(II) centre in both molecules through the two bidentate domains presented by the *cis* orientation of the pyridyl and imino nitrogen atoms forming bite angles of 68.93(7)°, 70.19(7)° (N1-Mn1-N2, N5-Mn1-N6, respectively), 69.60(7)° and 68.47(7)° (N7-Mn2-N8, N11-Mn2-N12, respectively). Coordination of both arms of **L1** to a single Mn(II) centre is achieved by significant twisting of several bonds in **L1**. The backbone is twisted with dihedral angles of 59.90(2)° (Mn1) and 60.40(2)° (Mn2) between the benzil groups, significantly less than found in the free ligand crystal structure. The hydrazone N-N bonds in both Mn1 and Mn2 display dihedral angles of 87.2(2)°, 83.7(2)° for Mn1 and 94.3(2)°, 106.0 (2)° for Mn2. The twisting of the ligand to form a mononuclear complex, as well as the enforced bite angles of the bidentate binding domains, results in the Mn(II) centre in both molecules adopting a distorted octahedral geometry.

*2.2.2 Crystal structure of {[Mn(L1)(CH$_3$CN)$_2$(H$_2$O)][Mn$_2$(L1)$_2$(CH$_3$CN)$_2$(μ$_2$-ClO4)$_2$]·(ClO$_4$)$_6$ (CH$_3$CN)$_2$} , Complex **2**.*

Crystals suitable for a single X-ray diffraction study were obtained by vapour diffusion of diisopropyl ether into an acetonitrile solution containing a 1:2 molar ratio of **L1** and $Mn(ClO_4)_2{\cdot}xH_2O$. Crystals were obtained at a yield of 45% after 2 weeks. The structure for complex **2** was solved and refined in the monoclinic $P2_1/c$ space group. The molecular structures found in the asymmetric unit with selected atomic labelling are shown in Figure 2.3. The asymmetric unit contains a mononuclear structure (Mn2), half of a dinuclear structure (Mn1), three perchlorate anions as well as a single acetonitrile solvent molecule.

The Mn(II) centre of Mn2 adopts a seven coordinate geometry which is best described as distorted pentagonal bipyramidal, with the coordination sphere being occupied by 4 nitrogen donor atoms from **L1**, two nitrogen atoms from two acetonitrile ligands and a single water molecule. The distortion is demonstrated by the *axial* angle of 171.89(8)° between the two pyridyl nitrogen atoms and the *equatorial* angles ranging from 71.49(8)° - 81.74(8)°, where in an ideal structure they would be 180° and 72°, respectfully. The degree of distortion is demonstrated by the large $\sum$ value of 23.87 derived from the five equatorial bond angles. Mn(II) adopting a seven coordinate geometry is well known in literature.[83,84,85]

The long bond lengths of the Mn(II) coordination sphere in Mn2, ranging from 2.193(2) Å to 2.469(2) Å suggest that the metal centre is in a high spin state.[80-82] **L1** coordinates to a single Mn(II) centre in Mn2 through two bidentate binding domains due to twisting of the backbone (dihedral angle of -66.2(3)°), with chelate bite angles of 70.09(8)° (N8-Mn2-N9) and 68.03(8)° (N12-Mn2-N13). As seen with complex **1** previously, the hydrazone bonds are highly twisted, with dihedral angles of -103.2(3)° (C34-N9-N10-C35) and -118.5(3)° (C42-N11-N12-C49). The

larger degree of twisting of one arm is exhibited in an elongated Mn(II)-hydrazone bond (2.469(2) Å), which is 0.134 Å larger than the Mn(II)-hydrazone bond length of the opposite arm.

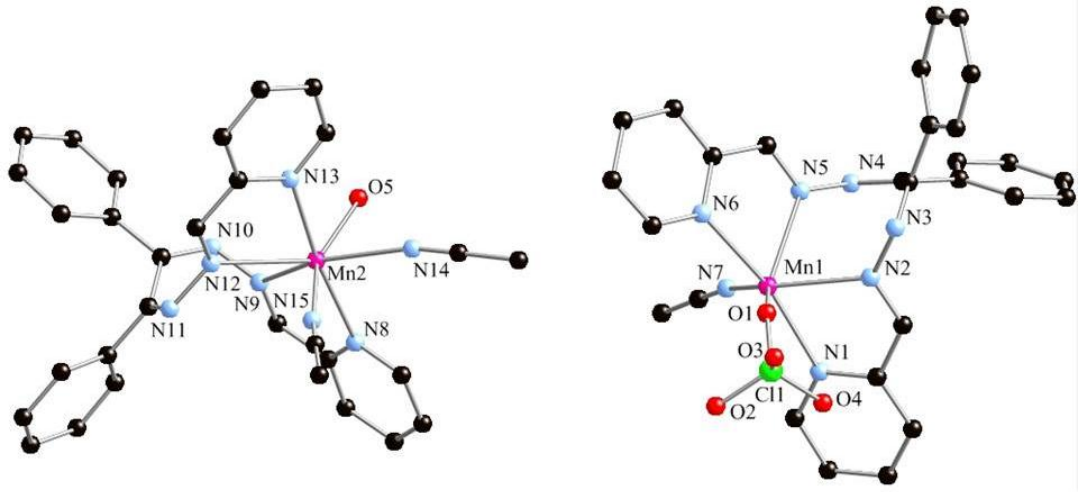

Figure 2.3 – Asymmetric unit of complex **2** showing the molecular structure and selected atomic numbering scheme. Hydrogen atoms, solvent molecules and anions omitted for clarity.

Mn1 forms a dinuclear structure with the two Mn(II) centres being linked by two μ_2 perchlorate ligands and is shown in Figure 2.4. An inversion centre in the middle of the molecule generates the two Mn(II) centres. As with Mn2, Mn1 also adopts a distorted seven-coordinate pentagonal bipyramidal geometry. The coordination sphere of Mn1 is fulfilled by 4 nitrogen donor atoms from **L1**, a single acetonitrile nitrogen atom and two oxygen atoms from two μ_2-perchlorate ligands. The degree of distortion is demonstrated by the small axial bond angle of 168.43(9)° and the equatorial bond angles varying between 73.09(8)° to 82.59(9)° resulting in a $\sum$ value of 24.06. The long coordinating bond lengths to the metal (2.262(3) Å – 2.412(2) Å) are indicative of a high spin centre.[80-82]

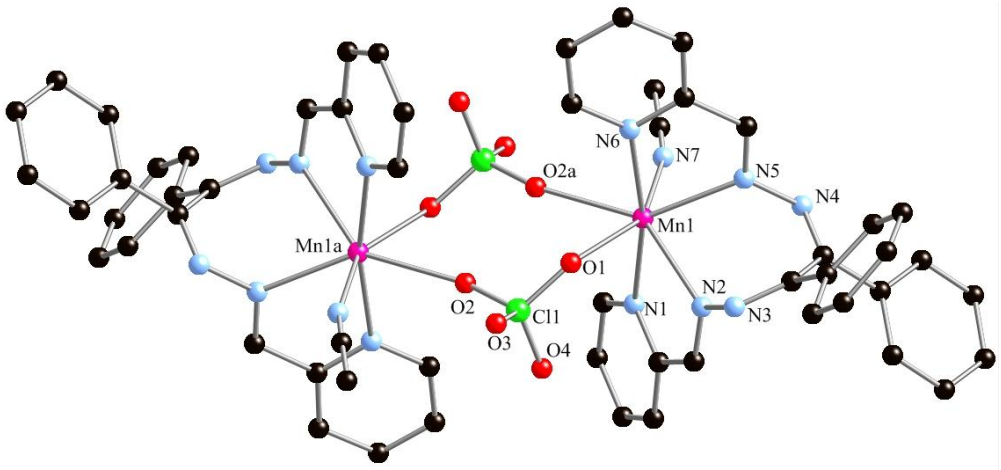

Figure 2.4 – Dinuclear structure of molecule *II* with selected atomic labelling. Equivalent atoms generated by inversion symmetry element. Equivalent atoms generated by the symmetry code: (1-x,1-y,1-z)[a]. Hydrogen atoms, solvent molecules and molecule *I* omitted for clarity.

A CSD search for two or more transition metal centres linked by at least a single perchlorate bridging ligand gave a total of 250 results, most of which involved bridging Cu(I) or Cu(II) and Ag(I) atoms. Of the 250 results, there were a total of 11 complexes (9 Ag(I), 1 Co(II), 1 Hg(II)) which had two μ_2-perchlorate bridges linking the two metal centres together. So far there are only 14 reported complexes of Mn(II) and Mn(III) which contain a perchlorate bridging two[86-91] or three metal[91-94] centres together, in combination with other ligands. Complex **2** therefore appears to be the first example of a Mn(II) complex where perchlorate acts as the sole bridging ligand, and also where two perchlorate ligands bridge two manganese centres together which has been crystallographically characterised.

There are two Mn1-O atom bond distances 2.329(2) Å (Mn1-O1) and a slightly longer Mn1-O2 distance of 2.412(2) Å. Previous complexes of Mn(II) containing μ_2-perchlorate bridges show the same effect of one elongated Mn-O bond and report Mn(II)···Mn(II) separations of approximately 3.8 Å. This is due to the presence of other bridging ligands holding the two Mn(II) centres closer together and subsequently contracting the bond angle of the perchlorate ligand.[86,87] In complex **2** the Mn(1)···Mn(1a) centres lie at distance of 8.565(5) Å from one another, substantially further apart than previously observed, and is due to the lack of a short contact ligand bridging the two metals together. The bond angle of the perchlorate is not contracted in this molecule, and is close to the 109° expected for a tetrahedral molecule, with a O1-Cl1-O2 angle of 108.49(14)°, with the perchlorate ligands adopting this optimal angle the Mn(II) centres are pushed away from one another.

L1 binds to a single Mn(II) centre in a tetradentate fashion, (70.44(8)°, N1-Mn1-N2; 70.37(8)°, N5-Mn1-N6) by twisting of the backbone, displaying a dihedral angle of -69.7(3)° between the benzil groups, showing the least amount of twisting of all three **L1** Mn(II) complexes. To allow for the two pyridyl nitrogen atoms to coordinate in a *trans* fashion, there is twisting of the hydrazone linker of both arms, with dihedral angles of -110.0(3)° and -103.0(3)° and this twisting aids in the coordination of **L1** to a single Mn(II) centre.

It is clear from the crystallographic studies that changing the anion source has a dramatic effect on the coordination preferences of Mn(II). With chloride anions the Mn(II) centre displays a distorted octahedral geometry (6-coordinate). Changing the anion to perchlorate resulted in Mn(II) adopting a distorted pentagonal bipyramidal geometry (7-coordinate). Both Mn(II) centres are in the high spin state, and this is indicated by the long bond lengths between donor atoms and the Mn(II) centres. The ligand arms of **L1** in both complexes bind in a bidentate fashion with very similar bite angles in both complexes. Complex **1** exhibits a large degree of twisting of the backbone and the arms of the ligand, allowing **L1** to wrap around a single metal centre. The twisting of **L1** minimises the steric strain around the Mn(II) centre. The steric strain placed upon **L1** in complex **1** is minimised in complex **2**, where there is ~10° less twisting of the backbone and

the arms of the ligand (~3° to ~35° less twisting) due to the smaller bond angle requirements of the 7-coordinate structure.

*2.2.3 Crystal structure of {[Fe(L1)(L1')]·$(BF_4)_2(CH_3CN)_2$}, Complex **3***

Crystals suitable for a single crystal X-ray diffraction study were obtained by the vapour diffusion of diisopropyl ether into an acetonitrile solution containing a 1:4 ratio of **L1** to $Fe(BF_4)_2 \cdot 6H_2O$. Single crystals were obtained after one month in a yield of 76%. Crystals were also obtained from 1:1 and 1:2, **L1**:$FeBF_4$ stoichiometry but were too small for a single X-ray diffraction study. IR spectroscopy indicated that the complexes were all identical to complex **3**. The structure of complex **3** was solved and refined in the triclinic *P*-1 space group and consists of a single Fe(II) bound to a molecule of **L1** and a rearranged ligand, **L1'**. Figure 2.5 shows the structural and selected atomic numbering scheme for complex **3**. The asymmetric unit for contains the complex, two tetrafluoroborate anions (one of which is disordered) and two acetonitrile solvent molecules per unit cell.

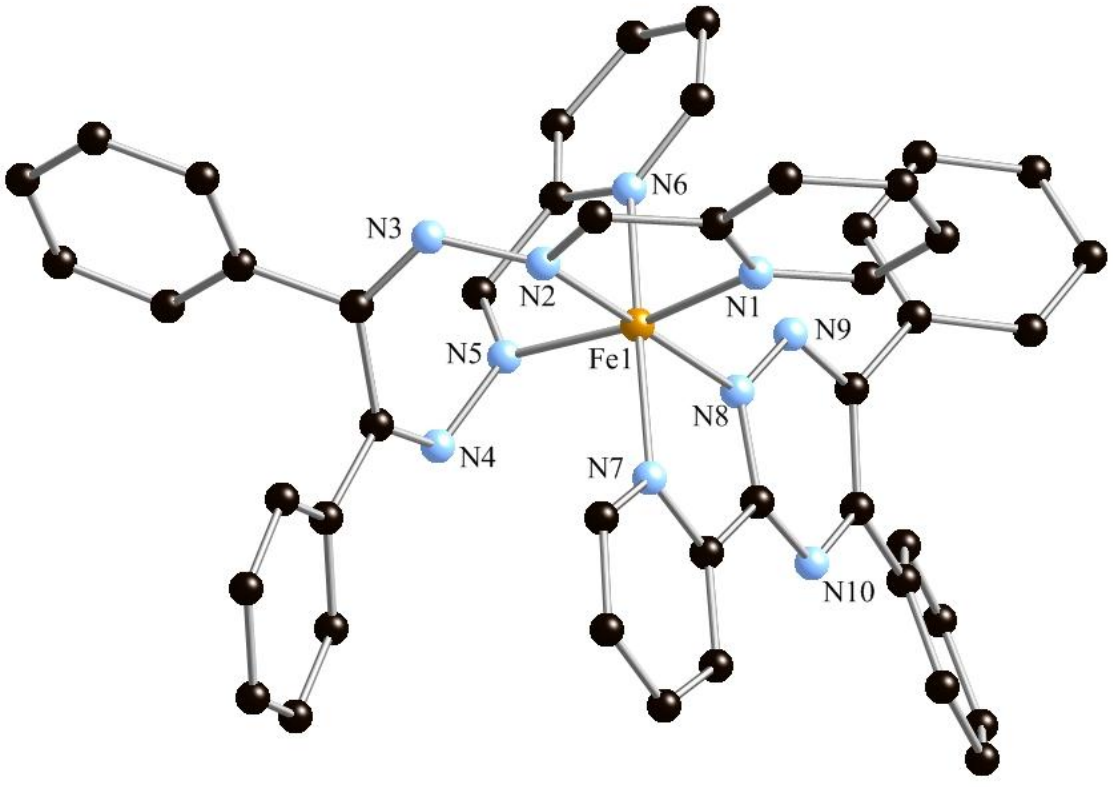

Figure 2.5 – Molecular structure and selected atomic numbering scheme for Complex **3**. Hydrogen atoms, solvent molecules and anions omitted for clarity.

The cationic complex consists of a six coordinate iron centre with the nitrogen donor atoms arranged in a distorted octahedral geometry. The degree of distortion is demonstrated by

the large ∑ value of 62.87, a large deviation from the idea value of zero for a perfect octahedral structure. The short bond lengths ranging from 1.913(3) Å to 1.973(3) Å between the nitrogen donor atoms and Fe(II) centre as well as the deep purple colour of the crystals indicates that the Fe(II) centre is in a *low-spin* state[95-99] (for full details on bond lengths and angles, see Table **2.6** in Appendix **3**).

L1 binds to the Fe(II) centre through two bidentate binding domains formed through the coordination of hydrazone and pyridyl nitrogen atoms with similar bite angles of 79.8191.(12)°, 81.38(12)°, 79.80(10)° and 81.56(9)°. The Fe-pyridyl bond lengths are nearly identical (1.970(3) Å and 1.971(3) Å) however the Fe(II)-hydrazone bond lengths display a greater variability in their lengths (1.913(3) Å and 1.953(3) Å). The shorter Fe(II)-hydrazone bond length results from a greater degree of twisting of the hydrazone linker (-101.10(4)° versus -150.20(3)°) and subsequently a greater degree of twisting of the bidentate binding domain (-9.10(3)° versus 3.50(3)°).

Coordination to a single Fe(II) centre results in reduction of twisting around the backbone, displaying a dihedral angle of -65.7(3)° when compared to the ideal angle found in the free ligand (85.9°[61], -99.5(3)).[63,65,75] This is consistent with previous studies that have found a reduction in the dihedral of the backbone of **L1** upon coordination to a metal centre.[77] As well as that observed in complexes **1** and **2.**

The second ligand (**L1'**) coordinated to Fe(II) is a 1,2,4-triazine ring, with two phenyl rings at the 4 and 5 positions and a pyridyl ring at the 3 position of the triazine ring. This ligand arises from an electrocyclic rearrangement of **L1** (see section 2.2.3.2). **L1'** is coordinated to the Fe(II) centre through the 2-nitrogen atom of the triazine ring at a length of 1.954(3) Å as well as the pyridyl nitrogen atom in a slightly longer bonding interaction of 1.973(3) Å. Coordination through these two nitrogen forms a bidentate binding domain, with a bite angle of 80.55(11)°. The shorter Fe(II)-triazine bond length arises from greater π-back bonding from the t_{2g} orbitals of the Fe(II) to the triazine π* orbitals. The two benzil groups are only slightly twisted about the C-C bond (-14.6(4)°) due to the planar nature of the aromatic triazine ring.

Changing the anion source from tetrafluoroborate to perchlorate consisting of the same stoichiometry (1:4, **L1**:$Fe(ClO_4)_2$) results in an isostructural complex. These crystals were grown by the slow vapour diffusion of benzene into an acetonitrile solution, and took approximately 6 weeks to grow (compared to three weeks taken with $Fe(BF_4)_2$). The crystal data was solved and refined in the triclinic *P*-1 space group, and the asymmetric unit contains the complex, two perchlorate anions, a single acetonitrile, water and benzene solvent molecule per unit cell and demonstrates similar bond lengths and angles to complex **3** (See Table **5** in Appendix **1** for crystal refinement data).

*2.2.3.1 ES-MS study for solution and crystal structure for $Fe(BF_4)$ and **L1***

To assess if the formation of **L1'** was immediate an ES-MS study was conducted. Crystals of complex **3** were dissolved in acetonitrile and the ES-MS scan was run immediately. A fresh solution containing an equimolar amount of $FeBF_4$ and **L1** in acetonitrile was also made up and the ES-MS scan again was run immediately. The ES-MS data for the crystal study shows evidence of two ligands, **L1** [M+H] = 417.1826 for $C_{26}H_{21}N_6$ and **L1'**, [M+H] = 311.1292 for $C_{20}H_{15}N_4$. As for the solution based study the ES-MS data only showed a peak at 417.1829, for that consisting of **L1** and no indication of the presence of the rearranged ligand, **L1'**. This indicates that the rearrangement of **L1'** does not occur immediately in solution and may occur slowly over a long period of time, as the crystals for both $Fe(ClO_4)_2$ and $Fe(BF_4)_2$ only appeared after 3 or 7 weeks respectively.

*2.2.3.2 Electrocyclic rearrangement of **L1** forming **L1'***

In organic chemistry electrocyclic reactions are an important class of reactions which are defined as: "*the formation of a new σ bond across the ends of a conjugated polyene or the reverse*"[71] and such reactions are also possible with C=C-C=C-C=N systems. Datta and co-workers observed the results of the rearrangement in the crystal structure of $[Ru(C_6H_6)(\mathbf{L1'})(Cl]^+$, when **L1** was refluxed with $[Ru(C_6H_6)Cl_2]_2$ in methanol.[75,76]

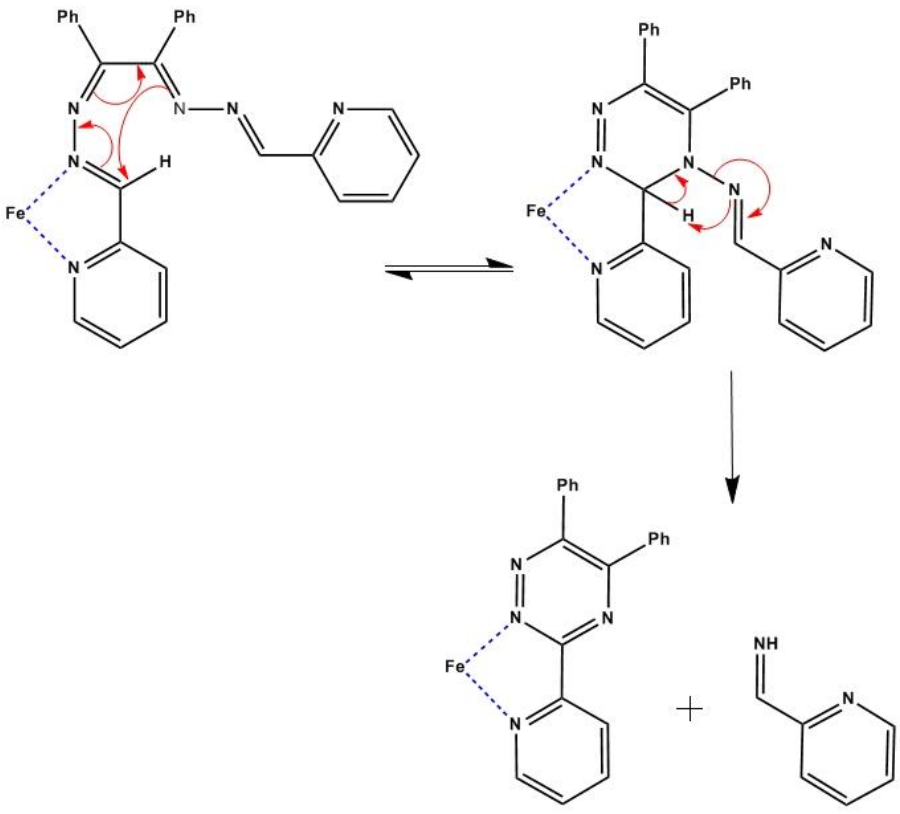

Figure **2.6** – Proposed mechanism for the formation of **L1'** from **L1**.[75,76]

As outlined in Figure 2.6, the first step involves the coordination of Fe(II) to a single bidentate binding domain (formed between the pyridyl nitrogen atom and a hydrazone nitrogen atom) of **L1**. This is followed by reorientation of the *p* orbitals, specifically aligning the HOMO and LUMO between the two carbon atoms where the new σ-bond is formed. After the new bond is formed the reaction is reversible, where breaking the newly formed σ-bond will restore aromaticity to the system. However, the reverse step does not occur and it is thought that the reaction progresses through the final step because this does not involve breaking a strong C-C bond, but a weak N-N bond, while the driving force of restoring aromaticity to the system remains.[75,76] Steric congestion around the Fe(II) centre due to the coordination of **L1'** prohibits the alignment of the HOMO and LUMO through bond rotation and thus prohibits a second electrocyclic rearrangement of **L1**.

*2.2.4 Crystal structure of , Complex **4***

Crystals suitable for a single crystal X-ray diffraction study were obtained by the slow evaporation of an acetonitrile solution containing an equimolar amount of **L1** and $CoCl_2 \cdot 6H_2O$. A yield of 76% of deep red crystals was obtained overnight. The structure for complex **4** was solved and refined in the triclinic *P*-1 space group. The atomic structure and selected numbering scheme for complex **4** is shown in Figure 2.7**.** The asymmetric unit contains two mononuclear neutral complexes, three acetonitrile solvent molecules and a partially occupied water molecule.

The geometry of both complexes with respect to the Co(II) centre is best described as a distorted octahedral structure. This is indicated by the *cis* bond angles ranging from 72.61(19)° to 112.50(19)° (Co1) and 71.41(18)° to 18.70(19)° (Co2), fluctuating greatly from the 90° expected for an ideal octahedral structure and results in the $\sum$ values of 125.25 (Co1) and 119.43 (Co2). Furthermore the three *trans* angles observed in both complexes vary considerably from the 180° expected for a perfect octahedral structure. Both complexes exhibit elongated Co-donor atom bond lengths ranging from 2.178(5) Å to 2.354(17) Å (Co1) and 2.166(5) Å to 2.238(16) Å (Co2) indicative of a high spin Co(II) complex[82,100] (for full details on bond lengths and angles see Table **2.7** in Appendix **3**).

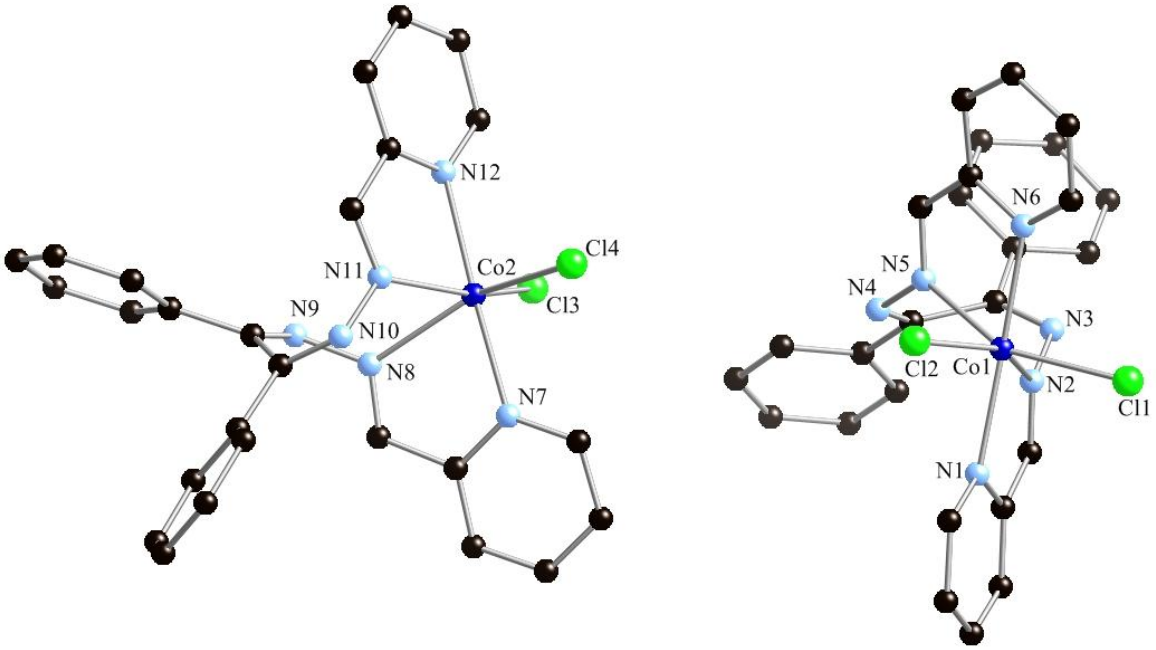

Figure 2.7 – Molecular structure and selected atomic numbering scheme for complex **4**. Hydrogen atoms, solvent atoms and carbon numbering omitted for clarity.

Each arm of **L1** binds to the Co(II) centre in both complexes through two bidentate chelating binding domains formed by the coordination of the pyridyl nitrogen atom and a hydrazone nitrogen atom with bite angles of 73.60(19)° (N1-Co1-N2), 72.61(19)° (N5-Co1-N6) and 73.33(19)° (N7-Co2-N8), 74.01(19)° (N11-Co2-N12). Significant twisting of the backbone (55.6(6)°, Co1 and 56.6(6)°, Co2) allows for **L1** to wrap around a single Co(II) centre. In addition to twisting of the backbone there is also twisting of the hydrazone bond of each arm of **L1** (which is flat in the free ligand[63,65,75]) displaying dihedral angles of 90.5(6)°, 98.7(6)° for Co1 and 84.2(6)°, 83.4(6)° for Co2. However the twisting of the ligand results in a single elongated Co-hydrazone nitrogen atom bond in each complex (2.234(5)°, Co1-N5; 2.250(5)°, Co2-N8), as well as a slight twist of binding domain (5.8(6)° vs 10.3(7)° in Co1; 5.2(6)° vs 8.7(6)° in Co2).

Complex **4** contains several significant π interactions influencing the packing of the structures in the crystal lattice. There is an offset face to face π-stacking interaction between two identical pyridyl rings with a centroid to centroid distance of 3.508(7) Å, a pyridyl C-H···π interaction with a benzil ring, with a C-H to centroid distance of 3.343(7) Å as well as an benzil to benzil C-H···π interaction with a C-H to centroid distance of 3.463(7) Å and an edge to face interaction between two benzil groups with a distance of 3.553(8) Å.

*2.2.5 Crystal structure of {[Co(L1)(NO_3)$_2$]·CH_3CN}, Complex **5***

Crystals suitable for a single crystal X-ray diffraction study were obtained by vapour diffusion of diisopropyl ether into a acetonitrile solution containing an equimolar ratio of **L1** and $Co(NO_3)_2·6H_2O$ and a yield of 75% was obtained after 3 weeks. The structure for complex **5** was refined and solved in the monoclinic $P2_1/c$ space group and the molecular structure and selected atomic numbering scheme is shown in Figure 2.8. The asymmetric unit contains a neutral complex and a single acetonitrile solvent molecule.

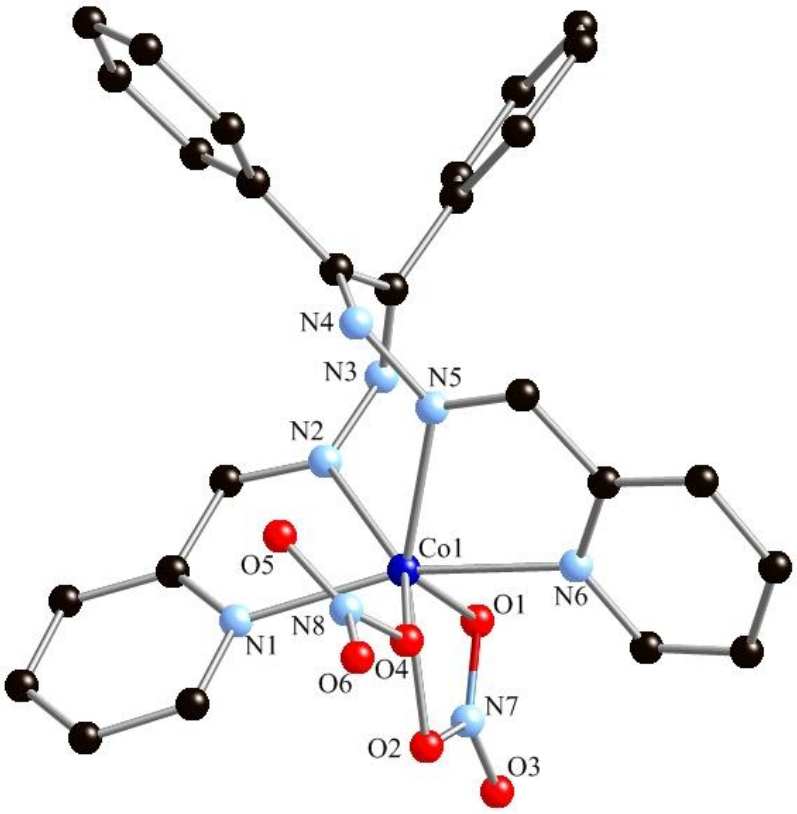

Figure 2.8 - Molecular structure and selected atomic numbering scheme for complex **5**. Hydrogen atoms, solvent atoms and carbon numbering omitted for clarity.

Complex **5** exhibits elongated Co-N and Co-O bond lengths ranging from 2.295(13) Å to 2.127(12) Å, indicative that the Co(II) centre is again in a high spin state.[82,100] Changing the ancillary ligand from chloride to nitrate results in the dispersal of donor atoms in a distorted pentagonal bipyramidal arrangement, brought on by the bidentate coordination of one of the nitrate ligands. This is demonstrated by the angles between donor atoms in the equatorial plane ranging from 55.99(5)° to 89.80(5)° where for an ideal pentagonal bipyramidal structure this angle is 72° and gives a $\sum$ value of 34.78. The expected equatorial to axial donor atom angles are expected to be 90° however in complex **5** these interactions range from 73.20(5)° to 125.23(5)°. Finally the axial-axial donor atom angle in complex **5** is 161.48(5)° (N1-Co1-N6), which in an ideal pentagonal bipyramidal arrangement this angle would be 180° (for full details on bond lengths and angles see Table **2.8** in Appendix **3**).

The distortion of the geometry arises from the enforced binding angles of the three bidentate binding domains of 55.99(5)° (O1-Co1-O2), 73.20(5)° (N1-Co1-N6) and 73.71(5)° (N5-Co1-N6). As seen with complex **4**, complex **5** exhibits a large degree of twisting to allow both arms of **L1** to bind to a single Co(II) centre. This is demonstrated by twisting of the backbone (62.21(16)°) and a large degree of twisting of the hydrazone bond of both arms of **L1**, with dihedral angles of 113.72(15)° and 104.23(15)° and both of these binding domains are relatively flat with dihedral angles of 0.51(16)° (N1-C5-C6-N2) and 3.63(16)° (N5-C21-C26-N6).

Complex **5** contains two significant π interactions that influence the crystal packing of the structure. There is an edge to face interaction with a distance of 3.586(19) Å and an C-H···π interaction with a C-H to centroid distance of 3.571(2) Å.

Changing the ancillary ligand from a monodentate to bidentate chelating ligand has a profound effect on the nature of the Co(II) centre. Where the ancillary ligand is chloride (complex **4**) the Co(II) centre adopts a distorted octahedral geometry. Changing the anion to nitrate (bidentate) leads the Co(II) centre to adopting a seven coordinate, pentagonal bipyramidal geometry due to the chelating nature of the ancillary ligand. Co(II) in complexes **4** and **5** adopts a high spin electron configuration, which is evident from the long bond lengths in both complexes. As seen in the previous sections for **L1** coordination studies, **L1** is able to bind to a single metal centre by twisting of the backbone and arms binding in a bidentate fashion. Complexes **1** and **2** showed that changing the coordination geometry from 6- to 7-coordinate resulted in less steric strain on the ligand, evident from less twisting of backbone (55.6(6)° and 56.6(6)° for complex **4** and 62.21(16)° for complex **5**) and the arms of **L1**.

*2.2.6 Crystal structure of {[$Cu_2(L1)_2$]·$(BF_4)_2$}, Complex **6***

Crystals suitable for a single X-ray diffraction study were synthesised by the vapour diffusion of diisopropyl ether into an acetonitrile solution containing an equimolar ratio of $Cu(BF)_2 \cdot xH_2O$ and **L1**. A yield of 73% of orange crystals were obtained after 4 weeks. The structure for complex **6** was solved and refined in the monoclinic *C*2/*c* space group. The asymmetric unit consists of a ligand of **L1** bound to two Cu(I) metal centres and a single tetrafluoroborate anion. Figure 2.9 shows the molecular structure of complex **6**, where the full molecule is related by an C_2 symmetry element, where the rotation axis lies along the axis between the two Cu(I) metal centres.

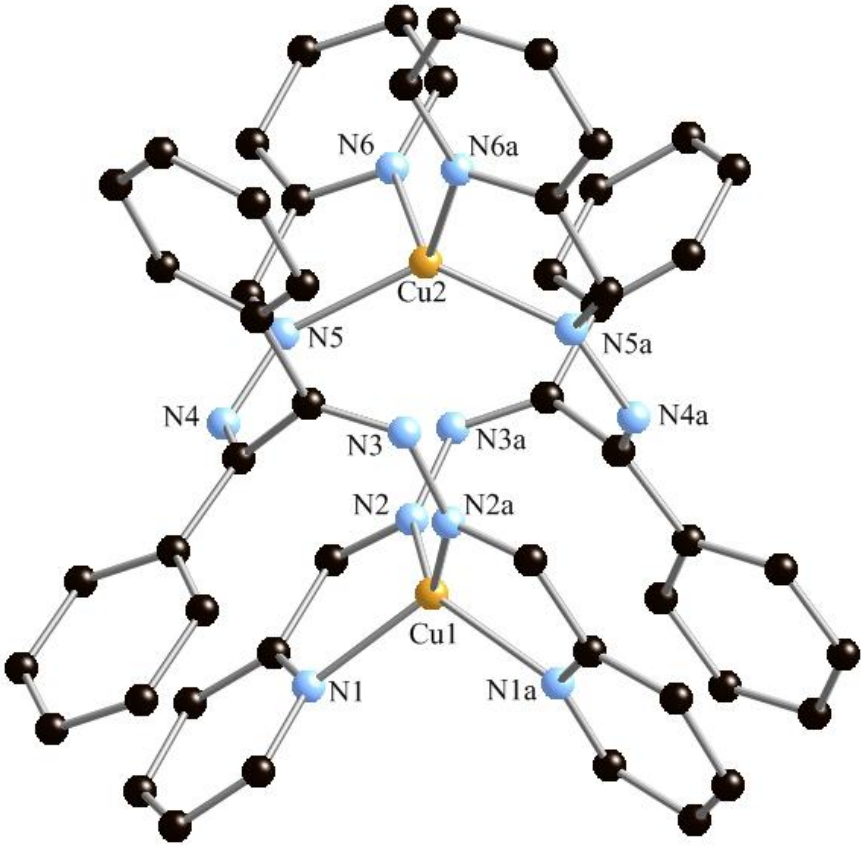

Figure 2.9 – Molecular structure and selected atomic numbering scheme of complex **6**. Equivalent atoms generated by the symmetry code: (1-x,+Y,3/2-z)[a]. Hydrogen atoms and anions omitted for clarity.

Both Cu(I) centres display a distorted tetrahedral geometry, shown by the τ_4 values of 0.85 for both Cu1 and Cu2 metal centres, using the bond angles determined between equivalent pyridine donor atoms and equivalent hydrazone donor atoms. **L1** binds through each arm to a Cu(I) centre in a bidentate fashion through the pyridine and hydrazone nitrogen atoms. The distortion of the metal centres arises from the enforced binding angle placed on the metal centre by the bidentate binding domains, exhibiting similar bite angles of 81.25(9)° (N1-Cu1-N2), 82.92(10)° (N5-Cu2-N6), far from the ideal 109.5° expected for an ideal tetrahedral geometry. For full details on bond lengths and angles see Table **2.9** in Appendix **3**.

Coordination to two metal centres is achieved by slight twisting of the backbone (-87.90(3)°), stopping the two arms from folding upon one metal centre. Each of the hydrazone arms is reasonably flat, with dihedral angles of 168.00(3)° and 163.40(2)° contributing to the formation of a structure which is best described as a *saturated homotopic dinuclear double helicate*. Figure 2.10 shows two molecules of complex **6**, showing the opposite handedness of the helices.

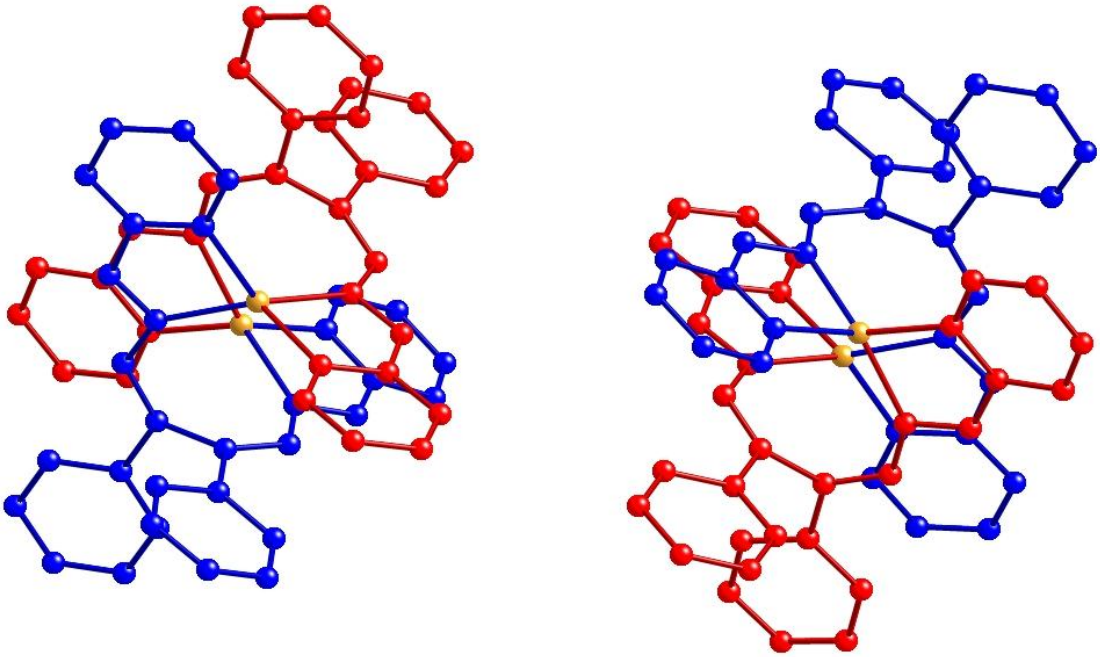

Figure 2.9 – The two handed helicates of $[Cu_2(\mathbf{L1})_2]$. Figure 2.10 right - right-handed helicate (P = Δ). Figure 2.10 left - left-handed helicate (M = Λ).

Complex **6** contains two weak intermolecular offset face to face π-π-interactions at 3.837(17) Å and 4.031(2) Å, between pyridine and benzil groups and aiding in stabilizing the discrete species. The packing of the molecules in the crystal lattice is influenced by two offset face to face π-stacking interactions, linking two helices of the same handedness to one another, at a distance of 3.848(17) Å, forming an infinitely linked helix. These chains are neighboured by like-handed helices, with opposite handed helicates separated by a channel, which is filled by tetrafluoroborate anions.

Complex **6** is isostructural to a dinuclear double helicate synthesised and crystallographically characterised by Drew and co-workers. This helicate was synthesised using a Cu(I) starting material,[63] whereas the copper source used for the synthesis of complex **6** is in a 2+ oxidation state. Reduction of Cu(II) is due to the reaction occurring in acetonitrile. Complex **6** shows the smallest amount of twisting of the backbone and arms of **L1** due to the bis-bidentate binding nature of **L1** observed in complex **6**.

*2.2.7 Crystal structure of {[Zn(L1)(NO$_3$)$_2$]·CH$_3$CN}, Complex **7***

Crystals suitable for a single crystal X-ray diffraction study were grown by vapour diffusion of diisopropyl ether into a acetonitrile solution containing a equimolar amount of $Zn(NO_3)_2 \cdot 6H_2O$ and **L1**. After 2 weeks a yield of 79% of yellow crystals were obtained. The structure for complex **7** was solved and refined in the monoclinic $P2_1/c$ space group, the

molecular structure and selected atomic numbering scheme is shown in Figure 2.11. The asymmetric unit contains a single Zn(II) complex and one acetonitrile solvent molecule.

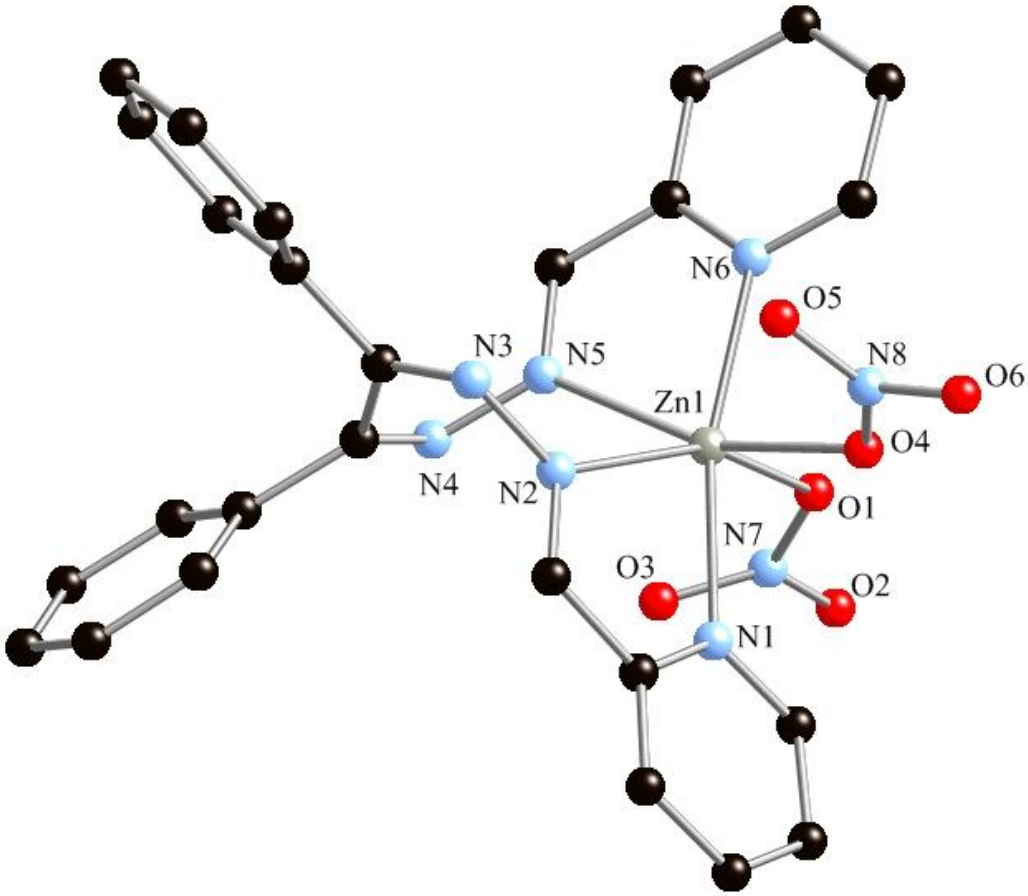

Figure 2.11 – Structure of complex **7** showing the selected atomic labelling. Hydrogen atoms and solvent molecules omitted for clarity.

The coordination sphere of the distorted octahedral Zn(II) complex contains four nitrogen donor atoms from **L1** (Zn-N bond lengths ranging from 2.1645(15) Å to 2.2330(14) Å) and two oxygen atoms from two nitrate ligands (2.0947(12) Å, Zn1-O1; 2.1137(12) Å, Zn1-O2). The geometry about the Zn(II) centre is best described as a distorted octahedral structure, exhibiting a distortion parameter of $\Sigma = 140.48$. The distortion arises due to the enforced bond angles upon the metal centre by the coordination of **L1**. This is shown by the small bond angles of 73.77(5)° (N1-Zn1-N2) and 74.01(5)° (N5-Zn1-N6) enforced by the bidentate binding domains, which are greatly deviated from the 90° in a perfect octahedral structure. The nitrate ligands, which are not constrained in their binding mode to Zn(II) are able to adopt a more ideal *cis* binding angle of 92.41(5)° (O1-Zn1-O2) and this demonstrates the degree of restriction placed upon the ideal bond angles of Zn(II) by **L1**.

As seen previously both arms of **L1** are able to coordinate to a single metal centre by rotation about the backbone and hydrazone bond, displaying a dihedral angle of 61.01(16)°

between the pyridyl groups and 101.96(16)°, 102.54(17)° for the hydrazone linkers, which are significantly twisted when compared to the angles observed in the free ligand.[61,63,65] See Table **2.10** in Appendix **3** for further details on bond lengths and angles.

The packing of the molecules of complex **7** in the crystal structure are influenced by several weak π-interactions, with three edge to face interactions at 3.570(19) Å, 3.578(19) Å, 3.742(19) Å each, as well as an offset face to face interaction at 3.670(19) Å.

In complex **5** the nitrate anion forces the geometry of the Co(II) centre into a 7-coordinate pentagonal bipyramidal structure. However in complex **7** this effect is not seen as the non-bonding oxygen atoms of the nitrate ligand lie at 3.04 Å and 3.08 Å from the Zn(II) centre. Interestingly the backbone and the hydrazone arms in complex **7** show the least amount of twisting of all the 6-coordinate complexes, and this is why the Zn(II) centre does not form a seven coordinate structure to minimise the steric strain place on **L1**.

2.3 Conclusion

The results with **L1** in this study have added to the library of complexes between **L1** and various transition metals, as well as providing interesting and unique results. **L1** shows the preference to form mononuclear complexes brought on by significant twisting of the backbone and the hydrazone bonds of both arms of the ligand. Changing the anion source for Mn(II) from chloride to perchlorate results in an increase in the coordination number of Mn(II) from six to seven. The same effect is seen when the metal salt source is changed from $CoCl_2$ to $Co(NO_3)_2$. Reaction with $Mn(ClO_4)_2$ has given rise to the first structurally characterised complex which contains two Mn(II) centres bridged by only μ_2-ClO_4 groups. Combining Zn(II) with **L1** gives rise to a mononuclear octahedral structure, however, less twisting of the ligand is not required for the formation of this octahedral structure.

Adding to results observed previously in the literature, Cu(II) is reduced to Cu(I) in solution and gives rise to a *saturated dinuclear double helicate* that is isostructural to that found previously in literature.[63] Using both $Fe(BF_4)_2$ and $Fe(ClO_4)_2$ results in a slow room temperature electrocyclic rearrangement of **L1**, an effect previously obtained by refluxing **L1** with Ru(II)[75,76].

Chapter 3

Bis-2-imidazolyliminohydrazono-1, 2-diphenylethane, L2

3.1 Synthesis and characterisation of *Bis-2-imidazolyliminohydrazono-1, 2-diphenylethane,* L2

L2 has previously been synthesized and structurally characterised in the Kruger research group,[73] however the data is not published currently in literature. The original preparation of the ligand has been modified in this study, to achieve a greater yield of product. To a methanolic solution of benzil dihydrazone containing four drops of acetic acid, two molar equivalents of imidazole-2-carbaldehyde was added and the resulting cloudy white solution was stirred at reflux overnight resulting in a clear bright yellow solution. The solvent was evaporated under vacuum until a small amount of yellow precipitate appeared and the solution was refrigerated for 4 days, to give a pale yellow powder at 92% yield. Micro analytical data was consistent with the proposed structure. ES-MS indicated a molecular ion (*m/z* = 395.4481), which is expected for the protonated species [**L2 + H**]$^{+}$. IR spectroscopy indicated a stretch at 1619 cm^{-1} which confirms the presence of an imine group, and the ^{1}H NMR data are consistent with the proposed structure (Figure 3.1).

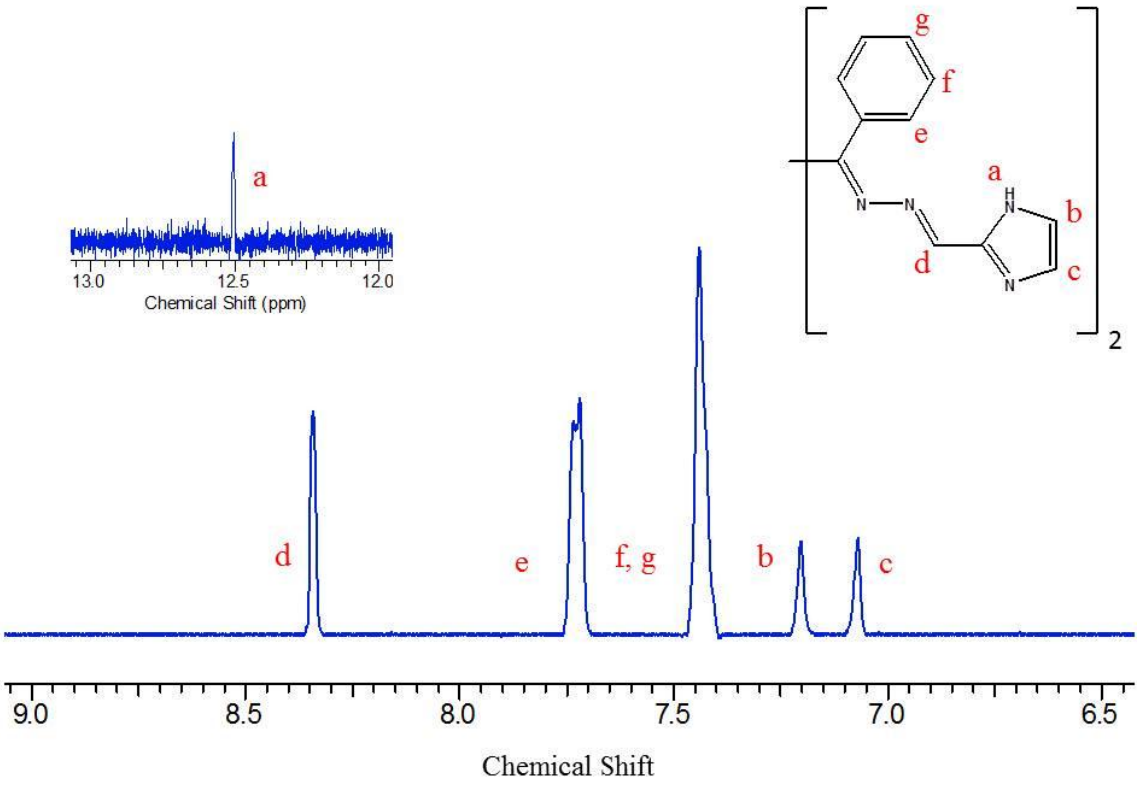

Figure 3.1 - ^{1}H NMR spectrum and peak assignment of **L2** (DMSO). ^{1}H NMR run at 400 MHz, protons b and c determined by 1D NOESY experiment.

The crystal structure of **L2** is consistent with that found previously in the Kruger research group (Figure 3.2).[73] As noted previously for similar ligands there is a twist of the backbone between the two arms of the ligand, brought on by a steric repulsion of the benzil groups on the

backbone, and is demonstrated by a dihedral angle of 91.19(11)°. This is the smallest observed dihedral angle when compared with literature for similar ligand structures.[61,63,65,67] **L2** contains two potential *cis* binding domains brought about by the orientation of a hydrazone nitrogen atom (N3, N6) and either a imidazole nitrogen atom (N2, N7) or subsequent deprotonation of the second nitrogen atom (N1,N8).

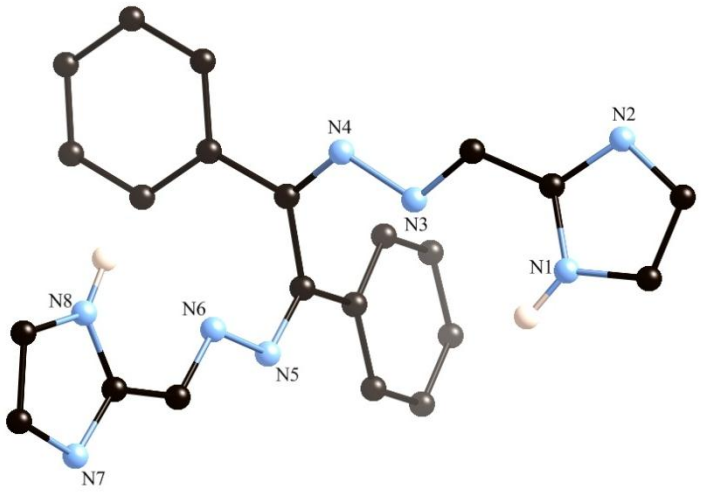

Figure 3.2 – Crystal structure of **L2**, as previously determined in the Kruger group.[73]

3.2 Synthesis and characterisation of complexes with Bis-2-imidazolyliminohydrazono-1, 2-diphenylethane, L2

3.2.1 C*rystal structure of {[Mn(L2)$_2$]·(ClO$_4$)$_2$(H$_2$O)$_4$CH$_3$CN}, Complex **8***

Crystals suitable for a single crystal X-ray diffraction study were grown by the slow diffusion of toluene into an acetonitrile solution containing an 1:2 ratio of **L2** to Mn(ClO$_4$)$_2$·xH$_2$O. Crystals of suitable size for data collection were grown at room temperature for 6 weeks and isolated in a yield of 33%. The structure for complex **8** was solved and refined in the tetragonal *P*4/*mnc* space group. Solvent disorder was attempted to be modelled however, Platon Squeeze[101] was required to remove residual electron density due to the large solvent accessible void of 182 Å^3. The asymmetric unit shows a single Mn(II) centre bound to half a molecule of **L2**, two water molecules, two partially occupied perchlorate anions and a disordered solvent molecule of acetonitrile. The full structure of complex **8** is realised by a 2-fold roto-inversion centre which lies through the backbone and Mn(II) centre. The molecular structure and the selected atomic labelling scheme of complex **8** are shown in Figure 3.3.

The four coordinate coordination sphere of the Mn(II) ion is completed by the coordination of four symmetry related imidazole nitrogen donor atoms, from two molecules of **L2**, at a long distance of 2.233(6) Å indicative of a high spin Mn(II) centre.[80-82] The arrangement of the donor atoms around the Mn(II) centre is best described as a square planar arrangement with a small τ_4 value of 0.0695 arising from the nearly ideal *trans* angle of 175.10° between imidazole donor atoms. The square planar nature of complex **8** arises from significant twisting of the backbone (-63.7(5)°) and hydrazone linker (-106.5(7)°) which results in the hydrazone nitrogen atom lying a distance at 2.751(6) Å from the Mn(II) centre and therefore a distance too long to form a reasonable Mn1-N3 coordination bond.

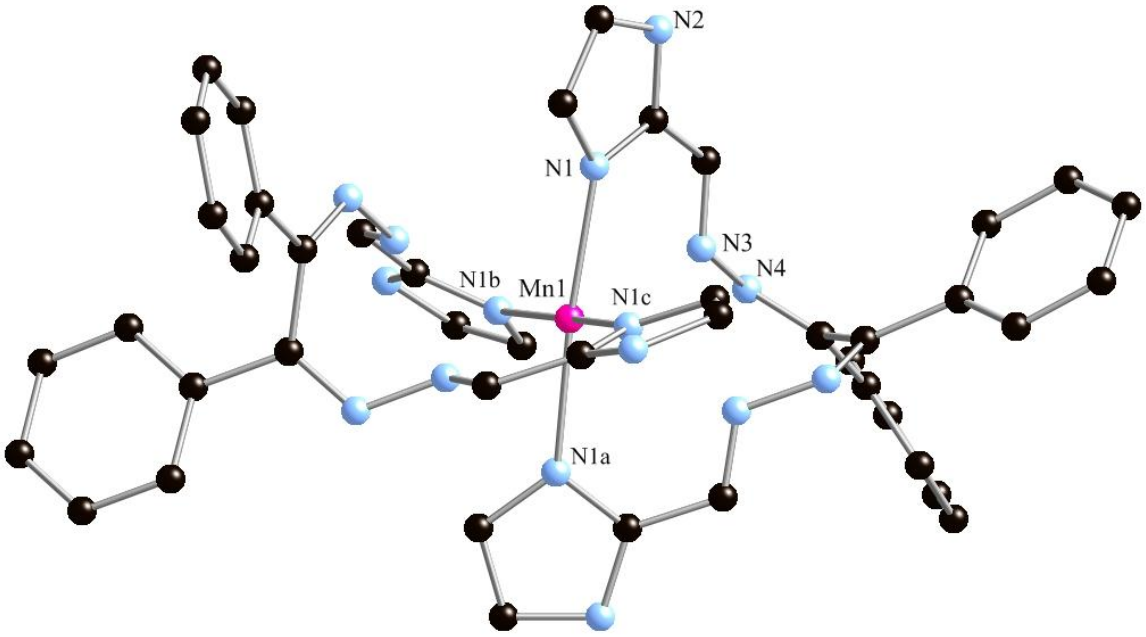

Figure 3.3 – Molecular structure of complex **8** generated by a 2-fold roto-inversion centre with selected atomic labelling. Symmetry code used to generate equivalent atoms: (1/2-x, 1/2 - y, 3/2-z)[a],(-1/2+x, -1/2+y, 3/2-z)[b],(1-x, -y, +z)[c]. Hydrogen atoms, solvent molecules and anions omitted for clarity.

Previous research has demonstrated manganese forming a square planar structure. Morris and co-workers formed a discrete mononuclear Mn(III) square planar complex when combining $Mn(acac)_3$ with an excess of methyl lithium[102]. Salavati-Niasari and co-workers have immobilised square planar Mn(II) coordinated to bis(2-mercaptoanil)benzil on alumina to catalyse the oxidation of cyclohexene with *tert*-buthylhydroperoxide and hydrogen peroxide.[103,104] The crystal structure of Mn(II) in a square planar geometry has been also determined in a tetranuclear Mn(II) cluster,[105] and acts as the central bridge between two macrocycles, with each ligand encapsulating a Cu(II) centre each.[106] Complex **8** demonstrates a discrete square planar Mn(II) complex.

Binding to Mn(II) through N1, allows the non-coordinating nitrogen atom to act as a proton donor, and this is demonstrated by two weak hydrogen bonds formed with the water molecules available in the asymmetric unit, with a proton donor to acceptor distance of 2.957(19) Å and 2.862(15) Å. These weak non-covalent binding interactions occur at all four available hydrogen donors in complex **8**, exhausting the hydrogen bonding capabilities of the imidazole nitrogen atoms. Hydrogen bonding aids in the packing of adjacent molecules of complex **8,** with the water molecules again involved as a proton acceptor forming two hydrogen bonding interactions between two discrete assemblies (Figure 3.4). In addition to hydrogen bonding influencing the packing of the crystal lattice there is also a single CH-π interaction at a distance of 3.512(9) Å between two equivalent benzil rings. See Table **3.7** in Appendix **3** for full details for hydrogen bonding parameters.

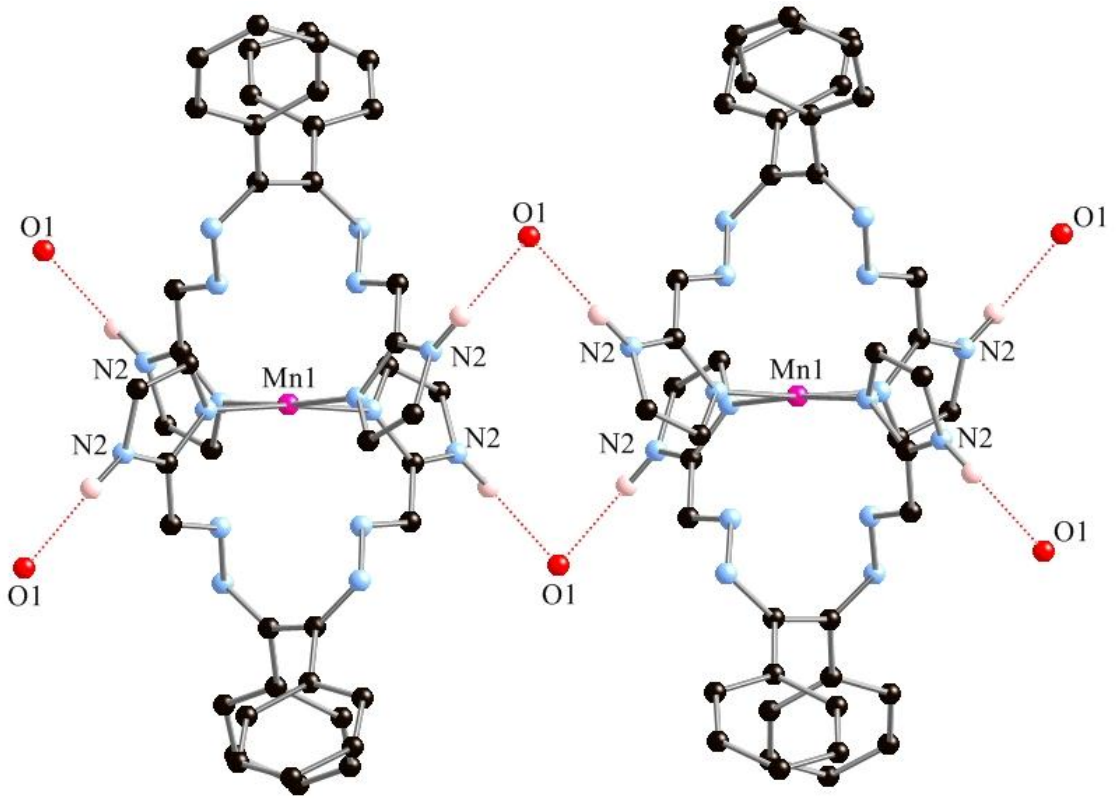

Figure 3.4 – Hydrogen bonding observed in complex **8**, linking two molecules together and exhausting all the sp^3 imidazole nitrogen proton donors. Non-hydrogen bonding hydrogen atoms omitted for clarity.

Figure 3.5 shows the space filling diagram of complex **8**. This diagram clearly shows how the Mn(II) centre is encapsulated by the two ligands, and does not allow space for any potential ancillary ligands to be able to bind to the hidden Mn(II) centre. The encapsulation of the metal, as well as the large distance between Mn(II) and the hydrazone nitrogen atom, brought about by the twisting of the backbone explains why the Mn(II) centre adopts a four coordinate, square planar structure.

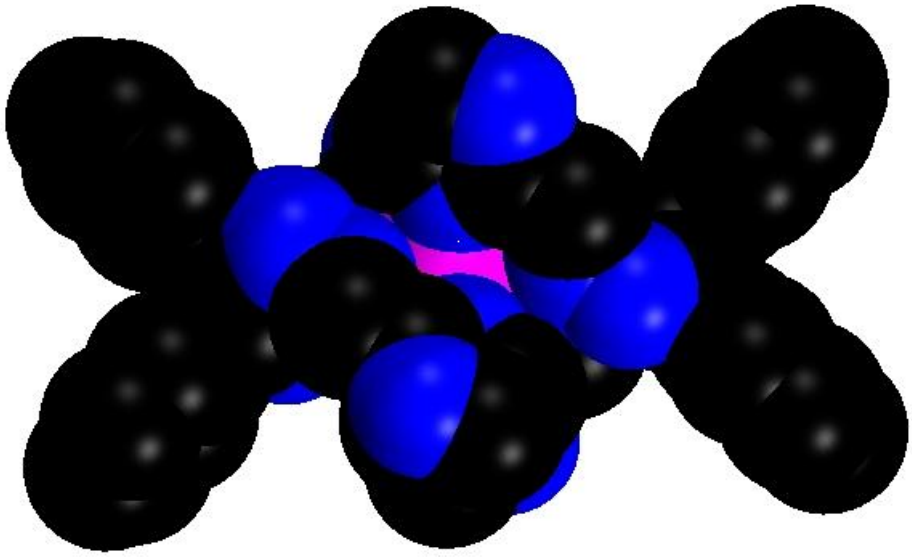

Figure 3.5 – Space filling diagram of complex **8** showing the encapsulation of the Mn(II) centre by two ligands of **L2**.

Changing the head group of the ligand from 2-pyridine (**L1**) to 2-imidazole (**L2**) results in a clear change in the nature of the structure formed. When pyridine is used, there is a large degree of twisting of the backbone and hydrazone arms, allowing **L1** to coordinate to a single metal centre, in a tetradentate fashion, resulting in either a octahedral (complex **1**) or pentagonal bipyramidal (complex **2**) structure, where the coordination sphere is satisfied by the coordination of ancillary ligands. Changing to imidazole results in **L2** binding in a bidentate fashion through two arms of the ligand, and the coordination sphere of Mn(II) is only satisfied by the presence of two ligands, encapsulating Mn(II) and blocking any ancillary ligands from binding to Mn(II). Upon changing the head group from pyridine to imidazole, the size of the bidentate binging domain increases due to the size of the head group decreasing by one atom.

*3.2.2 Crystal structure of {[$Ni_2(L2)_2(OH_2)_6$]·$(NO_3)_4(H_2O)_2CH_3CN$}, Complex **9***

Crystals suitable for a single X-ray diffraction study were synthesised by the slow evaporation of an acetonitrile solution over several days consisting of an equimolar amount of **L2** and $Ni(NO_3)_2{\cdot}6H_2O$ isolated in a yield of 40%. The structure for complex **9** was solved and refined in the monoclinic $P2_1/n$ space group. The asymmetric unit consists of a Ni(II) centre bound to an imidazole nitrogen atom and three water molecules, making up half the molecular structure of complex **9**. There are also two disordered nitrate anions, a disordered water molecule and half an acetonitrile solvent molecule per asymmetric unit. Figure 3.6 shows the molecular

structure of complex **9**, with selected atomic labelling scheme. The full structure of complex **9** is derived by an inversion centre which lies between the two Ni(II) centres.

The coordination sphere of Ni(II) is occupied by three nitrogen donor atoms from **L2** and three water molecules (2.064(4) Å – 2.076(4) Å) in a geometry which is best described as a slightly distorted octahedral geometry, indicated by the Σ value of 43.33. **L2** binds in a heterotopic fashion bridging two Ni(II) centres together. One arm of **L2** binds in a monodentate fashion at a distance of 2.045(5) Å (Ni1-N8) through the imidazole nitrogen atom only. The other arm binds to the second Ni(II) centre in a bidentate fashion, displaying significantly different bond lengths from one another, with the imidazole nitrogen atoms binding at a distance of 2.076(4) Å and the hydrazone nitrogen atom at 2.165(5) Å. This large distance is brought on by a combination of effects; firstly the backbone does not significantly twist when compared to the 'free' ligand crystal structure, with a dihedral angle of 97.90(5)° between benzil groups. Secondly the hydrazone linker undergoes significant twisting (168.9(5)° for the bidentate binding domain arm and 110.6(5)° for the monodentate binding arm) to form a reasonably flat bidentate binding site (7.7(7)°). Finally the desire for the Ni(II) to adopt an octahedral geometry with minimal distortion forces the ligand to bind in a more idealized fashion. See Table **3.8** in Appendix **3** for bond lengths and angles.

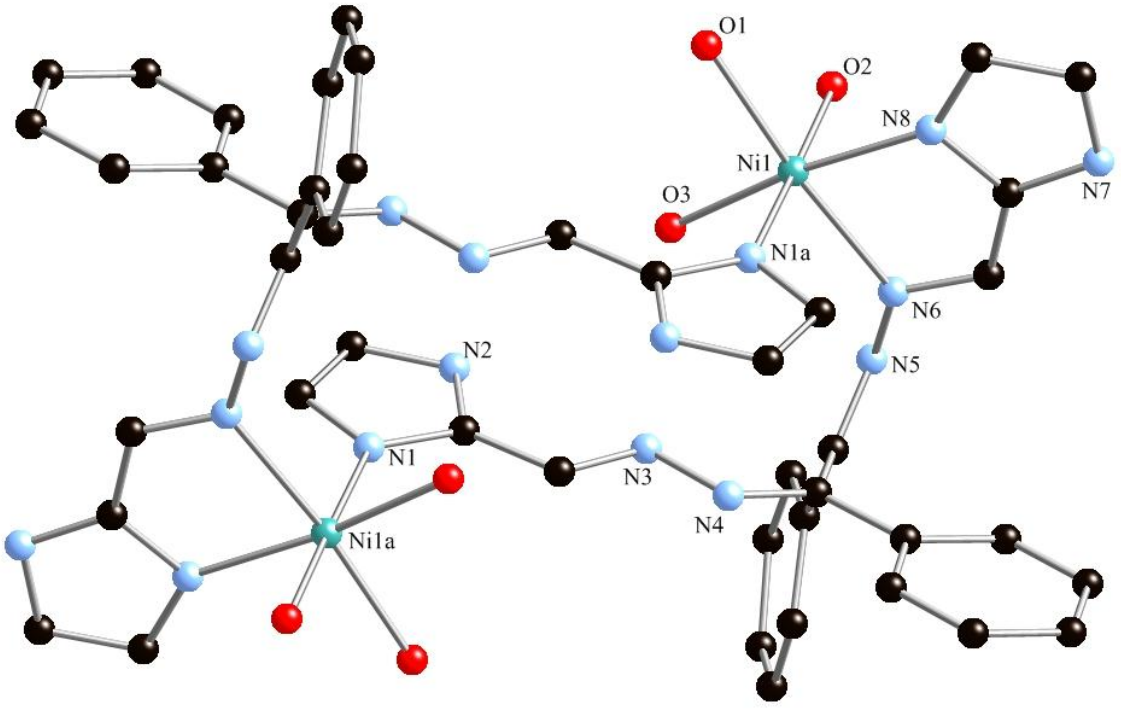

Figure 3.6 – Full molecular structure of complex **9** derived by a central inversion centre, with selected atomic labelling. Equivalent atoms generated by the symmetry code: (1-x,1-y,1-z)[a]. Hydrogen atoms, anions and solvent molecules omitted for clarity.

Binding through the non-protonated nitrogen atom of the imidazole group frees the protonated nitrogen atom to act as a proton donor and all four of these atoms act as excellent proton donors in weak hydrogen bonding interactions with the disordered nitrate anions (donor to acceptor distances ranging from 2.758(13) Å to 2.980(4) Å). The water ligands also act as proton donors forming weak hydrogen bonding interactions with the disordered nitrate oxygen atom acting as a proton acceptor with donor to accepter interactions ranging from 2.640(2) Å to 3.049(10) Å, and a disordered nitrate nitrogen atom (3.070(5) Å) acting as a proton acceptor. A disordered nitrate nitrogen atom links two water ligands and an imidazole head group together through a weak hydrogen bonding network. See Table **3.4** in Appendix **2** for full details on hydrogen bonding parameters.

Linking two molecules of complex **8** is a weak offset face to face π-interaction between a benzil group and imidazole at a distance of 3.828 (3) Å and an edge to face interaction at 3.675(7) Å between two benzil groups. Hydrogen bonding also assists in the arrangement of molecules in complex **8**, with a disordered nitrate linking two molecules together, with two disordered oxygen atoms acting as a proton acceptor to the imidazole nitrogen atom proton donor on one molecule (N7-H7···O9, 2.800(2) Å; N7-H7···O10 (2.758(13) Å). A single oxygen atom on the nitrate links to the second molecule with a water ligand and completing the bridge (O1-H1···O8, 3.049(10) Å).

*3.2.3 Crystal structure of {[$Co_2(L2)_2(NO_3)_4$]·($CH_3CN)_4$}, Complex **10***

Crystals suitable for a single crystal X-ray diffraction study were synthesised by the slow diffusion of diisopropyl ether into a acetonitrile solution containing an equimolar amount of $Co(NO_3)_2·6H_2O$ and **L2**. Crystal growth took two weeks, however, crystals were not stable out of solution and decomposed into an orange oil. The crystal data was solved and refined in the monoclinic $P2_1/n$ space group. The asymmetric unit consists of half a molecule of complex **10** and two acetonitrile solvent molecules. The full structure is derived by an inversion centre which lies in the middle of the molecule, and the full molecular structure with selected atomic labelling is shown in Figure 3.7.

The Co(II) coordination sphere consists of three nitrogen atoms (2.072(16) Å – 2.2085(15) Å) and three oxygen atoms (2.111(14) Å – 2.199(13) Å) dispersed in what is best described as a trigonal prismatic geometry, where $\sum = 126.76$, far from the ideal value of zero for a perfect octahedral structure. This geometry arises from the two small chelate bond angles formed by a nitrate ligand (60.00(5)°, O1-Co1-O2) and one arm of **L2** (76.96(6)°, N6-Co1-N7) which is significantly smaller than the 90° required for a perfect octahedral structure. The long bond lengths of complex **10** as well as the dark red colour of the crystals indicate that the Co(II) centre is in a high spin state.[82,100]

The arms of **L2** adopts two different binding modes in complex **10**, with one arm showing very little twisting (177.20(17)°) and coordinating through the imidazole nitrogen atom in a monodentate fashion. The second arm binds to a second Co(II) centre in a bidentate fashion, and undergoes a significant amount of twisting (-105.66(18)°) to correctly align the molecular orbitals (containing a lone pair of electrons) of the hydrazone and imidazole nitrogen atoms to form a bidentate binding domain. The backbone shows a very small degree of twisting (-95.31(17)°) when compared to the dihedral found in the free ligand structure (91.19(11)°. See Table **3.9** in Appendix **3** for full details on bond lengths and angles.

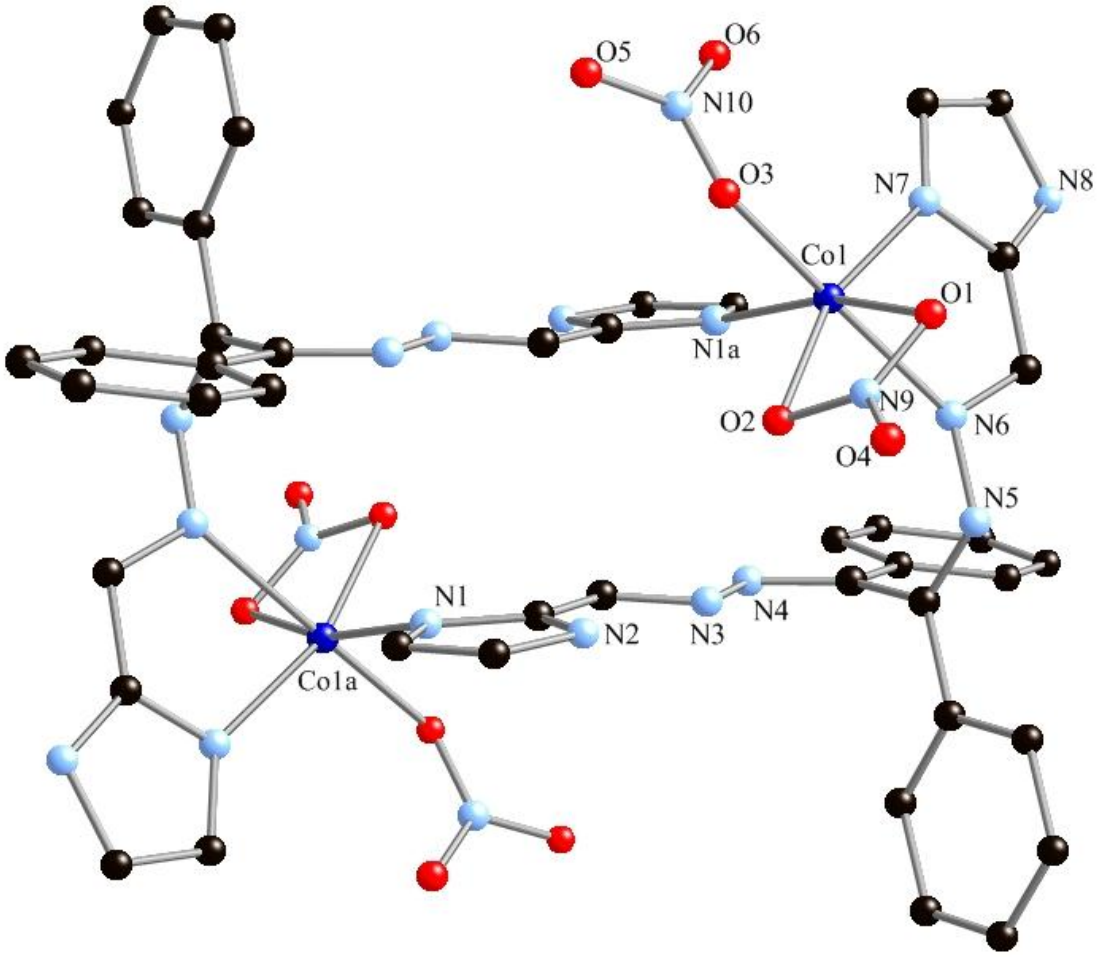

Figure 3.7 – Molecular structure of complex **10** generated by an inversion centre lying in the centre of the molecule. Selected atomic numbering shown. Symmetry code to generate equivalent atoms: (-x,1-y,1-z)[a]. Hydrogen atoms and solvent molecules are omitted for clarity.

All four protonated nitrogen atoms of the imidazole form hydrogen bonding interactions. One imidazole nitrogen atom acts as a proton donor and forms a hydrogen bond with an acetonitrile solvent molecule with a donor to acceptor distance of 2.826(5) Å (N2-H2···N12). The second hydrogen bonding interaction is formed between neighbouring molecules of complex **10**. Once again the imidazole nitrogen acts as a proton donor and a coordinated oxygen atom from a

neighbouring molecule acts as the proton acceptor, with a donor to acceptor distance of 2.967(2) Å. This weak hydrogen bonding interaction aids in the packing of the molecules in the crystal lattice.

Changing the head group from pyridine (complex **5**, section 2.2.5) to imidazole, keeping the stoichiometry and Co(II) source consistent changes the binding preferences of the ligand and coordination geometry of the metal centre. With pyridine as the head group Co(II) adopts a seven coordinate distorted pentagonal bipyramidal geometry, but with imidazole the Co(II) centre adopts a six coordinate distorted octahedral geometry. Furthermore complex **5** is only mononuclear and both arms of **L1** bind in a bidentate fashion. Due to the flexibility of the hydrazone and backbone, **L2** could potentially wrap about a single metal ion and bind via both arms in a bidentate fashion, however this is thermodynamically unfavourable as the ligand would then be under considerable strain and therefore does not form a mononuclear complex when combined with Co(II). This effect is seen with all complexes formed with **L2** in this study, where all structures are dinuclear.

*3.2.4 Crystal structure of {[Zn_2(L2)$_3$(μ_2OH)][(ClO_4)$_3$]·CH_3CN}, Complex **11***

Crystals suitable for a single crystal X-ray diffraction study were prepared by the slow diffusion of diisopropyl ether into an acetonitrile solution containing a 2:3, $Zn(ClO_4)_2$:**L2** ratio. Crystal growth took two weeks and gave a yield of 40 %. The structure for complex **11** was solved and refined in the orthorhombic *Pbca* space group. The atomic structure with selected atomic labelling of complex **11** is shown in Figure 3.8. The asymmetric unit consists of a single molecule of complex **11**, three perchlorate anions (two of which are disordered), and a disordered acetonitrile solvent molecule. The hydrogen atom of the μ_2-hydroxide bridge could not be modelled, and the large thermal ellipsoid of the oxygen atom indicates that the hydroxide is disordered over multiple locations, due to the several potential hydrogen bonding interactions to hydrazone and coordinated imidazole nitrogen atoms.

Complex **11** consists of two metal centres bridged by three winding ligands of **L2**, forming a *triple helicate*, with each arm binding to a single Zn(II) centre in a monodentate fashion through the sp^2 hybridized nitrogen atom of the imidazole ring. The complex exhibits similar Zn-N bond lengths of 2.024 (6) Å, 2.049(5) Å, 2.050(5) Å for Zn1 and 2.012(6) Å, 2.039(6) Å and 2.040(6) Å for Zn2. Completing the coordination sphere of both Zn(II) centres is a μ_2-hydroxide bridge separating the two centres by a distance of 3.712(12) Å and displaying similar Zn-μ_2OH bond distances of 1.854(5) Å and 1.878(5) Å for Zn1-O1 and Zn2-O1 respectively. The presence of a μ_2-hydroxide bridge is not uncommon and a CSD search for such a bridge (Zinc atoms bridged by a hydroxide bridge) results in over 500 known structures.

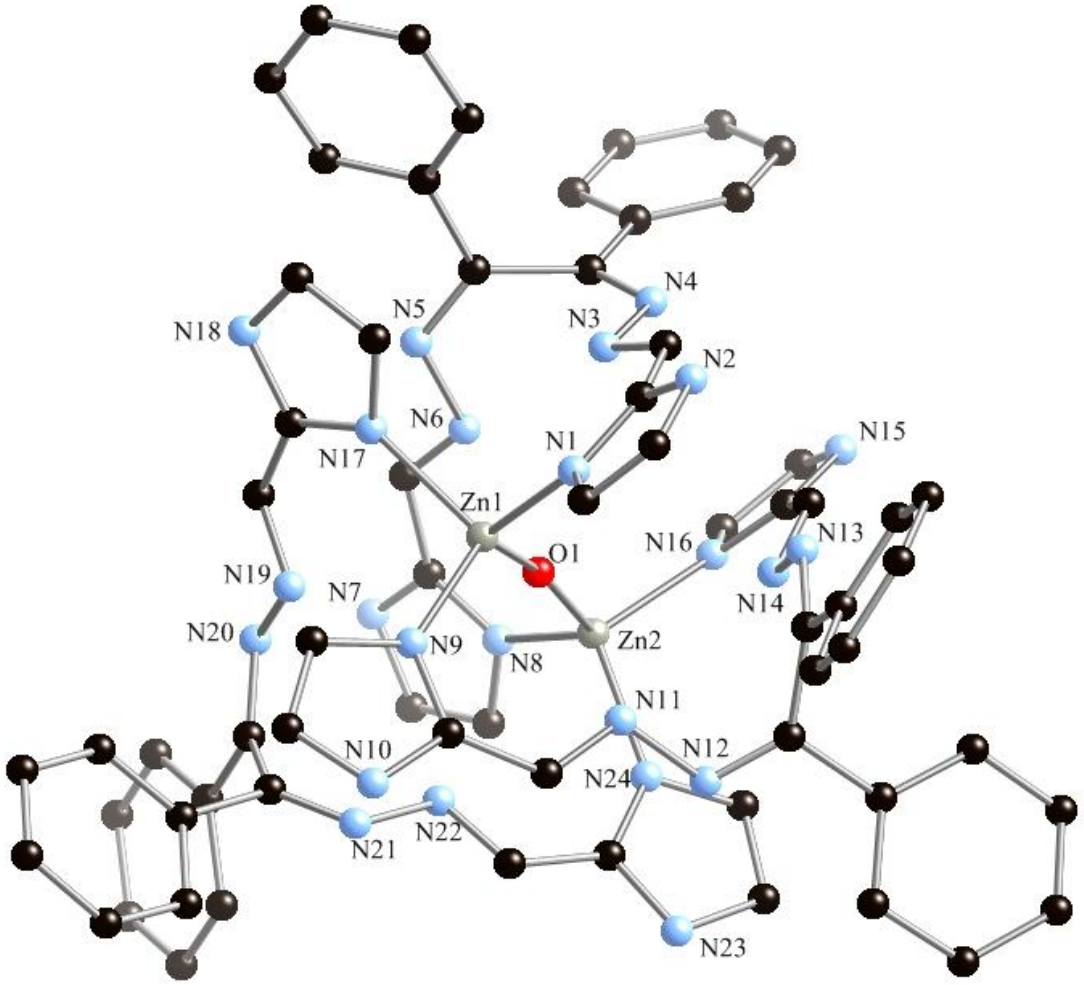

Figure 3.8 – Molecular structure and selected atomic numbering of complex **11**. Hydrogen atoms, anions and solvent molecules are omitted for clarity.

The geometry of both metal centres is best describe as tetrahedral and this is indicated by the τ_4 values of 0.97 using the bond angles of 115.1(2)° and 100.8(2)° for Zn1 and 0.99 for Zn2 using the bond angles of 118.8(3)° and 100.4(2)°. Adopting this geometry allows for the three ligands to wrap around two metal centres and forms a structure that is best described as an *unsaturated homotopic dinuclear triple helicate*. Figure 3.9 shows the handedness of a single structure of complex **11**. Complex **11** crystallises out as a racemic mixture of the left-hand (M = Λ) and right-handed (P = Δ) helices, where Zn1-O1-Zn2 represents the helical axis. See Table **3.10** in Appendix **3** for further details on bond lengths and angles. The space filling diagram also shows how well the helical axis is well protected, and shows several intramolecular offset face-to-face π-interactions between the π-conjugated arms of each ligand with distance ranging from 3.383(12) Å to 3.820(13) Å.

Complex **11** forms several hydrogen bonding interactions within the asymmetric unit. Each of the 6 available non-bonding imidazole nitrogen atoms act as a proton donor forming weak

hydrogen bonds with perchlorate oxygen atoms (2.670(3) Å – 3.051(10) Å, donor to acceptor distances), water oxygen atoms (2.945(11) Å, 3.000(2) Å, donor to acceptor distances) and acetonitrile nitrogen atoms (2.829(7) Å, donor to acceptor distances) acting as proton acceptors. Each molecule of complex **11** is further hydrogen bound to four opposite handed helixes, where a perchlorate acts as a bridging group (see Table **3.6** in Appendix **2** for hydrogen bonding parameters).

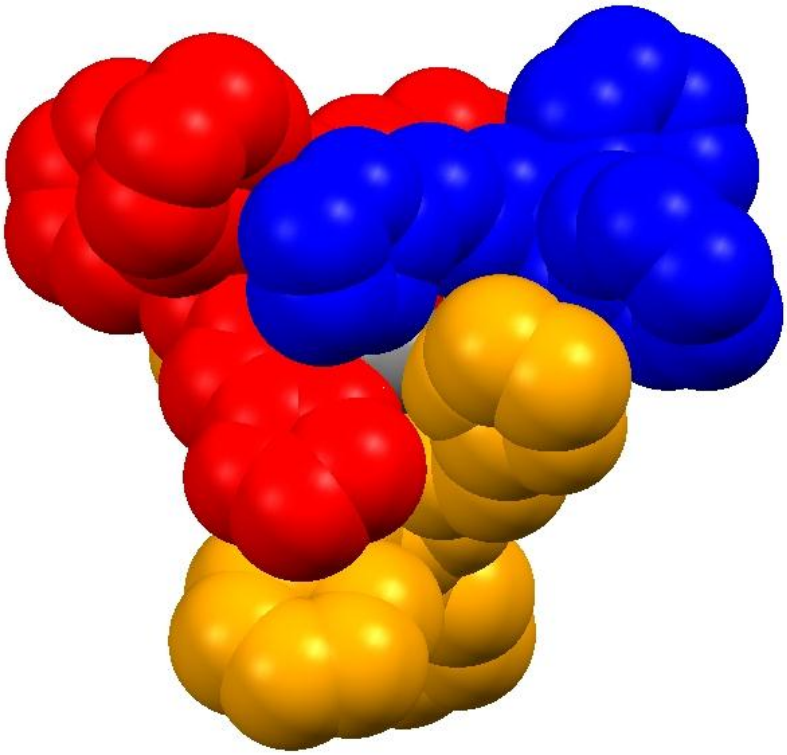

Figure 3.9 – Helicity of complex **11**, showing the right-handed (Δ=P) helicate. The space filling diagram also demonstrates the offset face-to-face π-interaction between the arms of **L2**.

An iso-structural complex was also grown by changing the metal salt source to $Zn(NO_3)_2$, and single crystals suitable for a single X-ray diffraction study were grown in a week by the evaporation of an acetonitrile solution containing a 2:3, Zn(II):**L2** ratio. The structure was solved in the cubic *Pa*-3 space group, and the crystallographic table is provided in Appendix **1**. The use of **L1** led to the formation of a mononuclear distorted octahedral complex, complex **7** once again generated by the bidentate coordination of two arms of **L1**, enforced by twisting of the backbone and arms of the ligand placing strain upon the ligand. However when **L2** is used, the coordination number of Zn(II) changes from 6 to 4 and the formation of a dinuclear triple helicate is realised. Once again **L2** demonstrates the preference to bind in a monodentate fashion through each arm, and Zn(II) centre and their large bulky nature prohibits any ancillary ligand from binding leading to the formation of two four coordinate Zn(II) centres. **L2** demonstrates little twisting of the backbone and arms, so the strain upon the ligand is minimised. Due to the monodentate binding

fashion of **L2**, the Zn(II) centres obtain a tetrahedral geometry, whereas the tetradentate binding fashion of **L1** resulted in the formation of an octahedral Zn(II) species.

3.3 Conclusion

From the results obtained in this chapter, **L2** shows a preference to bind in a monodentate fashion through both arms of the ligand, through the non-protonated imidazole nitrogen, resulting in interesting topologies. Where Mn(II) is used, two molecules of **L2** are able to bind and encapsulate the Mn(II) centre, forming the square planar complex **8**. This encapsulating effect is once again demonstrated in complex **11** where the helical axis of the dinuclear triple helicate is 'hidden' from the external environment. Encapsulations in complexes **8** and **11** results in the metal centres being well protected, and steric constraints does not allow the further binding of additional ligands to the metal centres to access higher coordination numbers.

Complexes **9** and **10** display identical binding modes of **L2** where both arms bind two different metal centres, with one arm binding in a monodentate fashion and the other arm binding in a bidentate fashion. The coordination spheres (both 6 coordinate) of Ni(II) and Co(II) are fully occupied by the aid of water and nitrate ancillary ligands, respectively and the ability of the ancillary ligands to bind the Ni(II) and Co(II) arises from no encapsulating effect on the metal centres as seen with complexes **8** and **11**.

Chapter 4

Bis-2-salicyliminohydrazono-1,2-diphenylethane, L3, and Bis-2-pyrroyliminohydrazono-1,2-diphenylethane, L4

4.1 Coordination clusters and magnetism – *a brief introduction*

For the following discussion the term *cluster* will be used to describe polynuclear supramolecular assemblies. Metal clusters can be prepared from transition metals and are typically bridged by one or more ligands.[68-70,107] Interest in clusters and their magnetic behaviour can be traced back to the work of Sessoli and Gatteschi. [70,108,109] Single molecule magnets (SMMs) are molecules that can be magnetised in a certain orientation by a magnetic field, and remain magnetised even after the magnetic field is switched off. This is a property of the molecule itself and does not require the interaction between molecules for this magnetic effect to occur.[110]

Recently a mixed nitrogen and oxygen donor ligand was synthesised and fully characterised. Combination of this ligand with Ni(II) resulted in the synthesis of an interesting cluster, which holds great promise for future research with this ligand. Described in further detail in the following sections is the synthesis, characterisation and crystallography of the ligand as well as the crystallography of the Ni(II) cluster.

4.1.1 Synthesis, and characterisation of Bis-2-salcyliminohydrazono-1,2-diphenylethane, H_2L3

H_2L3 has been used previously to form two mononuclear structures with Cu(II)[56] and Co(II),[49] however a detailed and fully characterised synthesis for this ligand has not been reported. Reported here is the detailed synthesis and characterisation of **H_2L3**.

To an ethanolic solution of benzil dihydrazone containing four drops of acetic acid, two molar equivalents of salcylicaldehyde was added and the resulting yellow solution was stirred at reflux overnight. The yellow solution was cooled to room temperature and a pale yellow powder was filtered under vacuum to obtain a yield of 83%. Micro analytical data is consistent with that expected for the proposed structure. ES-MS data (*m/z* = 447.1818) is consistent with that for the protonated structure, [**L5 + H**]$^+$. IR spectroscopy is indicative of the presence of imine functionality, with two strong stretches at 1625 cm^{-1} and 1602 cm^{-1} and ^{1}H NMR was consistent with the proposed structure (Figure 4.1).

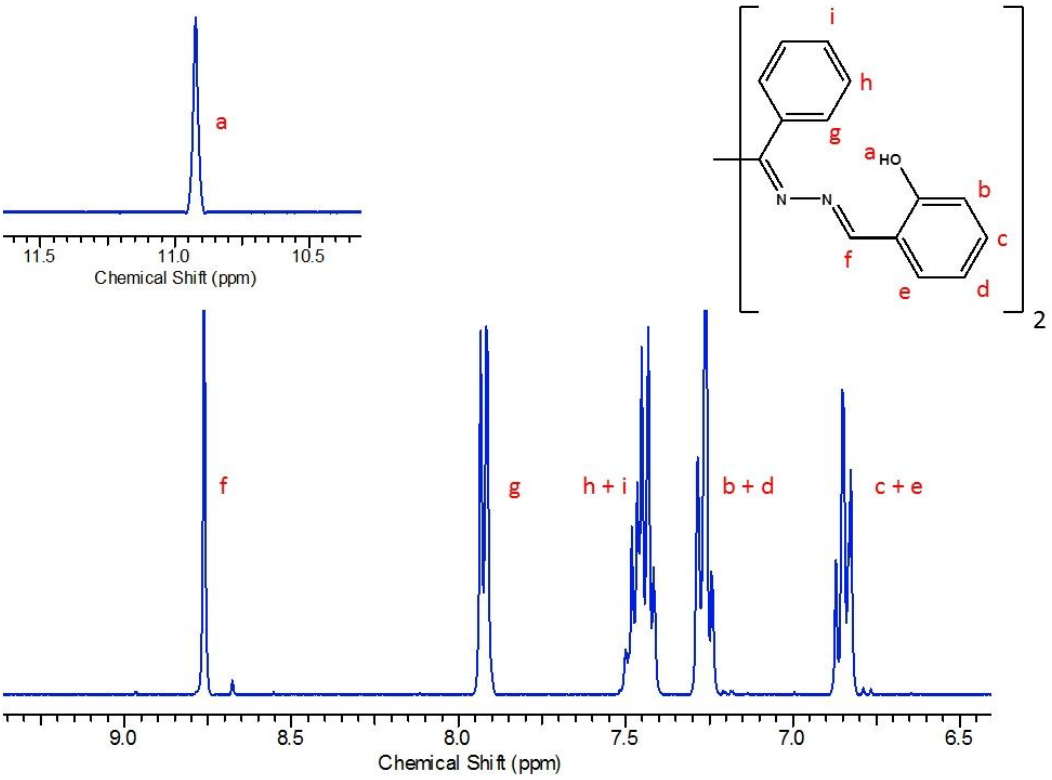

Figure 4.1 – ^{1}H NMR spectrum and assignment of **H_2L3** ($CDCl_3$). ^{1}H-NMR run at 400 MHz, protons g, h and i determined by 1D NOESY experiment.

4.1.2 Crystal structure of Bis-2-salcyliminohydrazono-1,2-diphenylethane, H_2L3

Crystals suitable for structural determination by single crystal X-ray diffraction were obtained by dissolving **H_2L3** in a hot methanol solution containing a molar excess of sodium methoxide. The bright orange solution was filtered and pale orange block shaped crystals were obtained by slow evaporation. Attempts to crystallise **H_2L3** without the presence of a base were unsuccessful despite the ligand remaining protonated. The structure of **L3** was solved and refined in the monoclinic *C*2/*c* space group. The asymmetric unit shows half a molecule of **L3** consisting of one arm of the ligand. Figure 4.2 shows the molecular structure, selected atomic numbering scheme and intramolecular hydrogen bonding for **L3**.

A 2-fold rotation symmetry element is used to generate the full molecule, with the rotation axis lying between the backbone of the molecule. The benzil backbone once again exhibits significant twisting between the two benzil groups, demonstrating a dihedral angle of 99.066(3)°. The double bond character of the imine groups (C=N) within this ligand is apparent from the short bond lengths of 1.28978(4) Å (C8-N2) and 1.28414 Å (C7-N1). The oxygen atom and hydrazone nitrogen atom, N1, are orientated in a *cis* fashion to one another, forming a

potential bidentate binding domain, which upon coordination to a metal centre will assemble a highly favourable 6-membered ring.

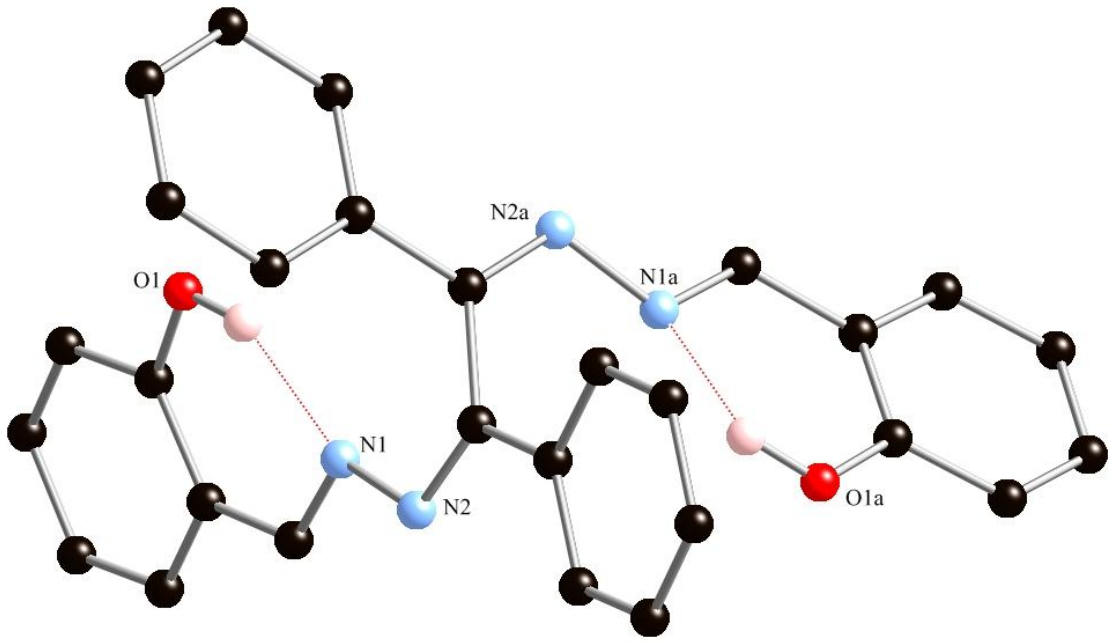

Figure 4.2 – Molecular structure, selected atom numbering scheme and intermolecular hydrogen bonding observed in **L3**. Non-hydrogen bonding atoms omitted for clarity. Symmetry code to generate equivalent atoms: a(1-x,+y,3/2-z).

The planarity of the arms of the ligand, are consistent with that expected of a π-conjugated system, due to the sp^2 hybridization of the hydrazone nitrogen atoms, and extends from the phenol ring to benzil ring of each arm of the ligand and is exhibited by the planar hydrazone bonds (169.7006(4)°).

The hydrogen bond arises between the oxygen atom (hydrogen bond donor) and the nitrogen atom of the hydrazone (hydrogen bond acceptor) with a donor-acceptor distance of 2.61151(14) Å (O1-H1···N1). The packing of the molecules is also influenced by a significant C-H···π-interaction between a benzil C-H and the aromatic phenol ring, exhibiting a distance of 3.5945(19) Å. The tightly ordered packing along all three axis is a contributing reason to why no solvent molecules are observed in the crystal structure of **L3**.

*4.1.3 Crystal structure of {[Ni_6(L3)$_4$(μ_3-OH)$_4$(H_2O)$_2$]·(CH_3CN)$_7$(H_2O)$_2$}, Complex **12***

Crystals suitable for a single crystal X-ray diffraction study were grown by the evaporation of an acetonitrile solution containing a equimolar ratio of $NiCl_2 \cdot 6H_2O$ and **H_2L3** as well as a three molar equivalent of sodium methoxide. Crystals of suitable size for data collection

were grown at room temperature after 4 days and isolated at a yield of 42%. The structure for complex **12** was solved and refined in the monoclinic $P2_1/n$ space group. The asymmetric unit consists of half the structure of the hexanickel cluster, three and half acetonitrile molecules and a disordered water molecule. The structure of the complex and the selected atomic labelling scheme are shown in Figure 4.3.

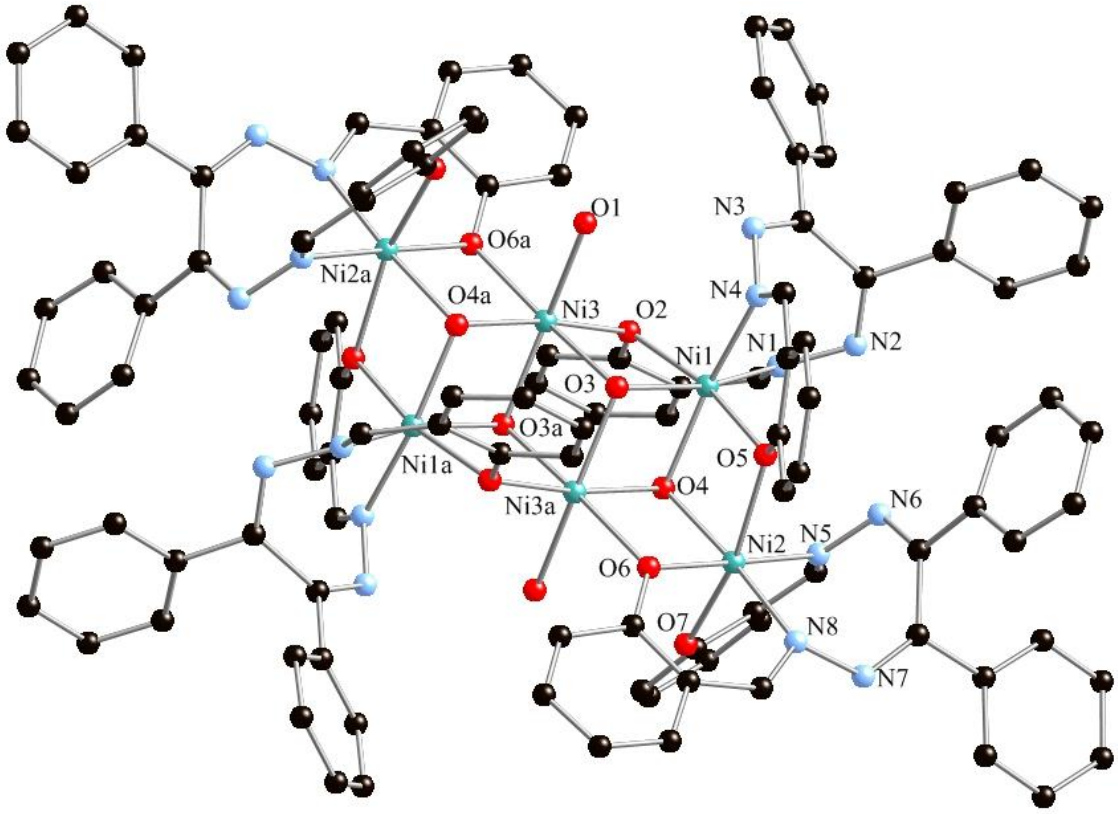

Figure 4.3 – Structure of complex **12** displaying selected atomic labelling. Hydrogen atoms, solvent molecules are omitted for clarity. Symmetry code to generate equivalent atoms: (-x,1-y,1-z).

The neutral cluster contains six Ni(II) metal centres, four doubly deprotonated ligands, four μ_3-hydroxide bridging ligands and two ancillary water molecules. The full structure of complex **12** is generated by a rotoinversion centre, which lies in the centre of cluster. The topology of the cluster resembles the two-dimensional ladder arrangement obtained with imine ligands containing nitrogen and oxygen donor atoms [68-70] and is shown in Figure 4.4. Each Ni(II) centre in complex **12** possess a geometry that is best described as distorted octahedral with $\sum$ values of 82.54 (Ni1), 55.07 (Ni2), 88.11(Ni3) and exhibit bond lengths ranging from 2.023(3) Å – 2.094(4) Å (Ni1), 2.013(3) Å - 2.185(3) Å (Ni2), 2.038(3) Å – 2.118(3) Å (Ni3).

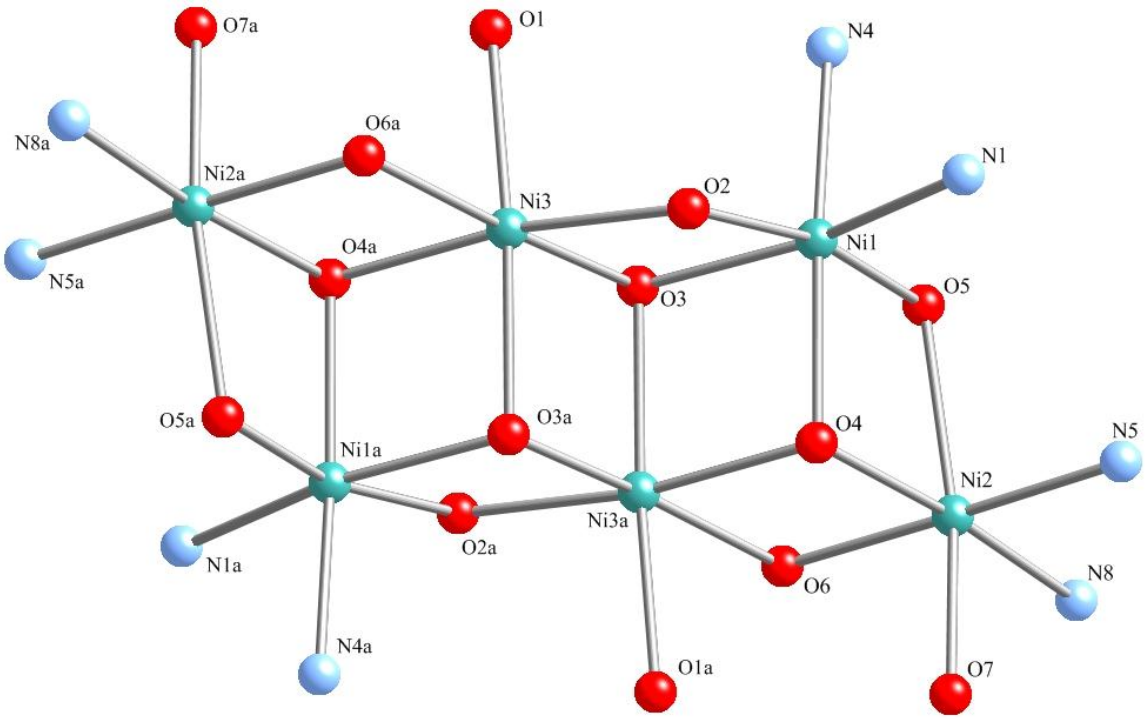

Figure 4.4 - Ni_6 cluster, with atom labelling. Solvent molecules, uncoordinated atoms and hydrogen atoms omitted for clarity. Symmetry code used to generate equivalent atoms; [a](-x,1 – y,1 – z).

L3 displays two binding modes. The first (**L3a**) binds to Ni1 through two bidentate binding domains brought on by significant twisting of the backbone (66.5(2)°), significantly less than that found in the 'free' ligand structure (99.066(7)°) and twisting of the once planar arms of the ligand (108.0(2)° and 113.8(2)°). Each arm binds with bite angles of 82.03(12)° and 88.26(13)°. The oxygen atom of one arm of **L3a**, O2, bridges Ni1 to Ni3 at an angle of 96.27(12)°, while the other arm, O5, bridges Ni1 to Ni2 at a slightly larger angle of 97.12(6)°. Figure 4.5 shows the bridging of Ni(II) centres by **L3a.** Ni1 is separated at a distance of 3.0927(5) Å from Ni3, 3.1776(6) Å from Ni2 and 3.0926(6) Å from Ni3a. The bridging oxygen atom, O2, acts as a proton acceptor in a hydrogen bonding interaction, where the benzil ring of an adjacent ligand acts as a proton donor (donor to acceptor interaction of 3.150(3) Å).

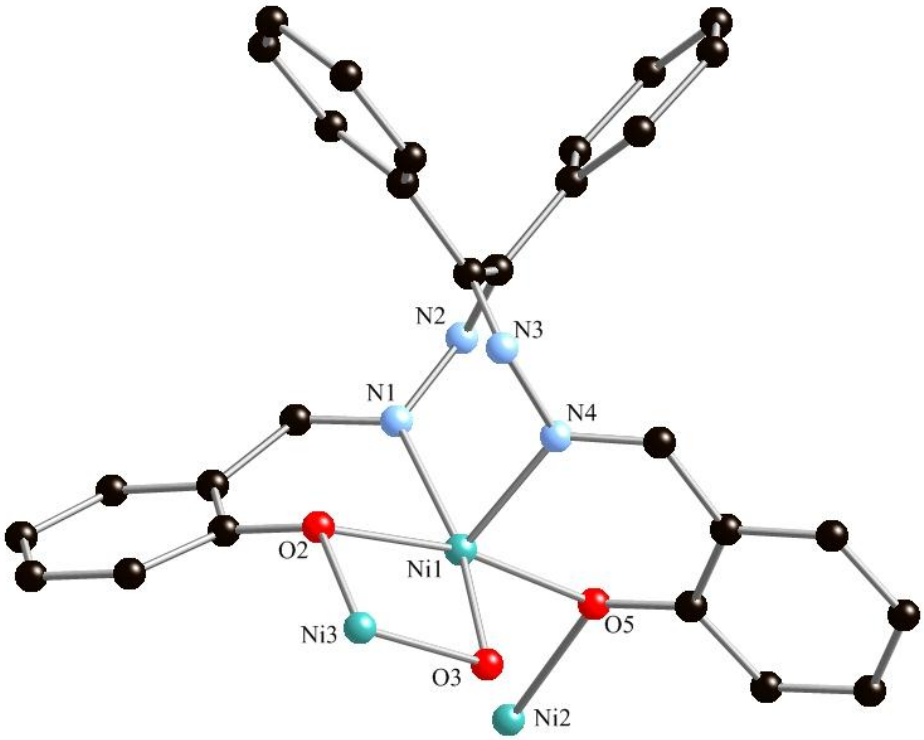

Figure 4.5 – Binding mode of **L3a**, bridging Ni1 to Ni2 and Ni3 through two separate arms of the ligand.

A second ligand of **L3**, **L3b**, binds to Ni2 in the asymmetric unit, once again through two bidentate binding domains brought about by significant twisting of the backbone (-68.8(3)°) and both arms of **L3b** (-157.8(12)° and 116.6(2)°), with one disordered benzil group on ligand. Each arm demonstrates bite angles of 88.21(13)° and 91.83(12)°. Only one arm of **L3b** bound (O6) links two metal centres together, Ni2 and Ni3, with an angle of 97.25(6)°. This bonding interaction leads to Ni2 being separated from Ni3a at a distance of 3.1043(5) Å. The phenolic oxygen atom not involved in linking the two metal centres together (O7) acts as a proton acceptor in an intramolecular hydrogen bonding interaction, to the water ligand bound to Ni3, with a donor to acceptor distance of 2.905(2) Å.

The coordination sphere of Ni1 is satisfied by the coordination of two hydrazone nitrogen atoms (N1, N4), two phenolic bridging oxygen atoms (O2, O5) and two μ_3-hydroxide bridging oxygen atoms (O3, O4). The coordination sphere of Ni2 consists of two hydrazone nitrogen atoms (N5, N8), two oxygen atoms from **L3b (**O6, O7), one oxygen atom from **L3a** (O5) and a μ_3-hydroxide bridging oxygen atom (O4).

Ni3 contains a coordination sphere fully satisfied by oxygen donor atoms. A μ_3-hydroxide bridges Ni1, Ni2 and Ni3 together, displaying bridging angles of 98.64(6)° (Ni1-O4-Ni3a), 103.02(6)° (Ni1-O4-Ni3a) and 99.05(6)° (Ni2-O4-Ni3a). Two symmetry related μ_3-hydroxide atoms bridges Ni3 to an equivalent atom of Ni3 and two cations of Ni1, with bonding angles of 98.85(6)° (Ni1-O3-Ni3), 98.62(6)° (Ni1-O3-Ni3a) and 99.65(6)° (Ni3-O3-Ni3a). Fulfilling the

coordination sphere of Ni3 is an ancillary water ligand (O1), and a bridging oxygen atom from **L3a** (O2) and **L3b** (O6). This water acts as a proton acceptor in a second hydrogen bonding interaction with a solvent acetonitrile molecule with a donor to acceptor distance of 3.344(4) Å. Ni3 lies at a distance of 3.0926(6) Å from Ni2 and 3.1194(8) Å from Ni3a. Ni3a and Ni1a are separated by a distance of 3.0927(5) Å.

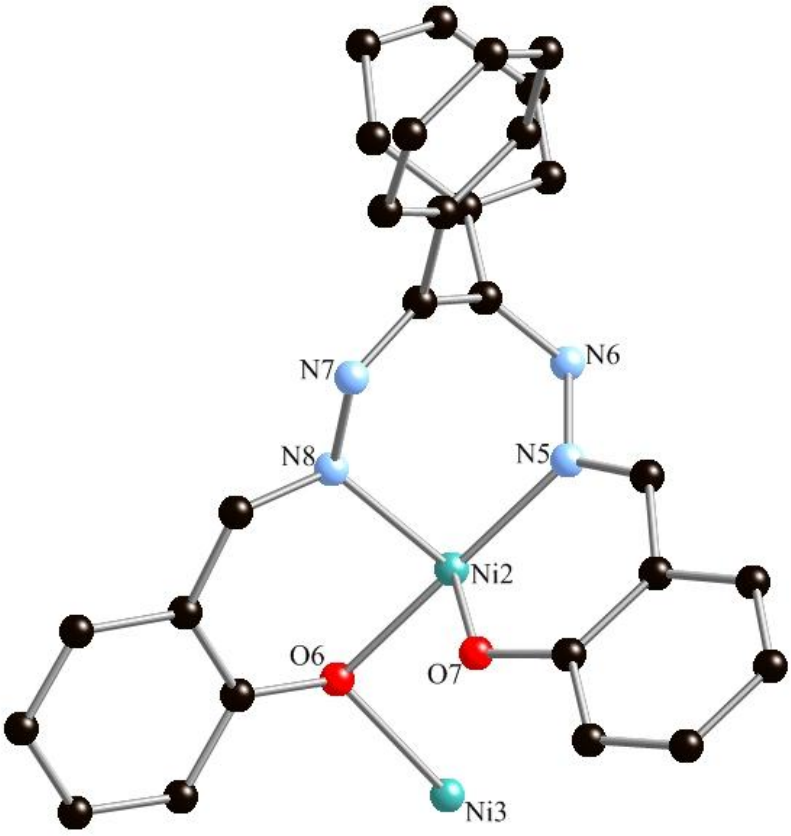

Figure 4.6 – binding mode of **L3b**, where only one phenolic oxygen atom bridges two metal centres together.

Previous research has used the imine functionality to design ligands with both nitrogen and oxygen donor atoms to assemble clusters containing Cu(II), Co(II) and Ni(II), all of which show interesting magnetic behaviour.[68-70,111] It is known that magnetic behaviour arises from the interaction between the metal centres, and the bond angles formed by the bridging ligands, which provide a pathway for the magnetic interaction.[69] The topology, bond angles as well as the metal-metal separation distances with respect to the Ni(II) centres in complex **12** are similar to that found for clusters with the same Ni_6 core.[68-70] Future work on this cluster should focus on acquiring magnetic measurements, as well as attempt to synthesise other clusters using Co(II), Mn(II) and Cu(II), metals ions which have previously shown to form single molecule magnets.[68-70,111] Polynuclear complexes are of considerable interest due to their potential applications in magnetic refrigeration, quantum computation, high density data storage and nanotechnological materials [68,69]

4.2 Studies of Bis-2-pyrrolyliminohydrazono-1,2-diphenylethane , L4

4.2.1 Synthesis and characterisation of Bis-2-pyrrolyliminohydrazono-1,2-diphenylethane, H_2L4

To a solution of benzil dihydrazone in ethanol, containing four drops of acetic acid, two molar equivalents of pyrrole-2-carbaldehyde was added. The resulting clear yellow solution was refluxed overnight and cooled to room temperature to obtain a yield of 83%. Micro analytical data was consistent with the proposed structure. ES-MS indicated a molecular ion (*m/z* = 393.1826) which is expected for the protonated species [**L4** + H]$^+$. IR spectroscopy indicated a strong stretch at 1613 cm^{-1}, confirming the presence of an imine functional group and ^{1}H NMR was consistent with that expected for the proposed structure (Figure 4.7).

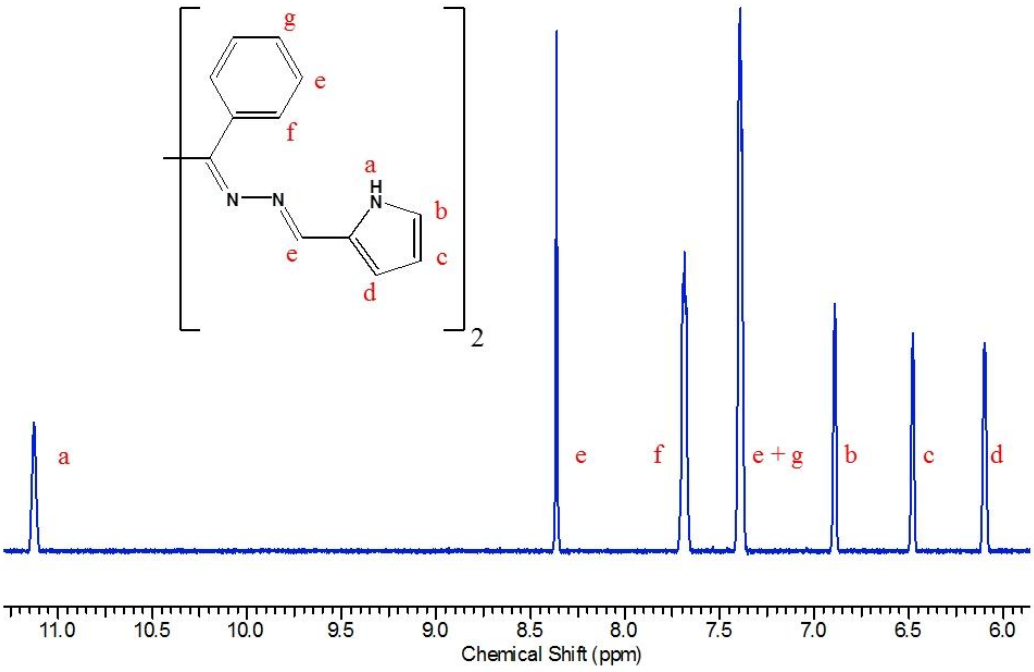

Figure 4.7 – ^{1}H NMR spectrum and peak assignment for **H_2L4** (DMSO), proton assignment was aided by the use of a 2D COSY experiment.

4.2.2 Crystal structure of Bis-2-pyrrolyliminohydrazono-1,2-diphenylethane, H_2L4

Crystals suitable for structural determination by single crystal X-ray diffraction were obtained by dissolving the pale yellow powder of **H_2L4** in hot methanol. The resulting clear yellow solution was filtered and the solvent was allowed to slowly evaporate at room temperature for one week to obtain bright yellow crystals. The structure of **H_2L4** was solved and refined in the triclinic *P* -1 space group. The asymmetric unit contains two molecules of **H_2L4**, both of which

exhibit similar bond lengths and angles. Figure 4.8 shows the molecular structure and the selected atomic numbering scheme for **H_2L4**.

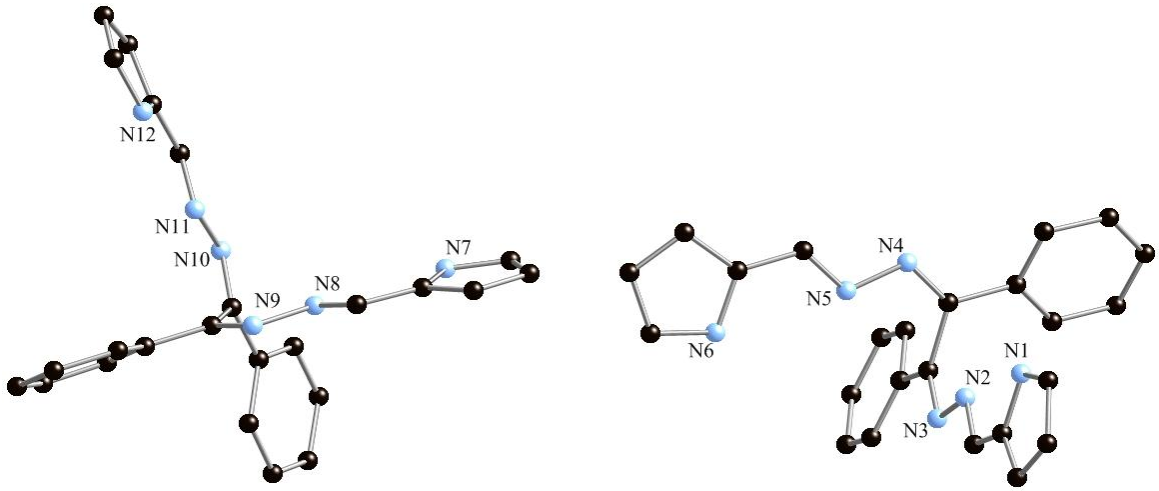

Figure 4.8 – Molecular structure and selected atomic numbering scheme for **H_2L4**. Hydrogen atoms omitted for clarity.

Both molecules in the asymmetric unit demonstrate significant twisting of the backbone with dihedral angles of 92.38(11)° and 91.50(12)° which is consistent with similar ligands found previously in the literature.[61,63,65,67] The double bond character of the imine groups (C=N) is apparent from the short bond lengths ranging from 1.2834(17) Å to 1.2936(17) Å. The pyrrolyl and hydrazone nitrogen atoms are orientated *cis* to each other, forming a potential bidentate binding domain. The planar nature of the arms of the molecules is consistent with the presence of a π-conjugated system due to the sp^2 hybridization of the nitrogen atoms of the hydrazone system. This π-conjugation extends into the benzil groups of each arm (for full details on bond lengths and angles see Table **4.8** in Appendix **3**).

Both the molecules in the structure form extensive hydrogen bonded one dimensional chains, with identical molecules (i.e. molecule containing N1 only hydrogen bonds to an adjacent molecule containing N1). All four pyrrole nitrogen atoms act as hydrogen bond donors, while the hydrazone nitrogen atoms act as acceptors, with donor-acceptor distances ranging from 2.9733(17) Å to 3.0390(16) Å (for full details on hydrogen bond parameters see Table **4.5** in Appendix **2**).

As well as the intermolecular hydrogen bonding interactions, the molecules also pack in the crystal through weak π-interactions. There are three C-H···π-interactions, between pyrrole C-H groups and the aromatic pyrrole rings, displaying carbon to centroid bond lengths of 3.7221(17) Å, 3.6360(16) Å and 3.551(16) Å.

*4.2.3 Crystal structure of [CuL4], Complex **13***

Crystals suitable for a single crystal X-ray diffraction study were obtained by the slow solvent evaporation of a methanolic solution containing an equimolar amount of **L4** and $Cu(CH_3COO)_2 \cdot H_2O$, as well as an excess of triethylamine to ensure the full deprotonation of the pyrrole nitrogen atoms. The structure for complex **13** was solved and refined in the triclinic *P*-1 space group. The molecular structure and selected atomic numbering scheme is shown in Figure 4.9. The asymmetric unit contains only a single mononuclear neutral complex per unit cell.

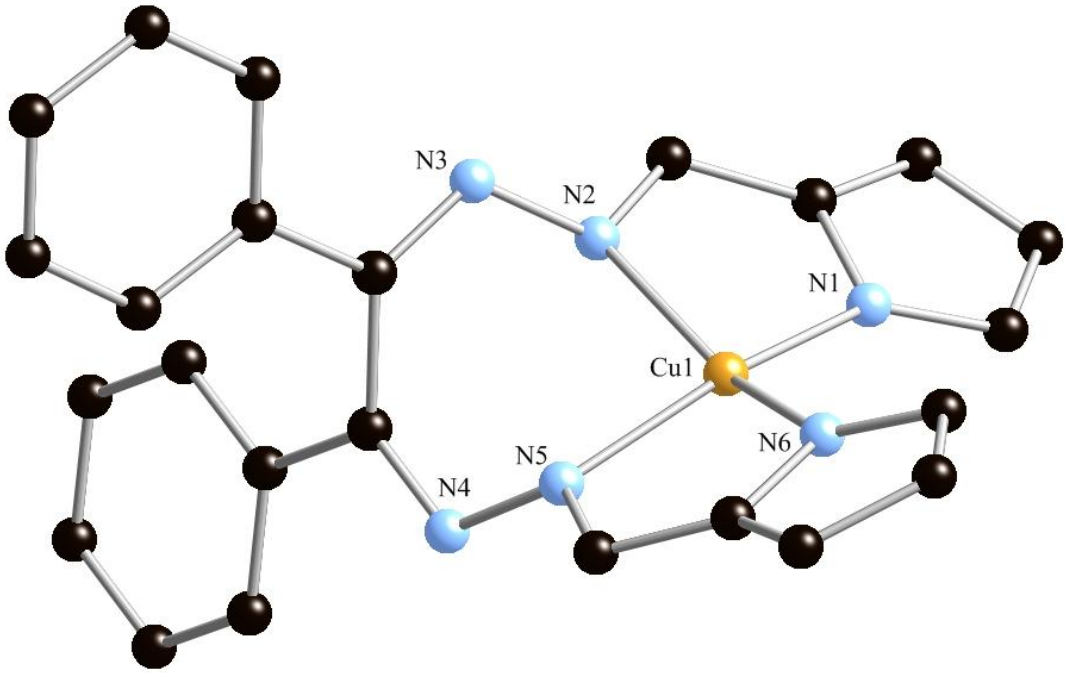

Figure 4.9 - Molecular structure and selected atomic numbering scheme for complex **13**. Hydrogen atoms omitted for clarity.

Using the two largest angles (*trans*) in the complex (161.65(7)°, 150.87(7)) a τ_4 value of 0.34 is obtained, which along with visual inspection of complex **13**, points towards a Cu(II) complex, with a distorted square planar geometry. Filling the coordination sphere are two bidentate binding domains formed by the pyrrole and hydrazone nitrogen atoms, with similar bite angles of 82.70(7)° and 82.74(7)° (N1-Cu1-N2 and N5-Cu1-N6), and similar acceptor-donor bond lengths (1.940(17) Å - 2.004(17) Å). The small bite angle enforced by the binding domains as well as folding of the ligand, results in the Cu(II) centre adopting the aforementioned distorted square planar geometry (*cis* angles are expected to be 90° for a square planar structure).

Coordination of the ligand to a single metal centre requires twisting of the backbone as well as the hydrazone functional groups in both arms of the ligand. The dihedral angle between

the two benzil rings on the backbone decreases from 91.52(13)° and 92.53(11)° in the free ligand to 74.53(7)° in the coordinated ligand. The hydrazone functional groups which are reasonably flat in the free ligand (~178°) show increased twisting about the hydrazone bond, with dihedral angles of 151.77(17)° (C5-N2-N3-C6) and 142.28(19)° (C13-N4-N5-C20).

There are four significant π interactions that influence the packing in the crystal lattice. There are three edge to face interactions (3.660(3) Å) between two benzil groups, a pyrrole-pyrrole interaction (3.371(2) Å) and a benzil edge to pyrrole face interaction (3.661(3) Å). The final significant interaction is a conjugated imine carbon to benzil interaction (3.447(2) Å).

By taking advantage of an imine condensation reaction, **H_2L4** demonstrates the synthesis of a new ligand. Combination of **L4** with with Cu(II) leads to the formation of a neutral mononuclear, distorted square planar structure. Once again the backbone and arms of **L4** twists significantly to coordinate to a single metal centre when compared to the free ligand structure as has been demonstrated for **L1** and **L2**.

Further work should focus on developing and expanding the library of complexes formed with **L4**. This can be achieved through manipulation of the solvents used in the growth of these crystals, as well as changing the reaction conditions used (e.g. temperature, use of different bases). Complexes formed between **L4** and various first row transition metals will indicate the importance and effect of hydrogen bonding interactions in the formation these supramolecular architectures.

4.3 Future studies with other ligands

New ligands can be designed based on the simple imine condensation reaction by simply changing the nature of the aldehyde used. For example **L5** has been previously used to assemble a Möbius cycle[67] using Ag(I) and a mononuclear complex, when combined with Cd(II).[61] The synthesis and full characterisation of **L5** is provided in the experimental section of this report. The full scope of the binding capabilities of this ligand have yet to be explored with first row transition metals, and the complexes formed would provide excellent contrast to those formed with **L2**. The presence of a slightly bulkier head group due to presence of a methyl group may show potential to affect the self-assembly of the final structure produced, when combined with similar metal salts used in this study. Complex formation using acetonitrile or methanol as the solvent and diisopropyl ether, diethyl ether, benzene and toluene as the antisolvent, as well as using an array of metal and ligand ratios have thus far proved fruitless.

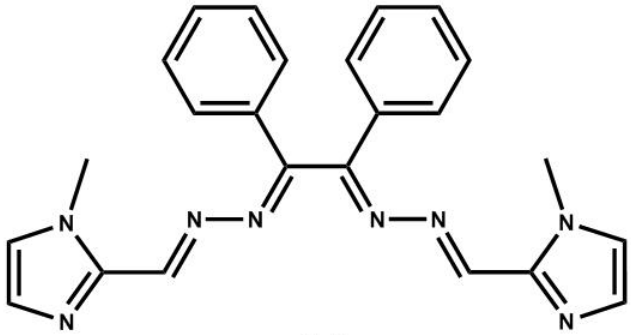

L5

Complexes **1** to **13** in this study all show characteristic twists of the backbone brought on by steric repulsion of the two benzil groups on the backbone. Modification of the backbone, and reducing the steric interaction on the backbone resulted in the use of butane-2,3-dihydrazone to synthesise **L6** – **L8**. Full experimental detail is provided in sections 5.2. Attempts to synthesise first row transition metal complexes with ligands, **L6 – L8** using the method described for **L5** previously did not provide single crystals suitable for X-ray diffraction studies. **L7** was insoluble in most solvents, but chloroform and THF were used to dissolve the ligand, and mixed solvent systems resulted in the ligand falling out of solution as a bright yellow precipitate. However strong colour changes upon addition of first row transition metals provides hope that suitable crystals for single crystal X-ray diffraction analysis can be obtained for **L7**.

Coordination studies with **L6** have shown formation of a one dimensional polymeric species with Ag(I).[65] The crystal structure of **L7** is known, as well mononuclear complexes formed between Cu(II). As shown previously, research within the Kruger group has focused on **L9** where a trinuclear triple helicate was formed when **L9** was combined with Fe(II).[73] It is clear from the small amount of complexes formed between ligands **6 - 9** and first row transition metals, that extensive work is required to be able to draw a sensible conclusion on the steric effects of the backbone for these ligands.

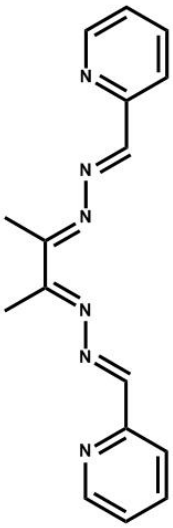

L6

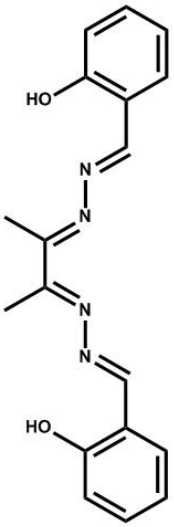

L7

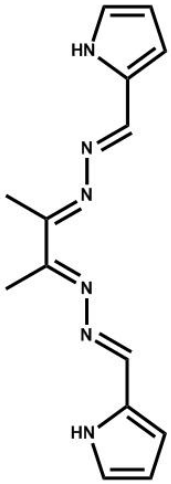

L8

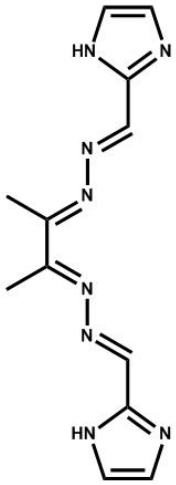

L9

Chapter 5

Conclusion

5.1 Conclusion

This study set out with several aims which involved exploiting the twisted nature of benzil dihydrazone and using the amine functionality of this molecule to synthesise ligands. All ligands were fully characterised.

Changing the ancillary ligand from chloride (complexes **1** and **4**) to either perchlorate (complex **2**) or nitrate (complex **5**), while using the pyridyl head group ligand, **L1**, for complex formation resulted in the coordination geometry of the metal centre changing from distorted octahedral to distorted pentagonal bipyramidal, as well as resulting in the synthesis of an interesting dinuclear Mn(II) complex bridged by two perchlorate ligands. The combination of **L1** with $Zn(NO_3)\cdot 6H_2O$ resulted in the mononuclear distorted octahedral complex **7**, where the nitrate anions are bound in a monodentate fashion, as opposed to the bidentate fashion one nitrate ligand adopts in complex **5**. The use of Fe(II) resulted in the electrocyclic rearrangement of **L1**, an effect previously seen with Ru(II).[75,76] In this study it was determined by ES-MS that rearrangement of **L1** did not occur instantaneously in solution. Previously Cu(I) has been used to form a dinuclear double helicate,[63] a isostructural complex was formed when Cu(II) was used in this study, which undergoes reduction to Cu(I) to form the helicate.

Coordination studies with the imidazole head group ligand, **L2**, resulted in the formation of a square planar Mn(II) complex, where the coordination sphere of the metal ion is satisfied by two ligands, with each ligand arm binding in a monodentate fashion. Both Ni(II) and Co(II) form dinuclear complexes and exhibit similar binding modes of **L2**, where the ligand binds through one arm in a bidentate fashion, while the other arm forms a monodentate interaction with the metal ion. A dinuclear triple helicate was formed when **L2** was combined with $Zn(ClO_4)\cdot 6H_2O$ or $Zn(NO_3)_2\cdot 6H_2O$, This topology arises from **L2** binding in a monodentate fashion to two Zn(II) ions.

All ligands exhibit similar dihedral angles that range between 89° to 99° of the backbone. Upon coordination to a metal ion, these ligands all show a reduction in the dihedral angle of the backbone when compared to their "free" ligand structure. The largest degree of twisting is seen where the ligand and metal ion form a mononuclear complex. Accompanying the large twist of the backbone there is further twisting of the arms, which allows the ligand to wrap about a single metal centre, forming a mononuclear complex. When these mononuclear complexes are compared to their dinuclear counterparts, the degree of twisting of the arms and backbone decreases.

Where the head group is changed from pyridine to imidazole, there is an instant effect on the intermolecular interactions taking place for the complexes. All complexes of **L2** exhibit hydrogen bonding interactions, where the protonated imidazole nitrogen acts as an excellent proton donor, to various solvent and anions available. Synthesis of **L4** introduces a new ligand

resembling the size of **L2** replacing a nitrogen atom of the head group with a carbon atom. Replacement of this nitrogen atom with a carbon atom has an immediate effect on the intermolecular interactions that complexes of **L4** can form and with the loss of a good hydrogen donor atom, no significant hydrogen bonding interactions were observed for complex **13**.

Changing the nature of donor atoms available on the ligand by the use of a phenolic head group achieved a mixed nitrogen and oxygen donor ligand. Upon coordination with Ni(II) a hexanuclear cluster was formed, with a topology that is best described as a two dimensional ladder. **L3** has the ability to bridge two metal centres through a single donor atom, due to deprotonation of the phenolic head group. The bridging of metal centres in this fashion with other ligands presented in this study is not possible, as the donor atoms on these ligands can only coordinate to a single metal ion, due to the presence of only a single pair of non-bonding electrons. The deprotonated phenolic oxygen atom however contains two pairs of lone pair electrons, which are able to form a bonding interaction to two metal centres.

Chapter 6

Experimental methods

6.1 Materials and methods

6.1.1 General information

Unless otherwise specified, all reagents and starting materials were reagent grade, purchased from standard suppliers and used as received. Water was purified by reverse osmosis *in-house*. Melting points were carried out on an Electrothermal melting point apparatus and are uncorrected. Elemental analysis was carried out by Campbell Microanalytical Laboratory, University of Otago. All reactions were carried out in air, using HPLC grade solvent.

6.1.2 Infrared spectroscopy

All infrared spectra were recorded on a Perkin-Elmer Spectrum One FTIR instrument operating in diffuse reflectance mode. Samples were prepared as KBr mulls. The following abbreviations are used; s: strong, m: medium; w: weak; br: broad.

6.1.3 Nuclear magnetic resonance

All spectra were recorded on a Varian INOVA 500 or Agilent 400-MR, operating at 500 MHz or 400 MHz respectively, for ^{1}H and 125 MHz and 100 MHz respectively, for ^{13}C. All samples were dissolved in commercially available deuterated solvents, DMSO or $CDCl_3$. Spectra were referenced to the residual solvent peaks. COSY, HSQC, HMBC, 1D-NOESY and 1D-TOCSY were employed where required for full characterisation of compounds using standard Varian pulse sequences.

6.1.4 Mass spectrometry

Mass spectra were recorded by Dr Marie Squire and Dr Meike Holzenkaempfer on either a DIONEX Ultimate 3000 or Bruker Maxis 4G spectrometer, both of which operated in high resolution positive ion electrospray mode. Samples were dissolved and diluted to the required concentration in HPLC grade MeCN or MeOH.

6.1.5 X-ray crystallography

Refinement data is presented in Appendix **1**. X-ray crystallographical data and refinement was carried out with an Oxford-Agilent SuperNova instrument with focused microsource Cu Kα (λ = 1.5418 Å) or Mo Kα (λ = 0.71073 Å) radiation and ATLAS CCD area detector. Assistance in selecting suitable crystals and mounting on the diffractometer was done by Dr Alan Ferguson. All structures were solved using direct methods with SHELXS[112] and refined on F^2 using all data by full matrix least-squares procedures with SHELXL-97[113] within OLEX-2.[114] Non-hydrogen atoms were refined with anisotropic displacement parameters where appropriate. Hydrogen atoms

were included in calculated positions, or were manually assigned from residual electron density where possible, with isotropic displacement parameters 1.2 times the isotropic equivalent of their carrier atoms. The functions minimised were $\Sigma w(F^2_o - F^2_c)$, with $w = [\sigma^2(F^2_o) + aP_2 + bP]^{-1}$, where $P = [\max(F_o)^2 + 2F^2_c]/3$. Graphical representations of crystallographic data were prepared using the CrystalMaker and Mercury 3.0 packages. As discussed in text, where voids containing highly disordered solvent molecules were present the SQUEEZE routine[101] was carried out and was only employed where sensible modelling of electron density due to solvent molecules was not possible. An electron count of 177 is due to the presence of disordered acetonitrile and water solvent molecules.

6.2 Ligand synthesis

Benzil dihydrazone (1,2-dihydrazono-1,2-diphenylethane)

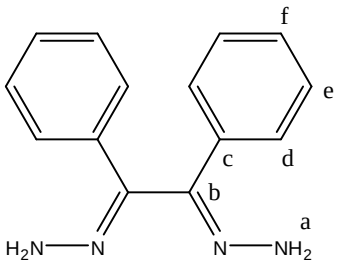

Modifying the preparation of butane-2,3-dihydrazone, 1.5 g (7.135 mmol) benzil was dissolved in 30 mL ethanol containing 4 drops of acetic acid. To the resulting bright yellow solution, 1.3 mL (26.80 mmol) hydrazine hydrate was added, the mixture was stirred at reflux overnight (14 hours), and the solution was allowed to cool to room temperature. The white microcrystalline product was filtered, washed with a small amount of ethanol and air dried. Yield 1.3 g (76%); MP 149 - 151 °C; δ_H (400 MHz, DMSO) 7.38 (d, 4H, J = 7.44 Hz, H^d), 7.26 (t, 4H, J = 7.44 Hz, H^e), 7.19 (t, 2H, J = 7.44 Hz, H^f), 6.66 (s, 4H, H^a); δ_C (100 MHz, DMSO) 138.5 (2C, C^c), 136.3 (2C, C^b), 129.0 (4C, C^e), 127.9 (2C, C^f), 125.3 (4C, C^d); *m/z* (ES-MS, MeCN) 239.1290 ([M+H^+], $C_{14}H_{15}N_4$ requires 239.2957); ν_{max}/cm^{-1}(KBr) 3352s, 3192s, 3060m, 1882w br, 1689m, 1581m, 1443s, 1333w, 1155m, 1095m, 941m, 765s, 691s.

Melting point and I.R. data consistent to that found in literature.[115]

Bis-2-pyridyliminohydrazono-1,2-diphenylethane. ***L1***

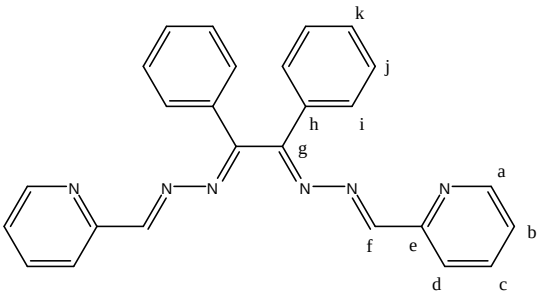

0.28 g (1.18 mmol) of benzil dihydrazone was added to 30 mL methanol containing four drops of acetic acid. To the resulting clear colourless solution two molar equivalents (0.25 mL, 2.35 mmol) of pyridine-2-carboxaldehyde was added. The resulting bright yellow solution was stirred at reflux overnight and the bright yellow solution was refrigerated for 24 hours and filtered to give a bright yellow block shaped crystalline product. Yield 0.23 g (48%); MP 161 - 163 °C; δ_H (400 MHz, $CDCl_3$) 8.56 (d, 2H, J = 5.09 Hz, H^a), 8.52 (s, 2H, H^f), 7.89 (d, 4H, J = 6.26 Hz, H^i), 7.81 (d, 2H, J = 7.83 Hz, H^d), 7.59 (dd, 2H, J = 7.83 Hz, 5.05 Hz, H^c), 7.44 – 7.39 (m, 6H, H^j + H^k), 7.22 (t, 2H, J = 5.08 Hz, H^b); δ_C (100 MHz, $CDCl_3$) 165.5 (2C, C^h), 160.2 (2C, C^f), 153.2 (2C, C^g), 149.3 (2C, C^a),136.5 (2C, C^c), 133.7 (2C, C^e), 131.1 (2C, C^k), 128.8 (4C, C^j), 127.8 (4C, C^i), 124.8 (2C, C^b), 121.9 (2C, C^d); *m/z* (ES-MS, MeCN) 417.1823 ([M+H^+] $C_{26}H_{21}N_6$ requires 417.4939); ν_{max}/cm^{-1}(KBr) 3056m, 2978m, 2929m, 1945w, 1819w, 1611s, 1589m, 1539s, 1494m, 1345m, 1246m, 1183w, 1084m, 991m, 915m, 868m, 772s, 749s, 687s.

Melting point[75] and ^{1}H NMR[64] analysis is in consensus with that found in literature.

Bis-2-imidazolyliminohydrazono-1,2-diphenylethane. ***L2***

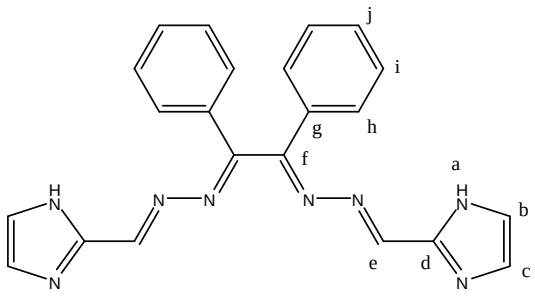

0.35 g (1.47 mmol) benzil dihydrazone was added to 30 mL methanol containing 4 drops of acetic acid. To the resulting solution two molar equivalents (0.28 g, 2.92 mmol) of imidazole-2-carbaldehyde was added. The resulting cloudy white solution was stirred at reflux overnight resulting in a bright, clear yellow solution. Solvent was evaporated off until a small amount of yellow precipitate appeared. The solution was refrigerated for 4 days, and the solution was filtered to yield a pale yellow powder. Crystals suitable for single crystal X-Ray diffraction were grown by recrystallization from hot methanol. Yield 0.54 g (92%); MP 234 - 237 °C; δ_H (400 MHz, DMSO) 12.54 (s, 2H, H^a), 8.35 (s, 2H, H^e), 7.74 (d, 4H, J = 8.07 Hz, H^h), 7.45 -7.43 (m, 6H, H^i + H^j), 7.20 (s, 2H, H^b), 7.07 (s, 2H, H^c); δ_C (100 MHz, DMSO), 162.6 (2C, C^g), 150.9 (2C, C^e), 142.1 (2C, C^f), 133.6 (2C, C^d), 131.5 (2C, C^j), 131.3 (2C, C^b), 129.4 (4C, C^i), 127.9 (4C, C^h), 121.0 (2C, C^c); *m/z* (ES-MS, MeOH) 395.4481([M+H] $C_{22}H_{19}N_8$ requires 395. 1727); ν_{max}/cm^{-1}(KBr) 3593m, 3066m br, 2780m br, 2599m, 1956w br, 1808w, 1619m, 1549m, 1445s, 1398m, 1287m, 1161m, 1028w, 975m, 824s, 769s.

Bis-2-salicyliminohydrazono-1,2-diphenylethane. ***L3***

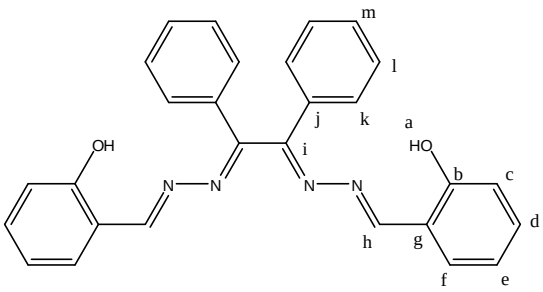

0.99 g (4.15 mmol) of benzil dihydrazone was added to 30 mL of ethanol containing 4 drops of acetic acid. To the resulting clear colourless solution 0.4 mL (8.333 mmol) of salcylicaldehyde was added and the resulting yellow solution was stirred at reflux overnight. The yellow solution was cooled to room temperature and a pale yellow precipitate was filtered off. Crystals suitable for a single crystal X-ray diffraction study were grown from the evaporation of a methanol solution containing 0.01 g (0.025 mmol) of **L3** and 0.004 g (0.074 mmol) sodium methoxide. (Yield 0.82 g (83%). MP 185 – 187 °C; δ_H (400 MHz, $CDCl_3$) 10.90 (s, 2H, H^a), 8.76 (s, 2H, H^h), 7.93 (d, 4H, J = 7.04 Hz, H^k), 7.48 – 7.41 (m, 6H, H^l + H^m), 7.29 – 7.24 (m, 4H, H^c + H^e), 6.87 – 6.83 (m, 4H, H^d + H^f); δ_c (100 mHz, $CDCl_3$) 166.1 (2C, C^j), 165.4 (2C, C^h), 159.8 (2C, C^b), 133.2 (2C, C^c), 132.9 (2C, C^i), 132.6 (2C, C^e), 131.8 (2C, C^m), 129.1 (4C, C^l), 127.9 (4C, C^k), 119.3 (2C, C^d), 117.6 (2C, C^g), 117.0 (2C, C^f); *m/z* (ES-MS, MeCN) 447.1818 ([M + H^+] $C_{28}H_{23}N_4O_2$ requires 447.1818); ν_{max}/cm^{-1}(KBr) 3055mbr, 2923m, 2758m, 2637w, 1959w, 1907w, 1698w, 1625s, 1602s, 1573m, 1491m, 1462m, 1440m, 1375w, 1355w, 1270s, 1237w, 1203m, 1152, 1120w, 1044w, 987w, 940w, 896w, 773m, 750s, 730s.

Bis-2-pyrroyliminohydrazono-1,2-diphenylethane. ***L4***

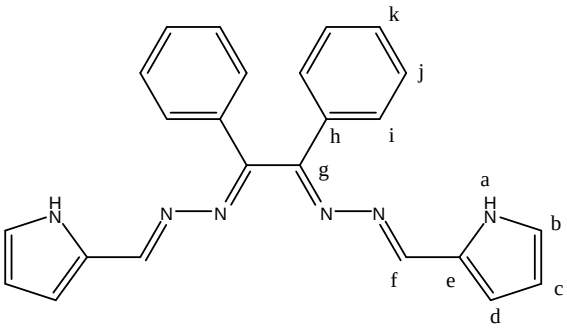

0.40 g (1.68 mmol) of benzil dihydrazone was added to 30 mL ethanol containing 4 drops of acetic acid. To the resulting clear colourless solution 0.31 g (3.26 mmol) of pyrrole-2-carbaldehyde was added. The clear yellow solution was refluxed overnight, and the solution was cooled to room temperature. The resulting pale yellow precipitate was filtered off under vacuum and recrystallized by dissolving the pure powder in methanol, and allowing the solvent to slowly evaporate to obtain crystals suitable for single crystal X-ray diffraction. Yield 1.07 g (83%); MP 203 - 205 °C; δ_H (400 MHz, DMSO), 11.13 (s, 2H, H^a), 8.36 (s, 2H, H^f), 7.69 (d, 4H, J = 3.99, H^i), 7.40 – 7.38 (m, 6 H, H^j + H^k), 6.89 (s, 2H, H^b), 6.48 (s, 2H, H^c), 6.10 (s, 2H, H^d); δ_C (100 MHz, DMSO) 162.2 (2C, C^h), 152.5 (2C, C^f), 134.8 (2C, C^g), 130.7 (2C, C^k), 129.2 (4C, C^j), 127.6 (4C, C^i), 127.3 (2C, C^e), 124.7 (2C, C^b), 116.3 (2C, C^c), 110.3 (2C, C^d); *m/z* (ES-MS, MeCN) 393.1826 ([M+H^+] $C_{24}H_{21}N_6$ requires 393.4719); ν_{max}/cm^{-1}(KBr) 3225m br, 3060m, 2830w br, 2533w, 2451w, 1951w br, 1901w, 1748w br, 1613s, 1583m, 1535m, 1473m, 1421s, 1342m, 1293m, 1240m, 1112s, 1095m, 1034s, 973m, 929s, 883m.

Bis-2-N-methyl-imidazolyliminohydrazono-1,2-diphenylethane. ***L5***

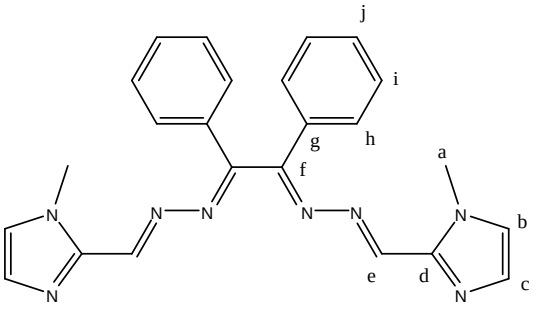

0.37 g (3.39 mmol) N-methyl imidazole-2-carbaldehyde was added to 30 mL methanol containing 4 drops acetic acid. To the resulting yellow solution 0.40 g (1.68 mmol) benzil dihydrazone was added. The yellow solution was stirred at reflux overnight to give a clear yellow solution. Removal of solvent gave a wet yellow product that was dried several times by slurrying in a small amount of THF and evaporating to dryness to give a pale yellow powder, which was recrystallized from a minimal amount of hot acetonitrile. Yield 0.21 g (30%); MP 197 - 201 °C; δ_H (400 MHz, $CDCl_3$) 8.66 (s, 2H, H^e), 7.88 (d, 4H, J = 7.44 Hz, H^h), 7.45 - 7.38 (m, 6H, H^i + H^j), 7.15 (s, 2H, H^c), 6.89 (s, 2H, H^b), 3.51 (s, 6H, H^a); δ_C (100 MHz, $CDCl_3$), 168.0 (2C, C^g), 152.1 (2C, C^e), 141.2 (2C, C^f), 133.4 (2C, C^d), 131.5 (2C, C^j), 129.2 (2C, C^c), 128.9 (4C, C^i), 127.9 (4C, C^h), 125.8 (2C, C^b), 36.1 (2C, C^a); *m/z* (ES-MS, MeCN) 423.2043 ([M+H] $C_{24}H_{23}N_8$ requires 423.5017); ν_{max}/cm^{-1}(KBr) 3110m, 2959m, 2723w, 2587w, 1903w br, 1767w, 1704w, 1616s, 1537m, 1432s, 1361m, 1290s, 1221m, 1154s, 1080w, 972m, 921m, 860m, 827s, 779s.

^{1}H NMR, ^{13}C NMR, I.R. data is consistent with that found in literature[61]

Butane dihydrazone (butane-2,3-dihydrazone)

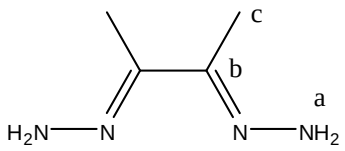

Following the literature preparation outlined by Hauer[116], 4 mL (45.58 mmol) 2,3-butanedione was added to 8 mL ethanol and the bright yellow mixture was added dropwise to a stirred solution of 10 mL hydrazine hydrate (206 mmol) in 100 mL ethanol over one hour and the resulting pale yellow solution was stirred at room temperature for 2 hours. The reaction mixture was sealed and cooled in a refrigerator for several days, resulting in clear colourless needle shaped crystals, which were filtered off and washed with a small amount of cold ethanol. Yield = 3.63 g (70%); MP 157 - 159 °C; δ_H (400 MHz, DMSO) 6.10 (s, 4H, H^a), 1.78 (s, 6H, H^c); δ_C (100 MHz, DMSO) 145.6 (2C, C^b), 9.3 (2C, C^c); *m/z* (ESMS, MeCN) 115.094 ([M+H^+], $C_4H_{11}N_4$ requires 115.1577); ν_{max}/cm^{-1}(KBr) 3340s, 3206s, 1645m, 1578m.

Melting point[116] and I.R.[117] analysis is in accordance with that found in literature.

Bis-2-phenyliminohydrazono-1,2-butane. ***L6***

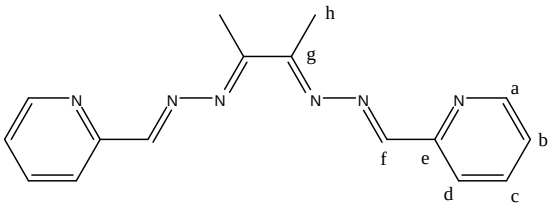

1.01 g (8.85 mmol) butane dihydrazone was added to 50 mL methanol containing four drops acetic acid. To the resulting clear colourless solution 1.69 mL (17.73 mmol) pyridine-2-carbaldehyde was added, and the clear yellow solution was heated to 70 °C and stirred for 15 minutes, during which time a bright yellow precipitate was formed. The solution was cooled to room temperature, filtered and washed with a small amount of cold methanol. Yield 0.87 g (35%); MP 153 - 155 °C; δ_H (400 MHz, $CDCl_3$) 8.69 (d, 2H, *J* = 4.00 Hz, H^a), 8.20 (s, 2H, H^f), 8.14 (d, 2H, *J* = 8.20 Hz, H^d), 7.80 (t, 2H, *J* = 7.5 Hz, H^c), 7.35 (t, 2H, *J* = 5.9 Hz, H^b), 2.31 (s, 3H, H^h); δ_c (100 MHz, $CDCl_3$) 162.2 (2C, C^g), 154.6 (2C, C^f), 153.2 (2C, C^e), 149.6 (2C, C^a), 136.7 (2C,C^c), 124.7 (2C, C^b), 121.7 (2C, C^d), 13.2 (2C, C^h); *m/z* (ES-MS, MeCN) 293.1512 ([M + H^+] $C_{16}H_{17}N_6$ requires 293.3523); ν_{max}/cm^{-1}(KBr) 2994m,1614s, 1590s, 1568s, 1468s, 1441s, 1359s, 1331m, 1224m, 1134m, 864w, 777s, 740s, 705m, 656m.

Melting point data[65] consistent with that found in literature.

Bis-2-salicyliminohydrazone-1,2-butane. ***L7***

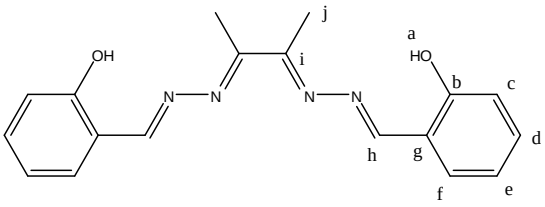

0.20 g (1.75 mmol) butane dihydrazone was added to 30 mL methanol. To this clear colourless solution 0.37 mL (3.47 mmol) salicylaldehyde and four drops acetic acid were added, giving a clear bright yellow solution. The solution was heated gently to 50 °C and stirred for 20 minutes, giving a large amount of yellow precipitate. The solution was cooled, filtered and the yellow powder was washed with a small amount of cold methanol. Yield 0.5313 g (92%); MP 234 - 238 °C; δ_H (400 MHz, $CDCl_3$) 11.80 (s, 2H, H^a), 8.65 (s, 2H, H^h), 7.40 – 7.35 (m, 4H, H^c + H^e), 7.04 (d, 2H, J = 8.33 Hz, H^f), 7.03 (t, 2H, J = 7.46 Hz, H^d), 2.11 (s, 6H, H^j); δ_c (100 MHz, $CDCl_3$) 164.2 (2C, C^h), 160.2 (2C, C^i), 133.5 (2C, C^c), 132.6 (2C, C^e), 119.6 (2C, C^d), 117.8 (2C, C^g), 117.2 (2C, C^f), 13.4 (2C, C^j); *m/z* (ES-MS, MeCN) 323.1503 ([M + H] $C_{18}H_{19}N_4O_2$ requires 323.3741); ν_{max}/cm^{-1}(KBr) 2755m br, 1946w.798w, 1699w br, 1609s, 1546s, 1494m, 1451m, 1417w, 1359s, 1344m, 1272s, 1211s, 1153m, 1117m, 1039m, 1023s, 984m, 934w, 893w, 788s, 749s, 642w.

IR data[50,117], MP and ^{1}H NMR[50] consistent with that found in literature.

Bis-2-pyrroyliminohydrazone-1,2-butane. ***L8***

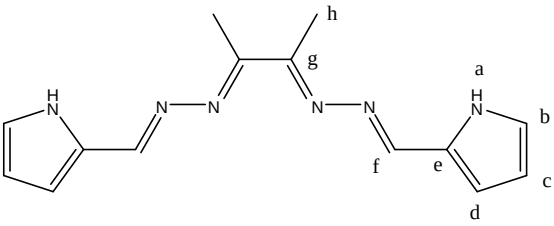

0.39 g (3.42 mmol) butane dihydrazone was added to 50 mL methanol containing four drops acetic acid. To the clear colourless solution two molar equivalents (0.65 g, 6.8 mmol) of pyrrole-2-carbaldehyde was added. The clear pale yellow mixture was heated at 50 °C and stirred overnight, during which time the solution had turned clear bright yellow. The solution was cooled to room temperature, where a small amount of precipitate was formed. The green precipitate was filtered off (0.013 g) and discarded. The solvent of the filtrate was evaporated under vacuum to give a dark brown oil, which was dissolved in hot acetonitrile, giving a dark brown solution. The solution was cooled to room temperature and a single drop of distilled water was added, causing immediate precipitation. The solution was allowed to stand over a week, until all solvent had evaporated, leaving a light brown powder. Yield 1.100 g (60%). MP 169 – 173 °C; δ_H (400 MHz, DMSO) 11.51 (s, br, 2H, H^a), 8.36 (s, 2H, H^f), 6.97 (s, 2H, H^b), 6.58 (s, 2H, H^c), 6.17 (s, 2H, H^d), 3.29 (s, 3H, H^h); δ_c (100 MHz, DMSO) 166.9 (2C, C^g), 151.4 (2C, C^f), 124.8 (2C, C^b), 116.0 (2C, C^c), 111.3 (2C, C^d), 13.9 (2C, C^h); *m/z* (ES-MS, MeOH) 269.1509 ([M + H] $C_{14}H_{17}N_6$ requires 269.3303); ν_{max}/cm^{-1}(KBr) 3419m br, 2987m br, 1959w, 1705w, 1592s, 1564s, 1468s, 1437m, 1349m, 1271m, 12157m, 1101m, 992m, 962m, 895w, 780m, 738m.

6.3 Complex synthesis

*{[Mn(L1)Cl_2]·(CH_3CN)$_3$ H_2O}, Complex **1***

10 mg (0.025 mmol) of **L1** was dissolved in 10 mL acetonitrile at 50 °C. To the resulting clear pale yellow solution 5 mg (0.025 mmol) $MnCl_2·4H_2O$ was added. The solution was filtered and yellow block shaped crystals suitable for a single crystal X-ray diffraction study were grown by the vapour diffusion of toluene. Yield 8 mg (60%); ν_{max}/cm^{-1}(KBr) 3256m br, 3004m, 2728w, 1972w, 1660m, 1628m, 1591s, 1567s, 1477m, 1441s, 1321m, 1307s, 1263m, 1155m, 1102w, 1011m, 990m, 968m, 887w, 777s, 753s, 700s, 636m; Found C, 57.31; H, 4.06; N, 17.24%. Required for $[C_{26}H_{20}N_6Cl_2Mn]·(CH_3CN)_{1.5}$,$(H_2O)_{0.25,}$ C, 57.25; H, 4.14; N, 17.26%.

*{[Mn(L1)(CH_3CN)$_2$(H_2O)][Mn_2(L1)$_2$(CH_3CN)$_2$(μ_2-ClO4)$_2$]·(ClO_4)$_3$ CH_3CN}, Complex **2***

10 mg (0.025 mmol) of **L1** was dissolved in 10 mL acetonitrile at room temperature. To the resulting clear pale yellow solution two molar equivalents (13 mg, 0.05 mmol) $Mn(ClO_4)_2·xH_2O$ was added. The clear yellow solution was filtered and yellow block shaped crystals suitable for a single crystal X-ray diffraction study were grown by the vapour diffusion of diisopropyl ether. Yield = 19 mg (45%); ν_{max}/cm^{-1}(KBr) 3059m, 2359w, 1996w, 1610w, 1563m, 1475m, 1259m, 1151m, 1099s, 1059s, 997m, 985s, 886w, 787m, 690m; Found C, 42.12; H, 3.69; N, 11.59%. Required for $[C_{82}H_{68}N_{20}OMn_3]·(H_2O)_{13}$, C, 41.99; H, 4.04; N,11.95.

*{[Fe(L1)(L1')]·(BF_4)$_2$ (CH_3CN)$_2$}, Complex **3***

10 mg (0.025 mmol) of **L1**, was dissolved in 10 mL acetonitrile at room temperature. To the resulting solution an excess (4 molar equivalents) of $FeBF_4·H_2O$ (37 mg, 0.1 mmol) resulting in the solution immediately turning dark purple. The solution was filtered and dark needle shaped single crystals suitable for single X-ray diffraction was obtained by the vapour diffusion of diisopropyl ether. Yield 6 mg (31%); ν_{max}/cm^{-1}(KBr) 3456m, 3110m, 2928w, 2865m, 1989w, 1727w, 1609m, 1557m, 1445m, 1373m, 1183s, 1051s, 1178w, 966m, 832s, 714s, 624s; Found C, 54.71; H, 3.64; N, 14.00%. Required for $[C_{46}H_{34}N_{10}Fe]·$ 2BF_4, 3H_2O, C, 54.68; H, 3.99; N, 13.86%.

*{[Co(L1)Cl_2]·$(CH_3CN)_3$ $(H_2O)_{0.66}$}, Complex **4***

10 mg (0.025 mmol) of **L1** was dissolved in 10 mL acetonitrile at 50 °C. To the resulting clear pale yellow solution 6 mg (0.025 mmol) $CoCl_2·6H_2O$ was added, causing the solution to immediately turn clear, pale red. The solution was stirred for a further minute, before being filtered, and the solvent was allowed to slowly evaporate off overnight to yield dark red block shaped crystals suitable for single crystal X-ray diffraction. Yield 11 mg (76%); ν_{max}/cm^{-1}(KBr) 3629m, 3065w, 2253m, 1976m, 1630m, 1590s, 1564s, 1477s, 1444s, 1364w, 1327m, 1307m, 1267m, 1181w, 1050m, 986s, 890m, 776s, 754s, 697s; Found C, 56.28; H, 4.06; N, 17.24%. Required for $[C_{26}H_{20}N_6Cl_2Co]·CH_3CN$, $(H_2O)_{0.5}$ C, 56.39; H, 4.06, N, 16.44%

*{[Co(L1)$(NO_3)_2$]·CH_3CN}, Complex **5***

10 mg (0.025 mmol) of **L1** was dissolved in 10 mL acetonitrile at 50 °C. To the solution of **L1** 7 mg (0.025 mmol) $Co(NO_3)_2·6H_2O$ was added causing to solution to turn light clear red/orange. The solution was filtered and red block shaped crystals suitable for single crystal X-ray diffraction were grown by the diffusion of isopropyl ether into the metal complex solution. Yield 11 mg (75%); ν_{max}/cm^{-1}(KBr) 3052w, 3017s, 2323w br, 1594m, 1567m, 1475s br, 1443s, 1357m, 1295s, 1228m, 1104w, 1054w, 1031s, 985m, 914m, 824w, 776m, 740m, 691m; Found C, 52.52; H, 3.62; N, 19.64%. Required for $[C_{26}H_{20}N_8O_6Co]·CH_3CN$, C, 52.51; H, 3.62; N, 19.68%.

*{[Cu_2($L1)_2$]·$(BF_4)_2$}, Complex **6***

10 mg (0.025 mmol) of **L1** was dissolved in 10 mL acetonitrile and stirred at 50 °C. An equimolar amount of $CuBF_4$ (8 mg, 0.025mmol) was added resulting in the solution turning clear dark green. The solution was filtered and single crystals suitable for single crystal X-ray diffraction were grown by the vapour diffusion of diisopropyl ether into the complex solution. Yield 11 mg (73%); ν_{max}/cm^{-1}(KBr) 3059m, 2915m, 2316w, 1921w, 1565m, 1470m, 1259m, 1223m, 1099s, 1059s, 969s, 844w, 787m, 601m; Found C, 53.35; H, 3.41; N, 14.35%. Required for $[C_{52}H_{40}N_{12}Cu_2]·$ $2BF_4$, $2H_2O$, C, 53.93; H, 3.79; N, 14.37%.

*{[Zn(L1)$(NO_3)_2$]·CH_3CN}, Complex **7***

7 mg (0.025mmol) of $ZnNO_3·6H_2O$ was added to a solution of **L1** (10 mg, 0.025 mmol) in 10 mL acetonitrile at 50 °C with constant stirring, resulting in no colour change of the pale clear yellow solution. The solution was filtered and clear colourless crystals suitable for single crystal X-ray diffraction were grown by the slow diffusion of isopropyl ether into the complex solution. Yield 12 mg (79%); ν_{max}/cm^{-1}(KBr) 3023w br, 2466w, 2254w, 1595m, 1572m, 1445s br, 1310s, 1294s, 1222m, 1154m, 1102w, 1032m, 981m, 886m, 817m, 776m, 694s, 641m; Found C, 51.89; H, 3.42; N, 19.39%. Required for $[C_{26}H_{20}N_8O_6Zn]·CH_3CN$, C, 51.98; H, 3.58; N, 19.49%.

*{[Mn(L2)$_2$]·(ClO$_4$)$_4$,(H$_2$O)$_4$ CH$_3$CN}, Complex **8***

3 mg (0.013 mmol) Mn(ClO$_4$)$_2$·xH$_2$O was added to a suspension of **L2** (10 mg, 0.025 mmol) in 10 mL acetonitrile, with constant stirring at room temperature, resulting in a clear pale yellow solution. The solution was filtered and yellow needle shaped crystals suitable for single crystal X-ray diffraction were obtained by the slow diffusion of toluene into the complex solution. Yield 7 mg (33%); ν_{max}/cm^{-1}(KBr) 3065m, 1985w, 1910w, 1654m, 1619m, 1547m, 1493w, 1447s, 1392w, 1326m, 1252w, 1101s br, 1000m, 931w, 889w, 826m, 771s, 693s, 629s. Found C, 45.92; H, 3.95; N, 19.25%. Required for [C$_{44}$H$_{36}$N$_{16}$Mn]· 2 ClO$_4$, 6 H$_2$O, C, 45.92; H, 4.20; N, 19.48%.

*{[Ni$_2$(L2)$_2$(OH$_2$)$_6$]·(NO$_3$)$_4$ (H$_2$O)$_2$ CH$_3$CN}, Complex **9***

8 mg (0.025 mmol) of NiNO$_3$·6H$_2$O was added to a suspension of **L2** (10 mg, 0.025 mmol) in 10 mL acetonitrile, with constant stirring at 50 °C resulting in the solution turning clear bright yellow. The solution was filtered and dark black crystals suitable for a single crystal X-Ray diffraction were obtained by the slow evaporation of the solution over one week at room temperature. Yield 10 mg (40%); ν_{max}/cm^{-1}(KBr) 3337 m br, 2621w, 2364w, 1914w, 1614m, 1549s, 1495s, 1475s, 1445s, 1387m, 1306s br, 1288s, 1183m, 1106m, 1079m, 1033m, 970w, 932w, 833m, 784m, 731w, 689s. Found C, 44.45; H, 3.38; N, 23.43%. Required for [C$_{44}$H$_{48}$N$_{16}$Ni$_2$]·(NO$_3$)$_4$, (CH$_3$CN)$_5$, C, 44.19; H, 4.32; N, 23.86%.

*{[Co$_2$(L2)$_2$(NO$_3$)$_4$]·(CH$_3$CN)$_4$}, Complex **10***

8 mg (0.025 mmol) of Co(NO$_3$)$_2$·6H$_2$O was added to a suspension of **L2** (10 mg, 0.025 mmol) in 10 mL MeCN, with constant stirring at room temperature, resulting in a clear red/orange solution. The solution was filtered and dark red crystals suitable for a single crystal X-ray diffraction study were obtained by vapour diffusion of diisopropyl ether. Crystals were not stable out of solution and decomposed to a red oil, therefore microanalytical studies were not possible.

*{[Zn$_2$(L2)$_3$(μ_2OH)][(ClO$_4$)$_3$]·H$_2$O CH$_3$CN}, Complex **11***

5 mg (0.013 mmol) of Zn(NO$_3$)$_2$·6H$_2$O was added to a stirred suspension of **L2 (**10 mg, 0.025 mmol) in 10 mL acetonitrile, at 50 °C. The clear pale yellow solution was filtered and pale yellow needle shaped crystals were grown by evaporation of the solution for 5 days at room temperature. Yield 13 mg (40%); ν_{max}/cm^{-1}(KBr) 3037m, 2323m, 1976w, 1897w, 1751w, 1667m, 1630m, 1561s, 1475s, 1452s, 1308s, 1241m, 1179w, 1115m, 1022m, 966w, 833m, 771s. An elemental analysis did not fit the proposed structure due to solvent loss, despite isolation of pure crystalline material. Sample lost crystallinity after 1 hour to form a pale green precipitate.

*{[Ni_6(L3)$_4$(μ_3-OH)$_4$(H_2O)$_2$]·(CH_3CN)$_7$ (H_2O)$_2$}, Complex **12***

10 mg (0.022 mmol) of Ligand **5** was dissolved in 10 mL acetonitrile at 50 °C. To the resulting clear pale yellow solution an excess (4 mg, 0.068 mmol) of sodium methoxide was added, causing the solution to immediately turn clear, bright, dark orange. To this solution 6 mg (0.026 mmol) $NiCl_2 \cdot 6H_2O$ was added and stirred for 30 minutes during which time the solution turned bright yellow and a precipitate formed. The solution was cooled to room temperature and filtered. The solution turned deep red after 48 hours and dark red/orange block shaped crystals suitable for single crystal X-ray diffraction were obtained by the slow evaporation of the solvent. Yield 19 mg (42%); ν_{max}/cm^{-1}(KBr) 3642w, 2927m, 2272w, 1615s, 1536s, 1467s, 1372m, 1340m, 1317s, 1252m, 1198s, 1125w, 1076m, 964m, 910m, 848m, 755m, 690m. Found C, 59.45; H, 4.08; N, 10.30%. Required for $[C_{112}H_{84}N_{16}O_{14}Ni_6] \cdot CH_3CN$, $(H_2O)_2$ C, 59.34; H, 3.98; N, 10.32%.

*[CuL4], Complex **13***

10 mg (0.025 mmol) of **L4** was added to 10 mL methanol. To this pale yellow suspension, 100 µL (0.078 mmol) of triethylamine was added to this solution, causing **L4** to dissolve into solution. To the bright yellow solution 3 mg (0.013 mmol) of $Mn(ClO_4)_2$ was added. Single block shaped crystals suitable for a single crystal X-ray diffraction study was grown by the vapour diffusion of toluene. Yield 7 mg (37%); ν_{max}/cm^{-1}(KBr) 3169w, 2907w, 2359m, 1844m, 1567s, 1487s, 1377m, 1289s, 1255m, 1154m, 1078m, 1031s, 930m, 827m, 748s, 692m. Found C, 63.49; H, 4.02; N, 15.71%. Required for $[C_{24}H_{18}N_6Cu]$, C, 63.69; H, 4.00; N, 18.51%.

Appendix 1

Crystallographic refinement data

Chapter 2

Table **2.1** – Crystallographic data for complexes **1**, **2** and **3**

Compound reference	Complex **1**	Complex **2**	Complex **3**
Chemical formula	$2(C_{26}H_{20}Cl\ MnN_6)\cdot 3(C_2H_3N), H_2O$	$2(C_{30}H_{28}MnN_8O), (C_{56}H_{46}Cl_2Mn\ N_{14}O_8)\cdot 6(ClO_4), 2(C_2H_3N)$	$(C_{46}H_{34}N_{10}Fe)\cdot 2(BF_4),2(C_2H_3N)$
Formula mass	612.91	3045.74	1038.41
Crystal system	Triclinic	Monoclinic	Triclinic
Space group	*P*-1	$P2_1/c$	P -1
a/Å	12.4610(4)	10.9416(3)	11.2212(8)
b/Å	12.6053(4)	30.4397(8)	14.3144(10)
c/Å	18.5860(6)	20.3641(4)	15.2176(8)
α/°	87.715(2)	90.00	105.843(5)
β/°	88.879(3)	96.132(2)	90.148(5)
γ/°	87.578(3)	90.00	96.404(6)
Unit cell volume/Å^3	2913.99(16)	6743.7(3)	2335.4(3)
Temperature/K	120.01(10)	120.01(10)	120.01(10)
No. Formula units per unit cell, Z	2	2	2
Crystal size max/mm	0.24	0.22	0.25
mid/mm	0.22	0.16	0.24
min/mm	0.21	0.08	0.16
Radiation type	CuKα	CuKα	CuKα
No. of reflections measured	31373	43581	15465
No. of independent reflections	10037	11600	8022
R_{int}	0.0302	0.0351	0.0458
Final *R*1 values (I > 2σ(I))	0.0392	0.0418	0.0630
Final wR(F2) values (I > 2σ(I))	0.1017	0.1146	0.1575
Final R1 values (all data)	0.0412	0.0492	0.0858
Final wR(F2) values (all data)	0.1033	0.1197	0.1740

Table **2.2** – Crystallographic data for complexes **4**, **5** and **6**

Compound reference	Complex **4**	Complex **5**	Complex **6**
Chemical formula	$2(C_{26}H_{20}Cl_2CoN_6)\cdot 3(C_2H_3N), 0.66(H_2O)$	$(C_{26}H_{20}CoN_8O_6)\cdot C_2H_3N$	$(C_{52}H_{40}Cu_2N_{12})\cdot 2(BF_4)$
Formula mass	1226.35	640.48	1133.66
Crystal system	Triclinic	Monoclinic	Monoclinic
Space group	*P*-1	$P2_1/c$	C2/*c*
a/Å	12.3763(4)	13.5372(2)	21.2206(7)
b/Å	12.4952(3)	14.39496(13)	10.9420(3)
c/Å	18.5144(7)	15.71276(18)	22.0250(7)
α/°	88.012(3)	90.00	90.00
β/°	89.126(3)	112.9836(15)	107.367(3)
γ/°	87.388(3)	90.00	90.00
Unit cell volume/Å^3	2858.20(16)	2818.85(6)	4881.0(2)
Temperature/K	120.00(10)	120.01(10)	120.01(10)
No. Formula units per unit cell, Z	2	4	4
Crystal size max/mm	0.20	0.24	0.40
mid/mm	0.15	0.18	0.28
min/mm	0.10	0.16	0.15
Radiation type	MoKα	CuKα	CuKα
No. of reflections measured	25710	36198	8525
No. of independent reflections	12463	4846	4398
R_{int}	0.0347	0.0362	0.0179
Final *R*1 values (I > 2σ(I))	0.0932	0.0269	0.0503
Final wR(F2) values (I > 2σ(I))	0.2330	0.0675	0.1512
Final R1 values (all data)	0.1010	0.0306	0.0529
Final wR(F2) values (all data)	0.2368	0.0694	0.1534

Table **2.3** – Crystallographic data for complexes **7**	
Compound reference	Complex **7**
Chemical formula	$(C_{26}H_{20}N_8O_6Zn)\cdot C_2H_3N$
Formula mass	646.95
Crystal system	Monoclinic
Space group	$P2_1/c$
a/Å	13.4651(3)
b/Å	14.8087(3)
c/Å	15.4643(3)
α/°	90.00
β/°	114.226(3)
γ/°	90.00
Unit cell volume/Å^3	2812.02(11)
Temperature/K	120.01(10)
No. Formula units per unit cell, Z	4
Crystal size max/mm	0.40
mid/mm	0.22
min/mm	0.18
Radiation type	CuKα
No. of reflections measured	10294
No. of independent reflections	4850
R_{int}	0.0214
Final *R*1 values (I > 2σ(I))	0.0270
Final wR(F2) values (I > 2σ(I))	0.0687
Final R1 values (all data)	0.0318
Final wR(F2) values (all data)	0.0722

Chapter 3

Table **3.1** – Crystallographic data for complexes **8**, **9** and **10**

Compound reference	Complex **8**	Complex **9**	Complex **10**
Chemical formula	$(C_{44}H_{36}MnN_{16})\cdot 4(Cl_{0.5}O_2)$, $4(H_2O)$, $0.25(C_8H_{12}N_4)$	$(C_{44}H_{48}N_{16}Ni_2O_6)\cdot 4(NO_3)$, C_2H_3N, $2(H_2O)$	$(C_{22}H_{18}CoN_{10}O_6)\cdot 2(C_2H_3N)$
Formula mass	1151.81	1337.52	659.50
Crystal system	Tetragonal	Monoclinic	Monoclinic
Space group	*P*4/*mnc*	$P2_1/n$	$P2_1/n$
a/Å	17.1205(4)	13.8779(4)	13.4518(2)
b/Å	17.1205(4)	17.7442(3)	16.8123(2)
c/Å	19.9562(7)	14.1630(4)	13.8453(3)
α/°	90.00	90.00	90
β/°	90.00	113.907(3)	105.2257(18)
γ/°	90.00	90.00	90
Unit cell volume/Å^3	5849.4(3)	3188.46(14)	3021.29(9)
Temperature/K	120.15	120.02(10)	120.01(10)
No. Formula units per unit cell, Z	4	2	4
Crystal size max/mm	0.17	0.22	0.21
mid/mm	0.15	0.19	0.18
min/mm	0.14	0.17	0.16
Radiation type	CuKα	CuKα	CuKα
No. of reflections measured	10931	10828	10552
No. of independent reflections	2604	5490	5205
R_{int}	0.0506	0.0187	0.0263
Final *R*1 values (I > 2σ(I))	0.1510	0.1261	0.0325
Final wR(F2) values (I > 2σ(I))	0.4297	0.3671	0.0786
Final R1 values (all data)	0.1720	0.1367	0.0389
Final wR(F2) values (all data)	0.4585	0.3903	0.0819

Table **3.2** – Crystallographic data for complexes **11**

Compound reference	Complex **11**
Chemical formula	$(C_{66}H_{54}N_{24}OZn_2)\cdot 2.67(ClO_4)$, C_2H_3N, $(Cl_{0.33}O_{1.28})$, $0.33(H_2O)$
Formula mass	1674.67
Crystal system	Orthorhombic
Space group	*Pbca*
a/Å	24.8041(3)
b/Å	24.6027(3)
c/Å	24.9591(3)
α/°	90.00
β/°	90.00
γ/°	90.00
Unit cell volume/Å^3	15231.3(3)
Temperature/K	120.02(10)
No. Formula units per unit cell, Z	8
Crystal size max/mm	0.20
mid/mm	0.18
min/mm	0.17
Radiation type	CuKα
No. of reflections measured	35831
No. of independent reflections	13098
R_{int}	0.0291
Final *R*1 values (I > 2σ(I))	0.0970
Final wR(F2) values (I > 2σ(I))	0.2525
Final R1 values (all data)	0.1039
Final wR(F2) values (all data)	0.2575

Chapter 4

Table **4.1** – Crystallographic data for ligand **3** complexes **12** and ligand **4**

Compound reference	Ligand **3**	Complex **12**	Ligand **4**
Chemical formula	$C_{28}H_{22}N_4O_2$	$C_{112}H_{88}N_{16}Ni_6O_{14}\cdot 7(C_2H_3N)\cdot 2(H_2O)$	$C_{24}H_{20}N_6$
Formula mass	446.50	2553.51	392.47
Crystal system	Monoclinic	Monoclinic	Triclinic
Space group	*C*2/*c*	$P2_1/n$	P-1
a/Å	24.2549(10)	17.5177(6)	10.0554(5)
b/Å	8.8108(3)	15.6151(5)	10.2055(5)
c/Å	11.2561(5)	22.8630(8)	20.1679(7)
α/°	90.00	90.00	97.844(4)
β/°	108.549(4)	107.898(4)	97.382(4)
γ/°	90.00	90.00	90.126(4)
Unit cell volume/Å^3	2280.54(15)	5951.3(4)	2032.86(16)
Temperature/K	293(2)	193.00(10)	286.54(10)
No. Formula units per unit cell, Z	4	2	4
Crystal size max/mm	0.27	0.26	0.25
mid/mm	0.25	0.14	0.22
min/mm	0.17	0.12	0.18
Radiation type	CuKα	Cu/Kα	CuKα
No. of reflections measured	5721	21392	14232
No. of independent reflections	2233	10232	7977
R_{int}	0.0419	0.0294	0.0238
Final *R*1 values (I > 2σ(I))	0.0560	0.0372	0.0370
Final wR(F2) values (I > 2σ(I))	0.1618	0.0942	0.0858
Final R1 values (all data)	0.0669	0.0477	0.0463

Table **4.2** – Crystallographic data for complex **13**

Compound reference	Complex **13**
Chemical formula	$(C_{24}H_{18}CuN_6)$
Formula mass	453.98
Crystal system	Triclinic
Space group	P-1
a/Å	7.9602(7)
b/Å	10.0139(8)
c/Å	12.9548(9)
α/°	86.289(6)
β/°	86.727(6)
γ/°	75.826(7)
Unit cell volume/Å^3	998.22(14)
Temperature/K	120.00(10)
No. Formula units per unit cell, Z	2
Crystal size max/mm	0.29
mid/mm	0.25
min/mm	0.21
Radiation type	Cu/Kα
No. of reflections measured	5926
No. of independent reflections	3443
R_{int}	0.0272
Final *R*1 values (I > 2σ(I))	0.0340
Final wR(F2) values (I > 2σ(I))	0.0934
Final R1 values (all data)	0.0357
Final wR(F2) values (all data)	0.0948

Table **5** – Crystallographic data for Isostructural complexes of **3** and **11**

Compound reference	Isostructural complex **3**	Isostructural complex **11**
Chemical formula	$(C_{46}H_{34}FeN_{10})\cdot 2(ClO_4)$, C_6H_6, C_2H_3N, H_2O	$(C_{66}H_{54}N_{24}O_1Zn_2)\cdot 5(H_2O)$, $3(NO_3)$
Formula mass	1118.76	1612.23
Crystal system	Triclinic	Cubic
Space group	*P*-1	*Pa*-3
a/Å	11.3991(5)	24.52358(17)
b/Å	15.2654(7)	24.52358(17)
c/Å	17.2244(7)	24.52358(17)
α/°	105.864(4)	90.00
β/°	103.699(4)	90.00
γ/°	110.121)4)	90.00
Unit cell volume/Å^3	2518.96(19)	14748.63(17)
Temperature/K	120.01(10)	290.81(10)
No. Formula units per unit cell, Z	2	8
Crystal size max/mm	0.24	0.22
mid/mm	0.15	0.15
min/mm	0.13	0.14
Radiation type	Cu/Kα	Cu/Kα
No. of reflections measured	16488	35544
No. of independent reflections	8673	4947
R_{int}	0.0427	0.0371
Final *R*1 values (I > 2σ(I))	0.0491	0.086
Final wR(F2) values (I > 2σ(I))	0.1241	0.2529
Final R1 values (all data)	0.0614	0.0988
Final wR(F2) values (all data)	0.1350	0.2659

Appendix 2

Hydrogen bond parameters

Table **3.3** – Hydrogen bonding parameters for complex **8**

D-H···A	D···A (Å)	D-H (Å)	H···A (Å)	D-H···A (°)
N2-H2···O1	2.957(19)	0.920(10)	2.060(10)	162.00(8)
N2-H2···O2	2.862(15)	0.920(10)	1.950(10)	170.00(8)

Table **3.4** – Hydrogen bonding parameters for complex **9**

D-H···A	D···A (Å)	D-H (Å)	H···A (Å)	D-H···A (°)
O1-H1···O8	3.049(10)	1.019(5)	2.097(8)	154.60(3)
O2-H2···O13	2.750(14)	1.073(6)	1.800(4)	145.70(14)
O3-H3···N11	3.070(5)	0.926(5)	2.160(5)	165.90(12)
O3-H3···O11	2.740(4)	0.926(5)	2.050(4)	130.50(12)
O3-H3···O13	2.990(4)	0.926(5)	2.130(4)	153.50(11)
O3-H3···O16	2.640(2)	0.926(5)	1.790(2)	150.20(7)
N2-H2···O11	2.980(4)	0.880(5)	2.120(4)	165.80(12)
N2-H2···O14	2.885(16)	0.880(5)	2.137(16)	142.50(5)
N7-H7···O9	2.800(2)	0.880(7)	1.960(2)	159.30(8)
N7-H7···O10	2.758(13)	0.880(7)	1.881(11)	173.40(5)

Table **3.5** – Hydrogen bonding parameters for complex **10**

D-H···A	D···A (Å)	D-H (Å)	H···A (Å)	D-H···A (°)
N2-H2···N12	2.826(5)	0.900(3)	2.070(3)	141.00(2)
N8-H8···O3	2.967(2)	0.860(3)	2.130(3)	166.00(2)

Table **3.6** – Hydrogen bonding parameters for complex **11**

D-H···A	D···A (Å)	D-H (Å)	H···A (Å)	D-H···A (°)
N2-H2···O5	2.836(8)	0.880(5)	2.006(5)	156.9(4)
N7-H7···^{1}O7	2.879(8)	0.880(6)	2.072(5)	152.1(4)
N10-H10···Cl2	3.197(12)	0.880(7)	2.354(10)	160.5(5)
N10-H10···O9	2.670(2)	0.880(7)	1.860(2)	152.3(8)
N10-H10···O10	2.790(3)	0.880(7)	2.150(3)	129.4(7)
N10-H10···O11	2.939(14)	0.880(7)	2.158(12)	147.(7)
N15-H15···O2	2.830(3)	0.880(6)	2.020(3)	153.5(8)
N15-H15···O3	2.945(11)	0.880(6)	2.158(9)	148.6(5)
N18-H18···O16	3.000(2)	0.880(6)	2.185(19)	133.1(7)
N18-H18···O17	3.051(10)	0.880(6)	2.457(7)	123.6(4)
N18-H18···O18	2.794(10)	0.880(6)	1.919(9)	173.3(5)
N23-H23···N26	2.829(7)	0.880(7)	2.004(15)	155.5(7)

Symmetry code: 1 (1/2-x,1-y,-1/2+z)

Table **4.3 -** Hydrogen bonding parameters for Ligand, **L3**

D-H···A	D···A (Å)	D-H (Å)	H···A (Å)	D-H···A (°)
O1-H1···N1	2.6115(14)	0.92357(4)	1.80997(16)	143.6007(2)

Table **4.4** – Hydrogen bonding parameters for complex **11**

D-H···A	D···A (Å)	D-H (Å)	H···A (Å)	D-H···A (°)
[1]O1-H1···O7	2.905(2)	0.850(4)	2.10(4)	158.00(3)
[1]C30-H30···O2	3.150(3)	0.950(2)	2.3140(4)	146.4(13)
C63-H63···O1	3.344(4)	0.980(3)	2.3880(16)	165.10(2)
Symmetry Code : 1 (-x,1-y,1-z)				

Table **4.5 -** Hydrogen bonding parameters for Ligand, **L4**

D-H···A	D···A (Å)	D-H (Å)	H···A (Å)	D-H···A (°)
N1-H1···N4	3.0390(16)	0.880(12)	2.2638(11)	146.87(8)
N6-H6···N3	2.9733(17)	0.880(12)	2.1782(11)	150.05(8)
N7-H7···N10	2.9919(15)	0.880(12)	2.9919(15)	150.59(8)
N12-H12···N9	3.0086(15)	0.880(12)	3.0086(15)	151.59(8)

Appendix 3

Selected bond lengths and angles

Table **2.4** - bond lengths (Å) and angles (°) for complex **1**

Mn1-Cl1	2.4273(7)	Mn1-N5	2.356(2)	Mn2-N7	2.342(2)
Mn1-Cl2	2.4261(7)	Mn1-N6	2.303(2)	Mn2-N8	2.330(2)
Mn1-N1	2.294(2)	Mn2-Cl4	2.4195(7)	Mn2-N11	2.415(2)
Mn1-N2	2.437(2)	Mn2-Cl3	2.3994(7)	Mn2-N12	2.327(2)
Cl1-Mn1-Cl2	108.18(3)	N2-Mn1-N5	68.30(7)	N7-Mn2-N8	69.60(7)
Cl1-Mn1-N1	91.03(6)	N2-Mn1-N6	106.58(7)	N7-Mn2-N11	110.68(7)
Cl1-Mn1-N2	146.40(5)	N5-Mn1-N6	70.19(7)	N7-Mn2-N12	176.18(7)
Cl1-Mn1-N5	94.67(5)	Cl3-Mn2-Cl4	111.54(3)	N8-Mn2-N11	70.96(7)
Cl1-Mn1-N6	93.35(5)	Cl3-Mn2-N7	89.60(6)	N8-Mn2-N12	113.10(7)
Cl2-Mn1-N1	89.27(6)	Cl3-Mn2-N8	146.42(5)	N11-Mn2-N12	68.47(7)
Cl2-Mn1-N2	98.58(5)	Cl3-Mn2-N11	93.77(5)	C6-N2-N3-C7	87.2(2)
Cl2-Mn1-N5	151.15(5)	Cl3-Mn2-N12	86.76(5)	C32-N8-N9-C33	94.3(2)
Cl2-Mn1-N6	90.63(5)	Cl4-Mn2-N7	92.45(5)	C8-C7-C14-C15	60.4(2)
N1-Mn1-N2	68.93(7)	Cl4-Mn2-N8	95.91(5)	C14-N4-N5-C21	83.7(2)
N1-Mn1-N5	108.14(7)	Cl4-Mn2-N11	146.00(5)	C40-N10-N11-C47	106.0(2)
N1-Mn1-N6	175.43(7)	Cl4-Mn2-N12	89.95(6)	C34-C33-C40-C41	59.9(2)

Table **2.5** - bond lengths (Å) and angles (°) for complex **2**

Mn1-1O1a	2.329(2)	Mn1-N6	2.281(2)	Mn2-N12	2.469(2)
Mn1-O2	2.412(2)	Mn1-N7	2.262(3)	Mn2-N13	2.311(2)
Mn1-N1	2.271(2)	Mn2-O5	2.193(2)	Mn2-N14	2.371(2)
Mn1-N2	2.357(2)	Mn2-N8	2.319(2)	Mn2-N15	2.246(3)
Mn1-N5	2.324(2)	Mn2-N9	2.335(2)	Mn1···Mn1a	8.565(5)
O1-Mn1-O2	75.65(8)	N2-Mn1-N6	117.80(8)	N9-Mn2-N12	71.49(8)
O1-Mn1-N1	93.41(8)	N2-Mn1-N7	129.12(9)	N9-Mn2-N13	117.67(8)
O1-Mn1-N2	76.94(8)	N5-Mn1-N6	70.37(8)	N9-Mn2-N14	147.89(8)
O1-Mn1-N5	121.21(8)	N5-Mn1-N7	82.59(9)	N9-Mn2-N15	120.08(9)
O1-Mn1-N6	81.28(8)	N7-Mn1-N6	93.55(9)	N12-Mn2-N13	68.03(8)
O1-Mn1-N7	151.19(9)	O5-Mn2-N8	92.09(8)	N12-Mn2-N14	140.54(8)
^{1}O2a-Mn1-N1	85.52(9)	O5-Mn2-N9	81.74(8)	N12-Mn2-N15	74.64(8)
^{1}O2a-Mn1-N2	142.06(8)	O5-Mn2-N12	127.15(8)	N13-Mn2-N14	85.50(8)
^{1}O2a-Mn1-N5	144.47(9)	O5-Mn2-N13	87.00(8)	N13-Mn2-N15	92.03(9)
^{1}O2a-Mn1-N6	83.20(9)	O5-Mn2-N14	77.41(9)	N14-Mn2-N15	77.76(9)
^{1}O2a-Mn1-N7	75.60(9)	O5-Mn2-N15	155.16(9)	C8-C7-C14-C15	-110.0(3)
N1-Mn1-N2	70.44(8)	N8-Mn2-N9	70.09(8)	C6-N2-N3-C7	-69.7(3)
N1-Mn1-N5	120.97(8)	N8-Mn2-N12	118.43(8)	C14-N4-N5-C21	-103.0(3)
N1-Mn1-N6	168.43(9)	N8-Mn2-N13	171.89(8)	C36-C35-C42-C43	-66.2(3)
N1-Mn1-N7	86.15(9)	N8-Mn2-N14	86.43(8)	C34-N9-N10-C35	-103.2(3)
N2-Mn1-N5	73.09(8)	N8-Mn2-N15	85.42(9)	C42-N11-N12-C49	-118.5(3)

Symmetry codes: 1 (1-x,1-y,1-z)

Table **2.6** - bond lengths (Å) and angles (°) for complex **3**

Fe1-N1	1.970(3)	Fe1-N5	1.913(3)	Fe1-N7	1.973(3)
Fe1-N2	1.953(3)	Fe1-N6	1.971(3)	Fe1-N8	1.954(3)
N1-Fe1-N2	81.38(12)	N2-Fe1-N8	176.11(12)	N5-C21-C22-N6	-9.10(3)
N1-Fe1-N5	169.50(12)	N5-Fe1-N6	79.81(12)	C14-N4-N5-C21	-101.1(4)
N1-Fe1-N6	96.81(12)	N5-Fe1-N7	94.52(12)	N7-C31-C32-N8	0.6(3)
N1-Fe1-N7	90.59(12)	N5-Fe1-N8	94.01(12)	N1-C5-C6-N2	3.5(3)
N1-Fe1-N8	95.87(12)	N6-Fe1-N7	167.78(12)	C8-C7-C14-C15	-65.7(3)
N2-Fe1-N5	88.91(12)	N6-Fe1-N8	89.00(12)	C6-N2-N3-C7	-50.2(3)
N2-Fe1-N6	94.04(12)	N7-Fe1-N8	80.55(11)	C34-C33-C40-C41	-14.6(4)
N2-Fe1-N7	96.68(12)				

Table **2.7** - bond lengths (Å) and angles (°) for complex **4**					
Co1-Cl1	2.3723(16)	Co1-N5	2.234(5)	Co2-N7	2.166(5)
Co1-Cl2	2.3541(17)	Co1-N6	2.184(5)	Co2-N8	2.250(5)
Co1-N1	2.198(5)	Co2-Cl3	2.3802(16)	Co2-N11	2.196(5)
Co1-N2	2.178(5)	Co2-Cl4	2.3824(16)	Co2-N12	2.176(5)
Cl1-Co1-Cl2	109.90(6)	Cl3-Co2-Cl4	106.94(6)	N8-Co2-N12	108.15(18)
Cl1-Co1-N1	88.39(14)	Cl3-Co2-N7	86.67(14)	N11-Co2-N12	74.01(19)
Cl1-Co1-N2	92.26(13)	Cl3-Co2-N8	95.52(13)	N7-C31-C32-N8	8.7(6)
Cl1-Co1-N5	150.91(14)	Cl3-Co2-N11	155.01(13)	N12-C48-C47-N11	5.2(6)
Cl1-Co1-N6	90.43(14)	Cl3-Co2-N12	90.89(14)	C32-N8-N9-C33	84.2(6)
Cl2-Co1-N1	89.97(15)	Cl4-Co2-N7	90.68(14)	C40-N10-N11-C47	83.4(6)
Cl2-Co1-N2	152.20(13)	Cl4-Co2-N8	151.71(14)	C41-C40-C33-C34	56.6(6)
Cl2-Co1-N5	92.29(14)	Cl4-Co2-N11	92.83(13)	N5-Co1-N6	72.61(19)
Cl2-Co1-N6	84.74(14)	Cl4-Co2-N12	88.86(13)	N1-C5-C6-N2	5.8(6)
N1-Co1-N2	73.60(19)	N7-Co2-N8	73.33(19)	N5-C21-C22-N6	10.3(7)
N1-Co1-N5	110.86(19)	N7-Co2-N11	108.70(19)	C6-N2-N3-C7	90.5(6)
N1-Co1-N6	173.84(19)	N7-Co2-N12	177.28(19)	C14-N4-N5-C21	98.7(6)
N2-Co1-N5	73.68(18)	N8-Co2-N811	71.41(18)	C8-C7-C14-C15	55.6(6)
N2-Co1-N6	112.50(19)				

Table **2.8** - bond lengths (Å) and angles (°) for complex **5**					
Co1-O1	2.2948(13)	Co1-N1	2.1503(14)	Co1-N5	2.2092(13)
Co1-O2	2.2767(12)	Co1-N2	2.1920(14)	Co1-N6	2.1776(13)
Co1-O4	2.1270(12)				
O1-Co1-O2	55.99(5)	O2-Co1-N5	162.74(5)	N2-Co1-N5	77.19(5)
O1-Co1-O4	133.85(5)	O2-Co1-N6	89.19(5)	N2-Co1-N6	125.23(5)
O2-Co1-O4	83.59(5)	O4-Co1-N1	88.08(5)	N5-Co1-N6	73.71(5)
O1-Co1-N1	103.53(5)	O4-Co1-N2	148.85(5)	N5-C21-C26-N6	3.63(16)
O1-Co1-N2	75.85(5)	O4-Co1-N5	89.80(5)	C2-N3-N4-C6	113.72(15)
O1-Co1-N5	121.82(5)	O4-Co1-N6	76.02(5)	N1-C5-C6-N2	0.51(16)
O1-Co1-N6	81.63(5)	N1-Co1-N2	73.20(5)	C14-N4-N5-C21	104.23(15)
O2-Co1-N1	79.52(5)	N1-Co1-N5	116.29(5)	C8-C7-C14-C15	62.21(16)
O2-Co1-N2	115.95(5)	N1-Co1-N6	161.48(5)		

Table **2.9** - bond lengths (Å) and angles (°) for complex **6**					
Cu1-N1	2.036(2)	Cu2-N5	2.030(2)	Cu2-N6	2.008(2)
Cu1-N2	2.054(2)				
N1-Cu2-N2	81.25(9)	N5-Cu2-N6	82.92(10)	C8-C7-C14-C15	-87.9(3)
^{1}N1a-Cu2-N2	129.54(9)	^{1}N5a-Cu2-N6	127.25(10)	C14-N4-N5-C21	-167.00(2)
N1-Cu2-^{1}N1a	112.62(13)	N5-Cu2-^{1}N5a	129.85(13)	C6-N2-N3-C7	-163.40(2)
N2-Cu2-^{1}N2a	128.22(12)	N6-Cu2-^{1}N6a	110.69(14)		
Symmetry Codes : 1(1-x, +Y, 3/2-z)					

Table **2.10** - bond lengths (Å) and angles (°) for complex **7**					
Zn1-O1	2.1137(12)	Zn1-N1	2.1885(15)	Zn1-N5	2.2330(14)
Zn1-O4	2.0947(12)	Zn1-N2	2.2124(14)	Zn1-N6	2.1645(15)
O1-Zn1-O4	92.41(5)	O4-Zn1-N2	101.75(5)	N2-Zn1-N5	76.58(5)
O1-Zn1-N1	88.48(5)	O4-Zn1-N5	160.17(5)	N2-Zn1-N6	116.50(5)
O1-Zn1-N2	154.46(5)	O4-Zn1-N6	89.66(5)	N5-Zn1-N6	74.01(5)
O1-Zn1-N5	96.99(5)	N1-Zn1-N2	73.77(5)	C14-N4-N5-C20	101.93(16)
O1-Zn1-N6	84.37(5)	N1-Zn1-N5	118.62(5)	C8-C7-C14-C15	61.01(16)
O4-Zn1-N1	78.92(5)	N1-Zn1-N6	166.27(5)	C6-N2-N3-C7	102.54(17)

Table **3.7** - bond lengths (Å) and angles (°) for complex **8**

Mn1-N1	2.233(6)				
N1-Mn1-^{1}N1a	175.1(3)	C4-N3-N4-C5	-106.5(7)	C6-C5-^{1}C5-^{1}C6	-63.7(5)
^{1}N1a-Mn1-^{2}N1b	97.0(3)				
N1-Mn1-^{2}N1b	83.2(3)				
Symmetry Codes: 1(1/2-x, 1/2 - y, 3/2-z) 2(-1/2+x, -1/2+y, 3/2-z)					

Table **3.8** - bond lengths (Å) and angles (°) for complex **9**

Ni1-O1	2.066(4)	Ni1-O3	2.064(4)	Ni1-N6	2.165(5)
Ni1-O2	2.076(4)	Ni1-N1	2.076(4)	Ni1-^{1}N8a	2.045(5)
O1-Ni1-O2	88.72(19)	O2-Ni1-N1	178.4(2)	N1-Ni1-N6	93.79(16)
O1-Ni1-O3	91.91(18)	O2-Ni1-N6	86.18(18)	N1-Ni1-^{1}N8a	92.40(18)
O2-Ni1-O3	85.8(2)	O2-Ni1-^{1}N8a	89.1(2)	N6-Ni1-^{1}N8a	79.35(19)
O1-Ni1-N1	91.39(17)	O3-Ni1-N1	92.69(18)	C12-N5-N6-C19	110.6(5)
O1-Ni1-N6	174.09(17)	O3-Ni1-N6	90.70(17)	C6-C5-C12-C13	97.9(5)
O1-Ni1-^{1}N8a	97.6(2)	O3-Ni1-N8	169.10(19)	C4-N3-N4-C5	168.9(5)
Symmetry codes: 1(1-x, 1-y, 1-z)					

Table **3.9** - bond lengths (Å) and angles (°) for complex **10**

Co1-^{1}N1a	2.0716(16)	Co1-O2	2.1986(13)	^{1}Co1a-^{1}N7a	2.0933(15)
Co1-N6	2.2085(15)	Co1-O3	2.1105(14)	^{1}Co1a-^{1}O1a	2.1234(14)
Co1-N7	2.0933(15)	^{1}Co1a-N1	2.0716(16)	^{1}Co1a-^{1}O2a	2.1986(13)
Co1-O1	2.1234(14)	^{1}Co1a-^{1}N6a	2.2085(15)	^{1}Co1a-^{1}O3a	2.1105(14)
^{1}N1a-Co1-O1	163.97(6)	N6-Co1-O2	90.85(5)	O1-Co1-O2	60.00(5)
^{1}N1a-Co1-O2	104.13(6)	N6-Co1-O3	166.88(6)	O1-Co1-O3	84.96(6)
^{1}N1a-Co1-O3	94.80(6)	N6-Co1-N7	76.96(6)	O2-Co1-O3	79.93(6)
^{1}N1a-Co1-N6	96.51(6)	N7-Co1-O1	103.84(6)	C4-N3-N4-C5	177.20(17)
^{1}N1a-Co1-N7	91.39(6)	N7-Co1-O2	161.36(6)	C5-C6-C12-C13	-95.31(17)
N6-Co1-O1	82.34(6)	N7-Co1-O3	109.43(6)	C12-N5-N6-C19	-105.66(18)
Symmetry codes: 1(-x, 1-y, 1-z)					

Table **3.10** - bond lengths (Å) and angles (°) for complex **11**

Zn1-O1	1.854(5)	Zn1-N17	2.049(5)	Zn2-N16	2.040(6)
Zn1-N1	2.050(5)	Zn2-O1	1.878(5)	Zn2-N24	2.012(6)
Zn1-N9	2.024(6)	Zn2-N8	2.039(6)	Zn1···Zn2	3.712(12)
O1-Zn1-N1	118.6(2)	O1-Zn2-N16	112.8(2)	C28-C27-C34-C35	75.4(6)
O1-Zn1-N9	120.0(2)	O1-Zn2-N24	118.8(3)	C50-C49-C56-C57	76.8(8)
O1-Zn1-N17	115.1(2)	N8-Zn2-N16	100.4(2)	C4-N3-N4-C5	157.9(6)
N1-Zn1-N9	100.8(2)	N8-Zn2-N24	104.0(2)	C12-N5-N6-C19	156.8(5)
N1-Zn1-N17	98.8(2)	N16-Zn2-N24	104.0(2)	C50-C49-C56-C57	76.8(8)
N9-Zn1-N17	99.8(2)	Zn1-O1-Zn2	168.2(4)	C4-N3-N4-C5	157.9(6)
O1-Zn2-N8	114.7(2)	C6-C5-C12-C13	83.8(6)	C12-N5-N6-C19	156.8(5)

Table **4.6** - bond lengths (Å) and angles (°) for ligand **3**

O1-C1	1.3551(18)	^{1}N1a-^{1}N2a	1.4018(18)	^{1}N1a-^{1}C7a	1.2842(19)
N1-C7	1.2842(19)	N2-C8	1.2897(18)	^{1}N2a-^{1}C8a	1.2897(18)
N1-N2	1.4018(18)	^{1}O1a-^{1}C1a	1.3551(18)		
C9-C8-^{1}C8-^{1}C9	99.066(3)	^{1}C8-^{1}N2-^{1}N1-^{1}C7	169.7006(4)	^{1}C8-^{1}N2-^{1}N1-^{1}C7	169.7006(4)
Symmetry codes: 1(1-x, +y, 3/2-z)					

Table **4.7** - bond lengths (Å) and angles (°) for complex **12**

Ni1-N1	2.094(4)	Ni2-O5	2.185(3)	Ni3-O1	2.112(3)
Ni1-N4	2.027(4)	Ni2-O6	2.020(3)	Ni3-^{1}O6a	2.115(14)
Ni1-O2	2.076(3)	Ni2-O7	2.050(3)	Ni3-O3	2.038(3)
Ni1-O3	2.035(3)	Ni1···Ni2	3.1776(6)	Ni3-^{1}O3a	2.043(3)
Ni1-O4	2.023(3)	Ni1···Ni3	3.0927(5)	Ni3-^{1}O4a	2.047(3)
Ni1-O5	2.052(3)	Ni1···^{1}Ni3a	3.0926(6)	Ni3-O2	2.118(3)
Ni2-N5	2.013(3)	^{1}Ni1a···Ni3	3.0926(6)	^{1}Ni2a···Ni3	3.1043(5)
Ni2-N8	2.075(3)	^{1}Ni1a···^{1}Ni2a	3.1776(6)	Ni3···^{1}Ni3a	3.1194(8)
Ni2-O4	2.029(3)				
N1-Ni1-N4	85.86(14)	N5-Ni2-N8	88.67(13)	O1-Ni3-O2	99.38(13)
N1-Ni1-O3	163.82(13)	N5-Ni2-O4	96.35(13)	O1-Ni3-O3	91.81(12)
N1-Ni1-O2	82.03(12)	N5-Ni2-O5	90.75(13)	O1-Ni3-^{1}O3a	166.29(13)
N1-Ni1-O4	100.47(14)	N5-Ni2-O6	178.97(13)	O1-Ni3-^{1}O4a	89.09(14)
N1-Ni1-O5	105.91(12)	N5-Ni2-O7	88.21(13)	O1-Ni3-^{1}O6a	83.56(12)
N4-Ni1-O2	100.45(13)	N8-Ni2-O4	174.75(13)	O2-Ni3-O3	81.84(11)
N4-Ni1-O3	95.10(13)	N8-Ni2-O5	104.40(12)	O2-Ni3-^{1}O3a	90.67(11)
N4-Ni1-O4	168.14(14)	N8-Ni2-O6	91.83(12)	O2-Ni3-^{1}O4a	171.51(13)
N4-Ni1-O5	88.26(13)	N8-Ni2-O7	91.58(12)	O2-Ni3-^{1}O6a	101.09(11)
O2-Ni1-O3	81.92(11)	O4-Ni2-O5	77.16(12)	O3-Ni3-^{1}O3a	80.23(13)
O2-Ni1-O4	90.42(12)	O4-Ni2-O6	83.18(12)	O3-Ni3-^{1}O4a	97.36(12)
O2-Ni1-O5	168.74(11)	O4-Ni2-O7	87.05(13)	O3-Ni3-^{1}O6a	174.85(12)
O3-Ni1-O4	81.63(13)	O5-Ni2-O6	88.25(11)	^{1}O3a-Ni3-^{1}O4a	80.87(13)
O3-Ni1-O5	90.27(12)	O5-Ni2-O7	163.97(11)	^{1}O3a-Ni3-^{1}O6a	103.76(11)
O4-Ni1-O5	80.38(12)	O6-Ni2-O7	92.68(11)	^{1}O4a-Ni3-O6a	80.37(12)
C9-C8-C15-C16	66.50(2)	C7-N1-N2-C8	113.80(2)	C35-N8-N7-C36	-157.80(2)
C15-N3-N4-C22	108.00(2)	C37-C36-C43C44	-68.80(3)	C43-N6-N5-C55	-116.60(2)
Symmetry codes: 1(-x, 1-y, 1-z)					

Table **4.8** - bond lengths (Å) and angles (°) for ligand **4**

N1-C1	1.357(18)	N5-C20	1.289(17)	N9-C30	1.294(17)
N1-C4	1.372(18)	N6-C21	1.378(17)	N10-N11	1.413(15)
N2-N3	1.411(15)	N6-C24	1.360(18)	N10-C37	1.290(17)
N2-C5	1.286(17)	N7-C25	1.357(19)	N11-C44	1.413(15)
N3-C6	1.288(16)	N7-C28	1.373(17)	N12-C45	1.373(17)
N4-N5	1.411(15)	N8-N9	1.411(15)	N12-C48	1.359(19)
N4-C13	1.289(17)	N8-C29	1.288(17)		
N1-C4-C5-N2	2.060(16)	C5-N2-N3-C6	177.99(11)	C31-C30-N9-N8	179.67(11)
N6-C21-C20-N5	1.570(14)	C30-N9-N8-C29	175.67(11)	C38-C37-C30-C31	179.68(11)
C7-C6-C13-C14	92.35(13)	N7-C28-C29-N8	4.270(15)	C20-N5-N4-C13	177.04(11)
C7-C6-N3-N2	179.82(11)	N12-C45-C44-N11	2.480(16)	C37-N10-N11-C44	179.17(11)
C14-C13-N4-N5	178.63(11)	C38-C37-C30-C31	91.52(13)		

Table **4.9** - bond lengths (Å) and angles (°) for complex **13**

Cu1-N1	1.940(17)	Cu1-N5	1.985117)	Cu1-N6	1.9375(17)
Cu1-N2	2.0038(17)				
N1-Cu1-N2	82.70(7)	C7-C6-C13-C14	74.53(17)	N2-Cu1-N6	150.87(7)
N1-Cu1-N5	161.65(7)	C20-N5-N4-C13	142.28(19)	N5-Cu1-N6	82.74(7)
N1-Cu1-N6	109.14(7)	N2-Cu1-N5	93.49(7)	C5-N2-N3-C6	151.77(17)

Appendix 4

Description of degree of distortion from idealised geometry

1.4 Description of degree of disorder from idealized geometry

Describing the geometry of structures can be difficult, especially when the structure is an intermediate between two common geometries. For example, the structure of four-coordinate Cu(I) and Cu(II) structures can reside between tetrahedral and square planar. Using the simple τ_4 parameter (equation 1.1**)** introduced by Houser and co-workers[118], it is easy to distinguish which four coordinate geometry has been obtained by using the two largest *trans* angles measured for the complex. A τ_4 value of 0.00 would be that of an ideal square planar structure, whereas a value of 1.00 would be for an ideal tetrahedral structure, variations from these ideal numbers points towards distorted four coordinate structures.[118]

$$\tau_4 = \frac{360° - (\alpha + \beta)}{141°}$$

Equation 1.1

When a metal centre contains six donor atoms, it can adopt either an octahedral or trigonal prismatic geometry. The equation used in the study for the description of the deviation from an ideal octahedral geometry is shown below in equation 1.2 and was used for the description of spin-crossover complexes using the twelve *cis* angles for a complex. A $\sum$ value of zero is obtained for perfect octahedral geometry where all *cis* bonds are the ideal 90°. [79]

$$\sum = \sum_{i=1}^{12} |90 - \alpha_i|$$

Equation 1.2

In the following study, several metal centres adopt seven coordinate geometries, which are best described as distorted pentagonal bipyramidal. To describe the degree of disorder of the metal ion for these complexes, modification of equation 1.2 and using the deviation of the five angles from the ideal 72° for the equatorial plane gives equation 1.3 below. Where a value of zero would be that expected for an ideal pentagonal bipyramidal geometry.

$$\sum = \sum_{i=1}^{5} |72 - \alpha_i|$$

Equation 1.3

References

(1) Lehn, J. M., *Chem. Scr.*, **1988**, *28*, 237-262.

(2) Cram, D. J., *Science*, **1988**, *240*, 760-767.

(3) Pedersen, C. J., *Angew. Chem. Int. Ed. Engl*., **1988**, *27*, 1021-1027.

(4) Steed, J. W., Atwood, J. L. and Gale, P. A. *Definition and Emergence of Supramolecular Chemistry. Supramolecular Chemistry: From Molecules to Nanomaterials.*; John Wiley and Sons Ltd., **2012**.

(5) Wilson, A. J., *Ann. Rep. Prog. Chem. Sect. B*., **2008**, *104*, 164-183.

(6) Dalgarno, S. J., *Ann. Rep. Prog. Chem. Sect. B*., **2009**, *105*, 190-205.

(7) Dalgarno, S. J., *Ann. Rep. Prog. Chem. Sect. B*., **2010**; Vol. 106; pp 197-215.

(8) Albrecht, M., *Nature*, **2007**, *94*, 951-966.

(9) Chang, R., *Chemistry*; 9 ed.; McGraw-Hill: New York, 2007.

(10) Steel, P. J., *Chemistry in New Zealand*, **2003**, *67*, 57-60.

(11) Janiak, C., *J. Chem. Soc.-Dalton Trans*., **2000**, 3885-3896.

(12) Hunter, C. A.; Lawson, K. R.; Perkins, J.; Urch, C. J., *J. Chem. Soc.-Perkin Trans*, **2001**, 651-669.

(13) Atkins, P.; De Paula, J., *Atkins' Physical Chemistry*; 9 ed.; Oxford University Press: United States of America, **2010**.

(14) Atkins, P. D. P., *Physical Chemistry*; 9 ed.; Oxford University Press: United States of America, **2010**.

(15) Atkins, P. D. P., *Elements of Physical Chemistry*; 5 ed.; Oxford University Press: United States of America, **2009**.

(16) Loudon, G. M., *Organic Chemistry*; 4 ed.; Oxford University Press: New York, **2002**.

(17) Leininger, S.; Olenyuk, B.; Stang, P. J., *Chem. Rev*., **2000**, *100*, 853-907.

(18) Pitt, M. A.; Johnson, D. W., *Chem. Soc. Rev*., **2007**, *36*, 1441-1453.

(19) Lehn, J. M.; Rigault, A., *Angew. Chem. Int. Ed. Engl*., **1988**, *27*, 1095-1097.

(20) Albrecht, M., *Chem. Rev.*, **2001**, *101*, 3457-3497.

(21) Pabo, C. O.; Sauer, R. T., *Annu. Rev. Biochem.* **1984**, *53*, 293-321.

(22) Steiner, T., *Angew. Chem. Int. Ed. Engl*., **2002**, *41*, 49-76.

(23) Nishio, M.; Umezawa, Y.; Honda, K.; Tsuboyama, S.; Suezawa, H., *CrystEngComm*., **2009**, *11*, 1757-1788.

(24) Housecroft, C. E.; Sharpe, A. G., *Inorganic Chemistry*; 3 Ed; Pearson Education Ltd, **2008**.

(25) Kotz, J. C. T., P. M.; Weaver, G. C., *Chemistry and Chemical Reactivity Enhanced Review Edition*; 6 ed.; Thomson Brooks/Cole: United States of America, **2006**.

(26) Nishio, M., *CrystEngComm*., **2004**, *6*, 130-158.

(27) Sinnokrot, M. O.; Valeev, E. F.; Sherrill, C. D., *J. Am. Chem. Soc*., **2002**, *124*, 10887-10893.

(28) Hunter, C. A.; Sanders, J. K. M., *J. Am. Chem. Soc*., **1990**, *112*, 5525-5534.

(29) Atkins, P. W. O., T. L.; Rourke, J. P.; Weller, M. T.; Armstrong, F. A.,; *Shiver and Atkins' Inorganic* Chemistry; 5 Ed; Oxford University Press: United States of America and Canada, **2010**.

(30) Tuna, F.; Lees, M. R.; Clarkson, G. J.; Hannon, M. J., *Chemistry*., **2004**, *10*, 5737-5750.

(31) Steel, P. J., *Chemistry in New Zealand*., **2011**, *75*, 194-197.

(32) Fatin-Rouge, N.; Blanc, S.; Pfeil, A.; Rigault, A.; Albrecht-Gary, A. M.; Lehn, J. M., *Helv. Chim. Acta*., **2001**, *84*, 1694-1711.

(33) Karlin, K. D., *Progress in Inorganic Chemistry*; John Wiley and Sons Inc, Britain, **1994**.

(34) Keegan, J.; Kruger, P. E.; Nieuwenhuyzen, M.; O'Brien, J.; Martin, N., *Chem. Commun.*, **2001**, 2192-2193.

(35) Conerney, B.; Jensen, P.; Kruger, P. E.; MacGloinn, C., *Chem. Commun*., **2003**, 1274-1275.

(36) Kruger, P. E.; Martin, N.; Nieuwenhuyzen, M., *J. Chem. Soc.-Dalton Trans*., **2001**, 1966-1970.

(37) Piguet, C. *J,. Incl. Phenom. Macro*., **1999**, *34*, 361-391.

(38) Safarowsky, O.; Windisch, B.; Mohry, A.; Vögtle, F., *J. Prakt. Chem.*, **2000**, *342*, 437-444.

(39) Metzler, R., *New J. Phys*., **2002**, *4*.

(40) Kazuhiro Miwa; Kaori Shimizu; Heejun Min; Yoshio Furusho; Yashima, E. *Tetrahedron* **2012**, 1-9.

(41) Jeazet, H. B. T.; Gloe, K.; Doert, T.; Kataeva, O. N.; Jager, A.; Geipel, G.; Bernhard, G.; Buchner, B., *Chem. Commun.*, **2010**, *46*, 2373-2375.

(42) Piguet, C.; Borkovec, M.; Hamacek, J.; Zeckert, K., *Coord. Chem. Rev.*, **2005**, *249*, 705-726.

(43) Piguet, C.; Bernardinelli, G.; Hopfgartner, G., *Chem. Rev.*, **1997**, *97*, 2005-2062.

(44) Kramer, R.; Lehn, J. M.; Marquisrigault, A., *Proc. Natl. Acad. Sci. USA*., **1993**, *90*, 5394-5398.

(45) Northrop, B. H.; Chercka, D.; Stang, P. J., *Tetrahedron*, **2008**, *64*, 11495-11503.

(46) Lawrence, D. S.; Jiang, T.; Levett, M., *Chem. Rev.*, **1995**, *95*, 2229-2260.

(47) Tecilla, P.; Dixon, R. P.; Slobodkin, G.; Alavi, D. S.; Waldeck, D. H.; Hamilton, A. D., *J. Am. Chem. Soc.*, **1990**, *112*, 9408-9410.

(48) Xu, L.; Chen, X. T.; Xu, Y.; Zhu, D. R.; You, X. Z.; Weng, L. H., *J. Mol. Struct.*, **2001**, *559*, 361-368.

(49) Bai, Y.; Dang, D. B.; Duan, C. Y., *Acta Crystallogr. Sect. E*., **2006**, *62*, M2599-M2601.

(50) Mukherjee, A.; Chakrabarty, R.; Ng, S. W.; Patra, G. K., *Inorg. Chim. Acta*., **2010**, *363*, 1707-1712.

(51) Lehn, J. M.; Rigault, A.; Siegel, J.; Harrowfield, J.; Chevrier, B.; Moras, D., *Proc. Natl. Acad. Sci. USA*., **1987**, *84*, 2565-2569.

(52) Li, S. G.; Jia, C. D.; Wu, B.; Luo, Q.; Huang, X. J.; Yang, Z. W.; Li, Q. S.; Yang, X. J., *Angew. Chem. Int. Ed. Engl.*, **2011**, *50*, 5720-5723.

(53) United States National Library of Medicine., **2013**.

(54) Archer, R. J.; Kruger, P. E., *Unpublished*.

(55) Piguet, C.; Bernardinelli, G.; Bocquet, B.; Quattropani, A.; Williams, A. F., *J. Am. Chem. Soc*., **1992**, *114*, 7440-7451.

(56) Bai, Y.; Liu, J.; Dang, D. B.; Duan, C. Y., *Acta Crystallogr*., **2006**, *62*, M1805-M1807.

(57) Yoshida, N.; Ichikawa, K., *Chem. Commun*., **1997**, 1091-1092.

(58) Yoshida, N.; Ichikawa, K.; Shiro, M., *J. Chem. Soc.-Perkin Trans*., **2000**, 17-26.

(59) Yoshida, N.; Ito, N.; Ichikawa, K., *J. Chem. Soc.-Perkin Trans*., **1997**, 2387-2392.

(60) Parajo, Y.; Malina, J.; Meistermann, I.; Clarkson, G. J.; Pascu, M.; Rodger, A.; Hannon, M. J.; Lincoln, P., *Dalton Trans.*, **2009**, 4868-4874.

(61) Drew, M. G. B.; De, S.; Datta, D., *Inorg. Chim. Acta*., **2008**, *361*, 2967-2972.

(62) Sun, Q. Z.; Bai, Y.; He, G. J.; Duan, C. Y.; Lin, Z. H.; Meng, Q. J., *Chem. Commun.*, **2006**, 2777-2779.

(63) Drew, M. G. B.; Chowdhury, S.; Datta, D., *Indian. J. Chem. A.*, **2004**, *43*, 51-55.

(64) Wei, M. L.; Sun, R. P.; Zhuang, P. F.; Yang, Y. H., *Russ. J. Coord. Chem.*, **2009**, *35*, 885-890.

(65) Chowdhury, S.; Drew, M. G. B.; Datta, D., *New J. Chem*., **2003**, *27*, 831-835.

(66) Keegan, J.; Kruger, P. E.; Nieuwenhuyzen, M.; Martin, N., *Cryst. Growth Des*., **2002**, *2*, 329-332.

(67) De, S.; Drew, M. G. B.; Rzepa, H. S.; Datta, D., *New J. Chem*., **2008**, *32*, 1831-1834.

(68) Tandon, S. S.; Bunge, S. D.; Rakosi, R.; Xu, Z. Q.; Thompson, L. K., *Dalton Trans.*, **2009**, 6536-6551.

(69) Tandon, S. S.; Bunge, S. D.; Sanchiz, J.; Thompson, L. K., *Inorg. Chem*., **2012**, *51*, 3270-3282.

(70) Mandal, D.; Bertolasi, V.; Ribas-Arino, J.; Aromi, G.; Ray, D., *Inorg. Chem*., **2008**, *47*, 3465-3467.

(71) Clayden, J.; Greeves, N.; Warren, S.; Wothers, P., *Organic Chemistry*; Oxford University Press, **2007**.

(72) Thompson, J. R., *Synthesis and analysis of Fe(II) spin crossover complexes*., University of Canterbury, **2010**.

(73) Williamson, K. E., *Towards the synthesis of trinuclear triple helicates*., University of Canterbury, **2011**.

(74) De, S.; Chowdhury, S.; Tocher, D. A.; Datta, D., *CrystEngComm*., **2006**, *8*, 670-673.

(75) Pal, P. K.; Chowdhury, S.; Drew, M. G. B.; Datta, D., *New J. Chem.*, **2000**, *24*, 931-933.

(76) Tocher, D. A.; Drew, M. G. B.; Nag, S.; Pal, P. K.; Datta, D., *Chemistry.*, **2007**, *13*, 2230-2237.

(77) Akkurt, M.; Khandar, A. A.; Tahir, M. N.; Hosseini-Yazdi, S. A.; Mahmoudi, G., *Acta Crystallogr. Sect. E.*, **2012**, *68*, m903-m904.

(78) Spingler, B.; Schnidrig, S.; Todorova, T.; Wild, F., *CrystEngComm.*, **2012**, *14*, 751-757.

(79) Halcrow, M. A., *Chem. Soc.* Rev., **2011**, *40*, 4119-4142.

(80) Woodruff, D. N.; McInnes, E. J. L.; Sells, D. O.; Winpenny, R. E. P.; Layfield, R. A., *Inorg. Chem.*, **2012**, *51*, 9104-9109.

(81) Bacciu, D.; Chen, C. H.; Surawatanawong, P.; Foxman, B. M.; Ozerov, O. V., *Inorg. Chem.*, **2010**, *49*, 5328-5334.

(82) Garcia, Y.; Gutlich, P., *Top. Curr.* Chem., **2004**, *234*, 49-62.

(83) Wittick, L. M.; Murray, K. S.; Moubaraki, B.; Batten, S. R.; Spiccia, L.; Berry, K. J., *Dalton Trans.*, **2004**, 1003-1011.

(84) Claramunt, A.; Escuer, A.; Mautner, F. A.; Sanz, N.; Vicente, R., *J. Chem. Soc.-Dalton Trans.*, **2000**, 2627-2630.

(85) Wu, G.; Wang, X. F.; Okamura, T. A.; Sun, W. Y.; Ueyama, N. *Inorg. Chem.* **2006**, *45*, 8523-8532.

(86) Jensen, K. B.; Johansen, E.; Larsen, F. B.; McKenzie, C. J., *Inorg. Chem.*, **2004**, *43*, 3801-3803.

(87) Larsen, F. B.; Boisen, A.; Berry, K. J.; Moubaraki, B.; Murray, K. S.; McKee, V.; Scarrow, R. C.; McKenzie, C. J., *Eur. J. Inorg. Chem.*, **2006**, 3841-3852.

(88) Inglis, R.; Jones, L. F.; Karotsis, G.; Collins, A.; Parsons, S.; Perlepes, S. P.; Wernsdorfer, W.; Brechin, E. K., *Chem. Commun.*, **2008**, 5924-5926.

(89) Inglis, R.; Papaefstathiou, G. S.; Wernsdorfer, W.; Brechin, E. K., *Aust. J. Chem.*, **2009**, *62*, 1108-1118.

(90) Inglis, R.; Katsenis, A. D.; Collins, A.; White, F.; Milios, C. J.; Papaefstathiou, G. S.; Brechin, E. K., *CrystEngComm.*, **2010**, *12*, 2064-2072.

(91) Stoumpos, C. C.; Inglis, R.; Karotsis, G.; Jones, L. F.; Collins, A.; Parsons, S.; Milios, C. J.; Papaefstathiou, G. S.; Brechin, E. K., *Cryst. Growth Des.*, **2009**, *9*, 24-27.

(92) Yang, C. I.; Cheng, K. H.; Hung, S. P.; Nakano, M.; Tsai, H. L., *Polyhedron.*, **2011**, *30*, 3272-3278.

(93) Inglis, R.; Taylor, S. M.; Jones, L. F.; Papaefstathiou, G. S.; Perlepes, S. P.; Datta, S.; Hill, S.; Wernsdorfer, W.; Brechin, E. K., *Dalton Tran.*,. **2009**, 9157-9168.

(94) Milios, C. J.; Inglis, R.; Jones, L. F.; Prescimone, A.; Parsons, S.; Wernsdorfer, W.; Brechin, E. K., *Dalton Trans.*, **2009**, 2812-2822.

(95) Murray, K. S., *Eur. J. Inorg. Chem.*, **2008**, 3101-3121.

(96) Kitchen, J. A.; Brooker, S., *Coord. Chem.* Rev., **2008**, *252*, 2072-2092.

(97) Weber, B., *Coord. Chem. Rev.*, **2009**, *253*, 2432-2449.

(98) Salitros, I.; Fuhr, O.; Eichhofer, A.; Kruk, R.; Pavlik, J.; Dlhan, L.; Boca, R.; Ruben, M., *Dalton Trans.*, **2012**, *41*, 5163-5171.

(99) Sunatsuki, Y.; Kawamoto, R.; Fujita, K.; Maruyama, H.; Suzuki, T.; Ishida, H.; Kojima, M.; Iijima, S.; Matsumoto, N., *Inorg. Chem*., **2009**, *48*, 8784-8795.

(100) Krivokapic, I.; Zerara, M.; Daku, M. L.; Vargas, A.; Enachescu, C.; Ambrus, C.; Tregenna-Piggott, P.; Amstutz, N.; Krausz, E.; Hauser, A., *Coord. Chem. Rev*., **2007**, *251*, 364-378.

(101) Van der Sluis, P.; Spek, A. L., *Acta Crystallogr., Sect. A.*, **1990**, *46*, 194-201.

(102) Morris, R. J.; Girolami, G. S., *Organometallics*., **1991**, *10*, 792-799.

(103) Salavati-Niasari, M.; Babazadeh-Arani, H., *J. Mol. Catal. A-Chem*., **2007**, *274*, 58-64.

(104) Salavati-Niasari, M.; Hassani-Kabutarkhani, M.; Davar, F., *Catal. Commun*., **2006**, *7*, 955-962.

(105) Kajiwara, T.; Kobashi, T.; Shinagawa, R.; Ito, T.; Takaishi, S.; Yamashita, M.; Iki, N., *Eur. J. Inorg. Chem*., **2006**, 1765-1770.

(106) Mang, L.; Sun, Y. Q.; Yang, G. M.; Yan, S. P.; Jiang, Z. H.; Liao, D. Z., *J. Coord. Chem*., **2003**, *56*, 1441-1445.

(107) Rinehart, J. D.; Long, J. R., *Chem. Sci*., **2011**, *2*, 2078-2085.

(108) Sessoli, R.; Gatteschi, D.; Caneschi, A.; Novak, M. A., *Nature*., **1993**, *365*, 141-143.

(109) Sessoli, R.; Tsai, H. L.; Schake, A. R.; Wang, S. Y.; Vincent, J. B.; Folting, K.; Gatteschi, D.; Christou, G.; Hendrickson, D. N., *J. Am. Chem. Soc*., **1993**, *115*, 1804-1816.

(110) Slageren, J. v., *Introduction to Molecular Magnetism, Lecture,*; Universität Stuttgart, **2008**.

(111) Murray, K. S., *Aust. J. Chem*., **2009**, *62*, 1081-1101.

(112) Sheldrick, G. M., *Acta Crystallogr., Sect. A*., **2008**, *64*, 112-122.

(113) Sheldrick, G. M. *Programs for X-ray Crystal Structure Refinement*., Ed., **1997**; p. University of Gottingen.

(114) O.V. Dolomanov; L.J. Bourhis; R.J. Gildea; J. A. K. Howard; Puschmeann, H., *J. Appl. Crystallogr*., **2006**, *42*, 339-341.

(115) Salavati-Niasari, M.; Hassani-Kabutarkhani, M., *Synth. React. Inorg. Met.-Org. Nano-Metal Chem*., **2005**, *35*, 469-475.

(116) Hauer, C. R.; King, G. S.; McCool, E. L.; Euler, W. B.; Ferrara, J. D.; Youngs, W. J., *J. Am.Chem. Soc*., **1987**, *109*, 5760-5765.

(117) Ardakani, M. M.; Sadeghi, A.; Salavati-Niasari, M., *Talanta*., **2005**, *66*, 837-843.

(118) Yang, L.; Powell, D. R.; Houser, R. P., *Dalton Trans*., **2007**, 955-964.